Durham University

Durham E-Theses

Electromagnetic interactions of muons

Rogers, I. W.

How to cite:

Rogers, I. W. (1965) *Electromagnetic interactions of muons*, Durham theses, Durham University. Available at Durham E-Theses Online: http://etheses.dur.ac.uk/8932/

Use policy

The full-text may be used and/or reproduced, and given to third parties in any format or medium, without prior permission or charge, for personal research or study, educational, or not-for-profit purposes provided that:

- a full bibliographic reference is made to the original source
- a link is made to the metadata record in Durham E-Theses
- the full-text is not changed in any way

The full-text must not be sold in any format or medium without the formal permission of the copyright holders.

Please consult the full Durham E-Theses policy for further details.

Academic Support Office, The Palatine Centre, Durham University, Stockton Road, Durham, DH1 3LE
e-mail: e-theses.admin@durham.ac.uk Tel: +44 0191 334 6107
http://etheses.dur.ac.uk

PLATE I

FRONTISPIECE

THE DURHAM EXPERIMENT

ELECTROMAGNETIC INTERACTIONS OF MUONS

by

I.W. Rogers, B.Sc.

Thesis submitted to the

University of Durham

for the degree of Doctor of Philosophy.

January, 1965.

DURHAM UNIVERSITY
SCIENCE
25 FEB 1965
LIBRARY

ABSTRACT

The electromagnetic interactions of muons in iron and lead have been studied, using cosmic ray muons, at Durham, 198 feet above sea level, and at London, 60 m.w.e. underground, respectively. The energies of the secondary particles from the interactions were determined from the cascade showers which these particles produced in layers of absorber.

As a result of these studies it has been shown that, over the range of transferred energies from 0.1 GeV to 30 GeV, there is no discrepancy between the results predicted on the basis of quantum electrodynamics and the experimental results. Since the production of knock-on electrons is the dominant process over most of this transferred energy range, there is thus no evidence for a breakdown of quantum electrodynamical theory in close collisions between muons and electrons.

By combining this result with the result of an accurate measurement of the anomalous magnetic moment of the muon it is further concluded that, at the present time, there is no evidence for the muon differing from a heavy electron.

PREFACE

This thesis describes investigations of the electromagnetic interactions of muons in iron and lead and the analysis and interpretation of the results obtained.

The whole of the work concerned with the interactions of muons in iron was carried out at Durham under the supervision of Dr. A.W. Wolfendale.

The data concerning the electromagnetic interactions of muons in lead were obtained from an experiment carried out by Dr. J.C. Barton of the Northern Polytechnic, London, and analysed at Durham.

Both the operation of the experiment at Durham and the analysis of the data from both this and the London experiment were the sole responsibility of the author. Dr. M.G. Thompson carried out the numerical calculations of the direct pair production probabilities used in the determination of the expected results.

CONTENTS

		Page
ABSTRACT		i
PREFACE		ii
CHAPTER 1	INTRODUCTION	1
CHAPTER 2	THEORETICAL CONSIDERATIONS OF THE ELECTROMAGNETIC INTERACTIONS OF MUONS	7
2.1	Introduction	7
2.2	Knock-on Interactions	8
2.3	Bremsstrahlung	9
2.4	Direct Pair Production	11
2.5	Comparison of the Energy Loss Probabilities	16
2.6	Discussion	17
CHAPTER 3	SURVEY OF PAST EXPERIMENTAL RESULTS	19
3.1	Introduction	19
3.2	The Knock-on Process	20
	3.2.1 Deery (1960)	20
	3.2.2 Stoker et al.	22
	3.2.3 McDiarmid and Wilson	23
	3.2.4 Backenstoss et al.	24
3.3	Bremsstrahlung	25
3.4	Direct Pair Production	25
	3.4.1 Introduction	25
	3.4.2 Roe and Ozaki	26
	3.4.3 Gaebler et al.	27
	3.4.4 Stoker et al.	28
	3.4.5 Chaudhuri and Sinha	31
3.5	Discussion	33

Page

CHAPTER 4 THE DURHAM EXPERIMENT

ELECTROMAGNETIC INTERACTIONS OF MUONS IN IRON 35

4.1 Introduction 35

4.2 The Selection System 36

4.2.1 The Geiger Counters 36

4.2.2 The Scintillation Counter 37

4.2.3 Calibration of the Scintillation Counter 38

4.2.4 The Anticoincidence Tray 39

4.2.5 Summary of Selection Criteria 40

4.3 The Flash Tube Trays 40

4.4 The Recording System 42

4.5 Running Time 43

CHAPTER 5 THE ANALYSIS OF THE DURHAM DATA 44

5.1 Introduction 44

5.2 The Standard Shower Curves 44

5.3 Estimation of Shower Energies. Method 1 45

5.3.1 Introduction 45

5.3.2 The Total Electron Track Length 46

5.3.3 Total Track Length from Standard Shower Curves 47

5.3.4 Determination of Total Track Lengths and Energies for Observed Showers 47

5.3.5 Accuracy of the Energy Estimates 48

5.4 Estimation of Shower Energies. Method II 49

5.4.1 Introduction 49

5.4.2 The Calibration Curves 50

Page

5.4.3 Estimation of the Number of Particles Traversing a Flash Tube Tray 50

5.4.4 Accuracy of the Energy Estimates 52

5.5 Conclusions 55

CHAPTER 6 RESULTS AND CONCLUSIONS FROM THE DURHAM EXPERIMENT 56

6.1 Introduction 56

6.2 Selection Criteria 57

6.3 Experimental Conditions and Running Times 58

6.4 The Theoretical Curves 60

6.5 Experiment A 60

6.5.1 Final Classification of Events 60

6.5.2 The Transferred Energy Spectrum 61

6.6 Experiment B 62

6.6.1 Final Classification of Events 62

6.6.2 The Transferred Energy Spectrum 63

6.7 Comparison between Predicted and Experimental Results 63

6.7.1 Introduction 63

6.7.2 Correction for Fluctuations 64

6.7.3 Correction for Detection Efficiency 66

6.7.4 Discussion of the Experimental Results 68

6.8 Conclusions 71

CHAPTER 7 THE LONDON EXPERIMENT

ELECTROMAGNETIC INTERACTIONS OF MUONS IN LEAD 72

7.1 Introduction 72

Page

7.2 General Description of Apparatus 72

7.3 The Scintillation Counters 73

7.3.1 Construction 73

7.3.2 Measurement of Output Pulse Heights 73

7.3.3 The Fourth Scintillation Counter as part of the Selection System 74

7.4 The Index Trays 75

7.4.1 Introduction 75

7.4.2 The Geiger Counter Index Trays 75

7.4.3 The Scintillation Counter Index Trays 76

7.5 The Selection and Recording of Events 77

7.6 The Dead Time of the Apparatus 78

7.7 The Resolving Time 79

7.8 Running Times 80

CHAPTER 8 ANALYSIS OF THE LONDON DATA 81

8.1 Introduction 81

8.2 The London Analysis 82

8.2.1 The Original Form of the Data 82

8.2.2 The Division of the Events 83

8.3 The Durham Analysis 84

8.3.1 Introduction 84

8.3.2 Grouping of the Events 85

8.3.3 Conversion from Channel Number to Number of Particles 85

8.3.4 The Calibration Curve 86

8.3.5 Discussion of Analysis 87

		Page
CHAPTER 9	RESULTS AND CONCLUSIONS FROM THE LONDON EXPERIMENT	90
9.1	Introduction	90
9.2	The Predicted Results	90
9.2.1	Introduction	90
9.2.2	The Basic Spectrum	91
9.2.3	The Target Thickness	91
9.2.4	The Effect of the Incident Angle of the Muon	94
9.2.5	The Effect of the Point of Interaction on the Estimated Energy of the Shower	95
9.2.6	The Predicted Energy Spectra	96
9.2.7	The Effect of Fluctuations	98
9.2.8	Discussion	98
9.3	The Experimental Results	99
9.3.1	Conversion from Maximum Channel Number to Energy	99
9.3.2	Final Selection of Data	99
9.3.3	The Unbiassed Results	100
9.3.4	The Biassed Results	101
9.4	Conclusions from the London Experiment	102
CHAPTER 10	CONCLUSIONS	103
ACKNOWLEDGMENTS		105
REFERENCES		106
APPENDIX	CASCADE SHOWERS	110
1	Introduction	110
2	Cascade Shower Development	110
3	Theoretical Results	111

		Page
	3.1 Introduction	111
	3.2 Approximation A (Rossi, 1952)	112
	3.3 Approximation B (Rossi, 1952)	112
	3.4 Buja (1963)	113
	3.5 Comparison of the Theoretical Results	113
4	Monte Carlo Calculations	115
	4.1 Wilson (1952)	115
	4.2 Crawford and Messel (1962)	116
	4.3 Discussion and Comparison of the Monte Carlo Results	117
5	Experimental Results	118
	5.1 Hazen (1955)	118
	5.2 Backenstoss et al. (1963a)	118
6	Comparison of Results	119
	6.1 Introduction	119
	6.2 Thin Plate Experiment	119
	6.3 Thick Plate Experiment	122
	6.4 Burst Experiment	122
7	Discussion	123

CHAPTER 1

INTRODUCTION

When it was first discovered that atomic nuclei were made up of a mixture of protons and neutrons it was realised that neither of the forces known at that time i.e. the electromagnetic force, which acts through the electromagnetic fields of charged particles, and the gravitational force, which acts between the masses of two particles, could be used to explain the binding of these particles in the nucleus. For this reason Yukawa (1935), working by analogy with the photon as the quantum of the electromagnetic force, postulated that the quantum of the nuclear force should be a particle of mass between 100 and 200 times the mass of the electron and that this particle should occur in both positive and negative charge states.

Shortly after this, Neddermeyer and Anderson (1937, 1939) found evidence for the existance in the cosmic radiation of charged particles with mass between that of the proton and that of the electron. When the mass and lifetime of these particles, now known as "muons", were measured they were found to be within the limits predicted for the Yukawa particle. However, an experiment carried out by Conversi et al. (1947), in which muons were stopped in absorbers of low atomic number, showed that, in carbon at least, a large proportion of negative muons decayed before interacting with a nucleus. This result was taken as indicating that the muon could

not be identified with the Yukawa particle, which was required to be strongly interacting, and so the search for the latter was intensified.

A short time after the work of Conversi, Lattes et al., (1947), working with nuclear emulsions exposed at mountain altitudes, found an event in which one charged particle decayed into a second one. On investigation it was found that this second charged particle was a muon. Further, a large number of tracks had been found in emulsions in which charged particles of the same type as the parent of the muon had interacted with the nuclei of the emulsion. Because of this it was thought that these incident charged particles could be identified with the Yukawa particle and that the muon was the decay product of the latter. Measurements of the mass, and lifetime of these particles, now known as "pions", confirmed that they fulfilled the requirements for the Yukawa particle. Thus it was concluded that the pion, and not the muon, was to be identified with the quantum of the nuclear force.

Since the discovery of the pion a large number of other elementary particles have been discovered using cosmic rays and beams of particles from high energy accelerators. The more common of these particles and their antiparticles are listed in table I.

TABLE I

Group	Type of Particle	Symbol	Rest Mass, m_e	Spin	Antiparticle
	Photon	γ	0	1	-
Leptons	Neutrino	ν	0	$\frac{1}{2}$	$\bar{\nu}$
	Electron	e^-	1	$\frac{1}{2}$	e^+
	μ-meson	μ^-	206.9	$\frac{1}{2}$	μ^+
Mesons	π-mesons	π^+	273.2	0	π^-
		π^0	264		π^0
		π^-	273.2		π^+
	K-mesons	K^+	966	0	K^-
		K^0	975 ± 3		$\bar{K}^0$
Baryons	Nucleons	p	1836.1	$\frac{1}{2}$	$\bar{p}$
		n	1838.6		$\bar{n}$
	Λ^0 hyperon	Λ^0	2182	$\frac{1}{2}$	$\bar{\Lambda}^0$
	Σ hyperons	Σ^+	2328	$\frac{1}{2}$	$(\bar{\Sigma}^-)$
		Σ^-	2342 ± 1		$(\bar{\Sigma}^+)$
		Σ^0	2330 ± 2		$(\bar{\Sigma}^0)$
	Ξ hyperons	Ξ^-	2584 ± 4	$\frac{1}{2}$	$(\bar{\Xi}^+)$
		Ξ^0	~2584		$(\bar{\Xi}^0)$

Reproduced from C.F. Powell, P.H. Fowler and D.H. Perkins, 'The Study of Elementary Particles by the Photographic Method', Pergamon Press Ltd., (1959).

In table I the particles are divided into four groups according to their masses and spins, namely:

1) The photon.

2) Leptons - particles with spin $\frac{1}{2}$ and mass less than the mass of the proton.

3) Mesons - particles with spin 0 and mass less than the mass of the proton, and

4) Baryons - particles of proton mass or greater and with spin $\frac{1}{2}$.

It is found that the interactions between the groups are as follows:

a) Between baryons and mesons the interactions are strong and proceed through the short range, or nuclear, force. These interactions have lifetimes of the order of 10^{-23} sec and an example of such an interaction is the proton-proton collision in which pions are produced, i.e. $p + p \rightarrow p + n + \pi^+$.

b) Between baryons and leptons and between mesons and leptons the interactions are weak and have a lifetime of the order of 10^{-10} secs. Examples of weak interactions are the β-decay of a nucleus and the decay of a muon ($\mu^{\pm} \rightarrow e^{\pm} + \nu + \bar{\nu}$).

Besides the two types of interactions described above charged particles also undergo a third type of interaction, the electromagnetic interaction, which takes place through the electromagnetic fields of the particles. Such interactions have lifetimes of the order of 10^{-21} secs and are thus weaker than the nuclear interactions by a factor of approximately 10^2 but stronger than the weak interactions.

Although the muon seems to fit quite nicely into the scheme of elementary particles given in table I it still presents a problem to physicists working in the field of elementary particles. Although it has been found possible, using quantum dynamics, to explain the existence of all other elementary particles and in many cases to predict the properties of particles before they are discovered e.g. the Ω^-, no theory has yet been put forward to explain the existence of the muon.

It has been found experimentally that, apart from its decay, the muon behaves as a heavy electron within the limits set by the experimental conditions. However, attempts are still being made to find deviations of the interactions of the muon from those of the electron. Such deviations, if found, would indicate that either the muon was interacting with a particle field which is, as yet, undiscovered, or that the muon has a structure which would lead to a breakdown in the theory of quantum electrodynamics.

Since the muon belongs to the lepton group it only undergoes two types of interactions, the weak and the electromagnetic interactions. Of these the electromagnetic interactions are most amenable to investigation. This thesis is concerned with two experiments carried out to study these interactions. Chapters 2 and 3 describe the theories of the electromagnetic interactions and past investigations of these. Chapters 4, 5 and 6 contain a description of an experiment carried out to investigate the electromagnetic interactions of muons in iron and the results obtained

from it. Chapters 7, 8 and 9 give the results of an experiment using lead instead of iron for a target and Chapter 10 contains the conclusions which are drawn from the two experiments and compares them with those drawn from other experiments which have been carried out to determine the properties of muons.

CHAPTER 2

THEORETICAL CONSIDERATIONS OF THE ELECTROMAGNETIC INTERACTIONS OF MUONS

2.1 Introduction

The electromagnetic interactions of muons, and of all charged particles, are classified according to the results of the interactions, namely:

i) Excitation and ionisation of the atoms of the medium through which the muon passes. In this type of interaction the muon passes at some distance from the atom and interacts with the atom as a whole. The energy transferred from the muon is then just sufficient to raise one of the electrons associated with this atom to a higher energy state (excitation) or remove it from the atom completely (ionisation).

ii) The knock-on process. This type of interaction is similar to the ionisation process except that the muon passes much closer to the atom. The energy transferred to the electron in the knock-on process is so large compared with the ionisation potential that the interaction may be taken as being between the muon and a free electron.

iii) Bremsstrahlung. Here the muon is scattered by the electromagnetic field of the nucleus and emits a photon.

iv) Direct pair production. This type of interaction is similar to bremsstrahlung except that when the muon is scattered by the electromagnetic field of the nucleus it produces an electron-positron pair rather than emitting a photon.

As well as undergoing the electromagnetic interactions described above the muon also undergoes what are commonly known as 'nuclear' interactions. Such interactions are not actually the interactions of the muons with nuclei, the muon being only weakly interacting, but are interactions between photons of the virtual photon cloud surrounding the muon, and the nucleus. Since, however, the cross-section for this process is small compared with those for interactions of types ii), iii) and iv) for incident muon energies below 1000 GeV the effect of muon nuclear interactions on measurements of the electromagnetic interactions can be allowed for.

The electromagnetic interactions with which this thesis is concerned are types ii), iii) and iv). A brief description of the theoretical results which have been obtained for these interactions is given in the following paragraphs.

2.2 Knock-on Interactions

The theoretical expression for the probability of a knock-on collision for a primary particle of spin $\frac{1}{2}$ has been derived by Bhabha (1938) and by Massey and Corben (1939). In the derivation it was assumed that the particle has a normal magnetic moment of unity. It is also assumed that the electromagnetic field of the particle can be described as being due to a point charge down to distances smaller than 10^{-13} cm from the centre of the particle.

The result of this work is given by equation 2.1:

$$\phi_{coll}(E,E')dE' = \frac{2Cm_e c^2}{\beta^2}\frac{dE'}{(E')^2}\left[1 - \beta^2\frac{E'}{E_m'} + \tfrac{1}{2}\left(\frac{E'}{E+mc^2}\right)^2\right] \quad \ldots 2.1$$

where $\phi_{coll}(E,E')dE'$ is the probability/g cm^{-2} that a particle of kinetic energy E and rest mass mc^2, will produce a knock-on electron with kinetic energy between E' and E' + dE'.

$C = 0.15\frac{Z}{A}$ $cm^2 g^{-1}$

Z is the atomic number of the absorber

A is the atomic weight of the absorber

β is the velocity of the incident particle in terms of the velocity of light

$m_e c^2$ is the rest mass of the electron

and E_m' is the maximum energy which can be transferred to the secondary electron and is given by

$$E_m' = 2m_e c^2\left(\frac{p^2c^2}{m_e^2c^4 + m^2c^4 + 2m_e c^2(p^2c^2 + m^2c^4)^{\frac{1}{2}}}\right)$$

where p is the momentum of the incident particle.

2.3 Bremsstrahlung

When a charged particle passes close to an atomic nucleus it experiences a force which causes it to undergo an acceleration resulting in the emission of a photon. The differential probability for the emission of radiation by charged particles of spin $\frac{1}{2}$ and normal magnetic moment has been calculated by Christy and Kusaka (1951) on the assumptions that 1) the kinetic energy of the incident particle is much

larger than its rest energy, 2) the potential of a nucleus can be described as being that due to a point charge for distances from the centre of the nucleus larger than the nuclear radius, r_n, and constant for distances less than r_n, and 3) the screening of the outer electrons is negligible. As a result of their analysis they obtained the following expression:

$$\phi_{rad}(E,E')dE' = \propto \frac{N}{A} Z^2 r_e^2 \left(\frac{m_e c^2}{mc^2}\right)^2 \frac{dE'}{E'} F(u, v) \qquad \ldots 2.2$$

where $\phi_{rad}(E,E')dE'$ is the probability/g cm^{-2} that a particle of rest mass mc^2 and kinetic energy E will emit a photon with energy between E' and E' + dE'

N = Avogadro's number

$\propto$ is the fine structure constant

Z, A and $m_e c^2$ are the same as in equation 1.1

r_e is the classical electron radius

and F(u, v) is a function of the total energy, u, of the incident particle and the fraction of this energy emitted in the form of a photon, v. This function is dependent upon the spin of the incident particle and for particles of spin $\frac{1}{2}$ is given by:

$$F(u,v) = 4\left[1 + (1-v)^2 - \tfrac{2}{3}(1-v)\right]\left[\ell n\left(\frac{2u}{mc^2}\frac{\hbar}{mcr_n}\frac{1-v}{v}\right) - \tfrac{1}{2}\right]$$

where $r_n = 0.49\, r_e\, A^{\frac{1}{3}}$ and

$\hbar = \frac{1}{2\pi}$ x Planck's constant.

2.4 Direct Pair Production

The original work onthe theory of the direct production of electron-positron pairs by relativistic charged particles passing close to atomic nuclei was that due to Bhabha (1935 A, B) who used quantum electrodynamics to derive the cross section for the interaction. In the derivation he assumed that the fields of the incident and target charged particles could be described classically, i.e. as being due to point charges, that the target nucleus was infinitely heavy and that the incident particle was not deflected during the interaction. As a result of the derivation he obtained the second order differential cross section for the process i.e. the cross section for the production by an electron of an electron-positron pair in which the electron has an energy between ϵ_- and $\epsilon_- + d\epsilon_-$ and the positron has an energy between ϵ_+ and $\epsilon_+ + d\epsilon_+$. For the region in which $m_e c^2 \ll \epsilon_-, \epsilon_+$; $\gamma m_e c^2 \gg \epsilon_-, \epsilon_+$, where γ is the energy of the incident particle in terms of the rest mass of that particle, and in the case of no screening the value of this cross section is given by

$$dQ = \frac{8}{\pi}\left(\frac{r_e Z}{137}\right)^2 \frac{\epsilon_+^2 + \epsilon_-^2 + \frac{2}{3}\epsilon_+\epsilon_-}{(\epsilon_+ + \epsilon_-)^4} \log \frac{k\,\epsilon_-\epsilon_+}{(\epsilon_- + \epsilon_+) m_e c^2} \log \frac{k' m_e c^2 \gamma}{(\epsilon_- + \epsilon_+)} d\epsilon_- d\epsilon_+ \quad \ldots 2.3$$

where k and k' are both numbers of the order of unity but are not always the same.

By integrating this cross section Bhabha then obtained an expression for the total cross section for direct pair production, namely,

$$Q = \frac{28}{27\pi}\left(\frac{r_e Z}{137}\right)^2 \log^3 k\gamma \quad \ldots 2.4$$

This crosssection is valid over the region in which the total energy of the pair is greater than $2m_e c^2$ and less than $m_e c^2 \gamma$.

About the time when Bhabha's results appeared theoretical values for the total cross section were obtained independently by Nishina et al. (1935) and Racah (1937) which were in good agreement with each other but led to numerical values a factor of two lower than those of Bhabha.

By carrying out a more precise integration of the second order differential equations given by Bhabha, Davisson (see Rossi, 1952) obtained expressions for the first order equations in four different regions,

1) the region where a low energy pair is produced and where there is no screening,

2) the region where a low energy pair is produced and there is complete screening,

3) the region where a high energy pair is produced and there is no screening, and

4) the region where a high energy pair is produced and there is complete screening.

The expressions obtained and the regions in which they can be taken as valid (Rossi, 1952) are:-

Region 1 $\dfrac{2m_e c^2}{E_o} < \dfrac{E_T}{E_o} < \dfrac{2m_e c^2}{mc^2}$; $\dfrac{E_T}{E_o} < \dfrac{(2m_e c^2/E_o)}{\alpha Z^{\frac{1}{3}}}$

$$\phi(E_o,E_T)dE_T dx = \frac{8}{\pi}\alpha^2 \frac{N}{A} Z^2 r_e^2 \cdot \frac{7}{9}\frac{1}{E_T} \ell n \left[\frac{k_1 m_e c^2}{mc^2}\frac{E_o}{E_T}\right] \times \ell n \left[\frac{k_1'}{6}\frac{1}{m_e c^2}\frac{1}{E_T}\right] dE_T\, dx \quad \ldots 2.5$$

where $m_e c^2$ is the rest mass of the electron.

mc^2 = rest mass of incident particle

E_o = energy of incident particle

E_T = total energy of created pair

α = fine structure constant

N = Avogadro's number

A = Atomic weight of absorber

Z = Atomic number of absorber

r_e = classical electron radius

$k_1, k_1', k_2', k_3, k_4$ = . . . numbers of the order of unity.

Region 2.

$$\frac{2m_e c^2}{E} < \frac{E_T}{E_o} < \frac{2m_e c^2}{mc^2} \; ; \quad \frac{E_T}{E_o} > \frac{(2m_e c^2/E_o)}{\alpha Z^{\frac{1}{3}}}$$

$$\phi(E_o,E_T)dE_T dx = \frac{8}{\pi}\alpha^2 \frac{N}{A} Z^2 r_e^2 \frac{7}{9} \frac{1}{E_T} \ell n \left[\frac{k_1 m_e c^2}{mc^2} \frac{E_o}{E_T}\right] \times \ell n \left(\frac{k_2'}{\alpha Z^{\frac{1}{3}}}\right) dE_T dx \quad \ldots 2.6$$

Region 3.

$$\frac{2m_e c^2}{mc^2} < \frac{E_T}{E_o} < 1; \quad \frac{E_T}{E_o} < \left(\frac{2m_e c^2}{mc^2}\right) \alpha Z^{\frac{1}{3}} \left(\frac{E_o}{mc^2}\right)$$

$$\phi(E_o,E_T)dE_T dx = \frac{8}{\pi}\alpha^2 \frac{N}{A} Z^2 r_e^2 \frac{E_o^2}{E_T^3}\left(\frac{m_e c^2}{mc^2}\right)^2 \ell n\left(\frac{k_3}{\alpha Z^{\frac{1}{3}}}\frac{mc^2}{m_e c^2}\frac{E_T}{E_o}\right) dE_T dx \quad \ldots 2.7$$

Region 4.

$$\frac{2m_e c^2}{mc^2} < \frac{E_T}{E_o} < 1; \quad \frac{E_T}{E_o} \gg \left(\frac{2m_e c^2}{mc^2}\right)\alpha Z^{\frac{1}{3}}\left(\frac{E_o}{mc^2}\right)$$

$$\phi(E_o,E_T)dE_T dx = \frac{8}{\pi}\alpha^2 \frac{N}{A} Z^2 r_e^2 \frac{E_o^2}{E_T^3}\left(\frac{m_e c^2}{mc^2}\right)^2 \ell n\left(2k_4 \frac{E_o}{mc^2}\right) \quad \ldots 2.8$$

Following this, Block et al. (1954) further improved the integration of equation 1.3 and obtained a total cross-section which is in good agreement with that due to Racah (1937).

A more recent treatment of the theory of direct pair production is that due to Murota et al. (1956) who calculate the cross-section using the Feynmann-Dyson method in which the incident charged particle is treated quantum dynamically and the target charged particle is taken as being a fixed Coulomb field. For the case of an incident charged particle of mass many times that of the electron they show that of the four lowest order Feynmann-diagrams for the process, shown below, only two, those labelled A and A', need be considered.

Using these two diagrams they obtain an expression for the cross-section, σ, for the production of an electron-positron pair in which the electron has energy between ϵ_- and $\epsilon_- + d\epsilon_-$ and the positron has energy between ϵ_+ and $\epsilon_+ + d\epsilon_+$, given by:

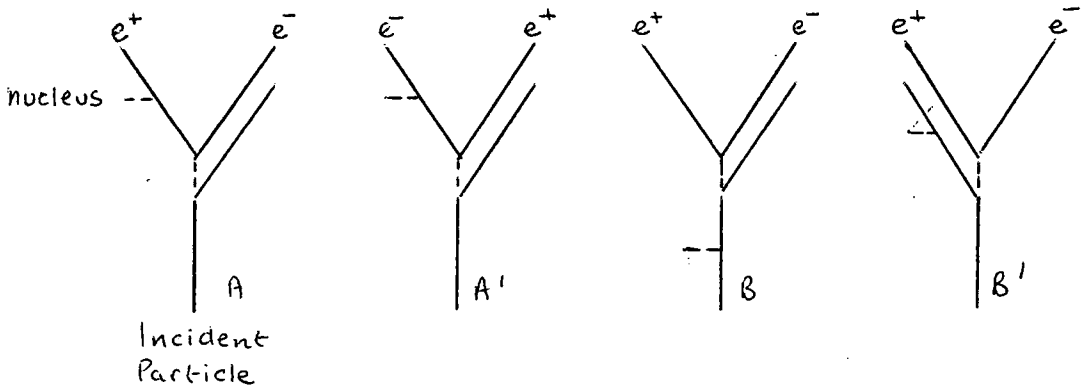

Fig. 2.1. Lowest order Feynmann-Dyson diagrams for Direct Pair Production

$$\sigma = \frac{2}{\pi}\,(Ze^2)^2\,(e^2/m_e c^2)^2\,d\epsilon_+\,d\epsilon_-\,L$$

$$\times\left\{\left[\frac{\epsilon_+^2+\epsilon_-^2}{\epsilon^4}\left\{\left(1+\tfrac{4}{3}x\right)\log\left(1+\frac{1}{x}\right)-\tfrac{4}{3}\right\}\right.\right.$$

$$\left.\left.+\tfrac{2}{3}\,\frac{\epsilon_+\epsilon_-}{\epsilon^4}\left\{(1+2x)\log\left(1+\frac{1}{x}\right)-2\right\}\right]\right.$$

$$\times\,\frac{E_1^2+E_2^2}{E_1^2}$$

$$+\tfrac{8}{3}\,\frac{\epsilon_+\epsilon_-}{\epsilon^4}\,\frac{1}{1+x}\,\frac{E_2}{E_1}$$

$$+\left[\frac{\epsilon_+^2+\epsilon_-^2}{\epsilon^4}\left\{\tfrac{1}{3}\,\frac{1}{1+x}+\frac{1}{x}-\tfrac{4}{3}\log\left(1+\frac{1}{x}\right)\right\}\right.$$

$$\left.\left.+\tfrac{2}{3}\,\frac{\epsilon_+\epsilon_-}{\epsilon^4}\left\{\frac{1}{1+x}+\frac{1}{x}-2\log\left(1+\frac{1}{x}\right)\right\}\right]\times\frac{\epsilon^2}{E_1^2}\right\} \quad \ldots\ 2.9$$

E_1, E_2 are the energies of the incident particle before and after the interaction

μc^2, $m_e c^2$ are respectively the mass of the incident particle and the mass of the electron

$x = (\mu^2 c^4 / E_1 E_2) \cdot (\epsilon_+ \epsilon_- / m_e^2 c^4)$

L is a term which depends upon the screening and is given by

$L = \log (2 \propto \epsilon_+ \epsilon_- / \epsilon M) - 1$ for no screening and

$L = \log (\propto .137\, Z^{-\frac{1}{3}}\, M/m_e c^2)$ for complete screening

$\propto$ is a constant of the order of unity

M is the matrix element for the two Feynmann-Dyson diagrams used and is

$$M^2 \equiv m_e^2 c^4 + (\epsilon_+ \epsilon_- / E_1 E_2) \mu^2 c^4$$

This expression for the cross section is valid when $\mu c^2 \gg m_e c^2$, $E_1 - \epsilon \gg \mu c^2$, $\epsilon \ll E_1$ and $\epsilon \gg m_e c^2$ where $\epsilon = \epsilon_+ + \epsilon_-$.

When equation 2.9 is integrated with respect to the fraction of the pair energy going to the electron a second undefined constant, $a = \frac{n\, m_e c^2}{\epsilon}$ where n is greater than one, appears as one limit of the integration. The minimum value of a is $a = \frac{m_e c^2}{\epsilon}$ in which case the integral is carried out from $\epsilon_- = 0$ to $\epsilon_- = m_e c^2$. However, since equation 2.9 is not valid for very low energy secondary electrons it is usual to take $n > 1$.

2.5 Comparison of the Energy Loss Probabilities

Curves are drawn in figures 2.2, 2.3, 2.4 and 2.5 of the probabilities of producing a given energy transfer by each of the three processes described above for the cases of 10 GeV and 100 GeV muons incident upon iron and lead absorbers. These curves were calculated from equations 2.1, 2.2 and 2.9 with k_1, k_1', k_2', k_3 and k_4 put equal to unity. Also shown are the results obtained using Bhabha's formulae as presented by Davisson, equations 2.5, 2.6, 2.7 and 2.8.

Figure 2.2

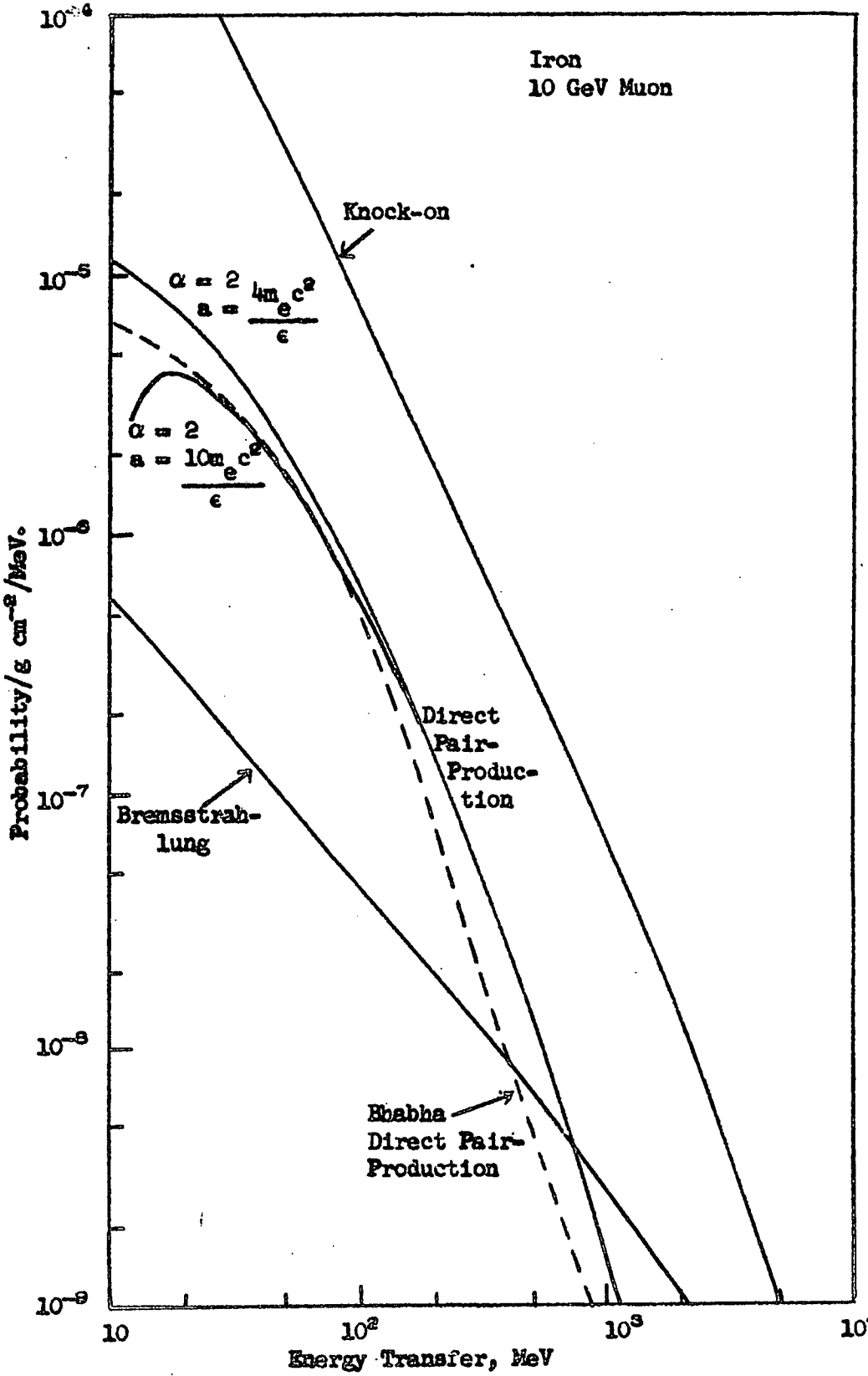

Differential Energy Transfer Curve for 10 GeV Muons in iron

Figure 2.3.

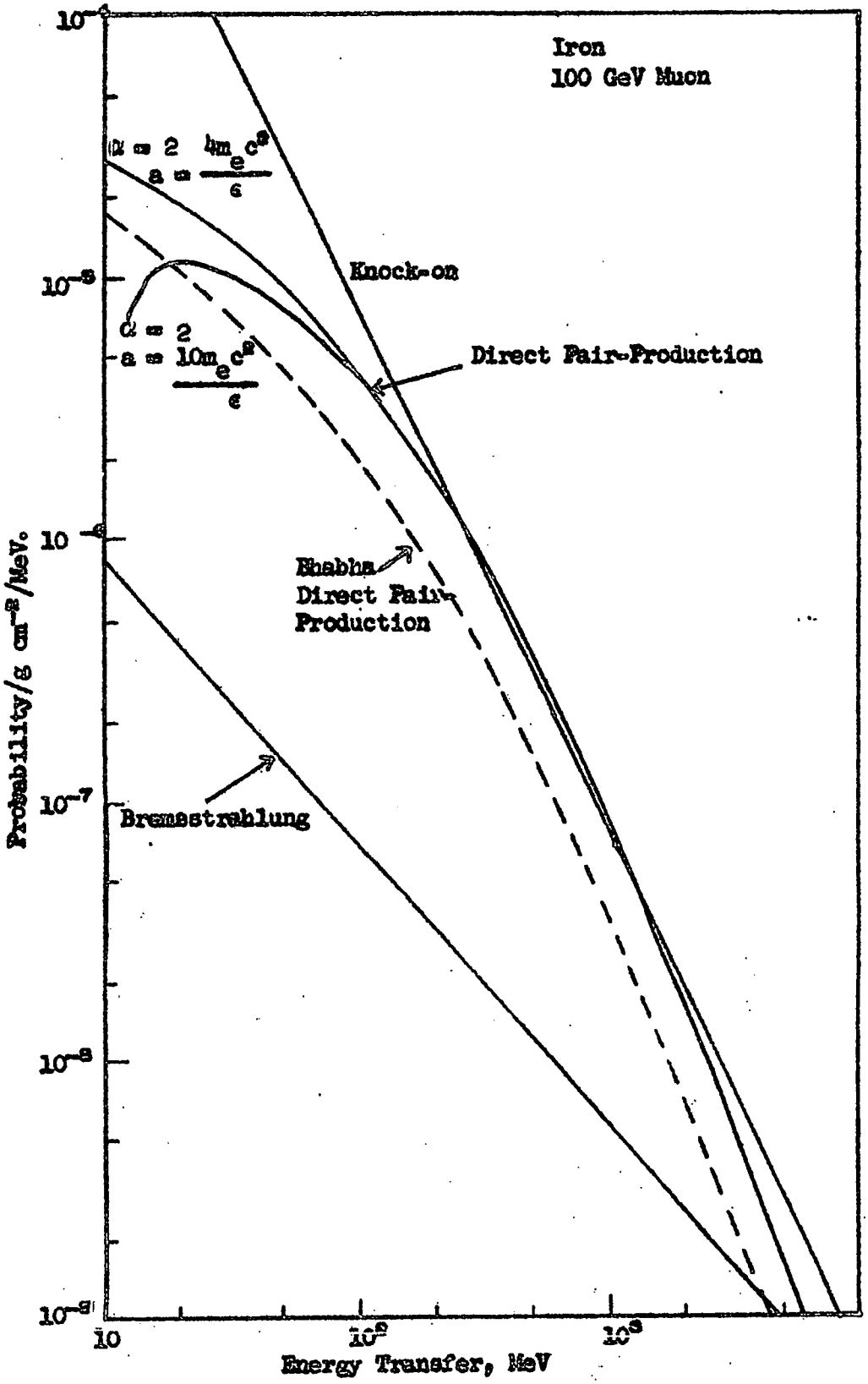

Differential Energy Transfer Curves for 100 GeV Muons in Iron.

Figure 2.4.

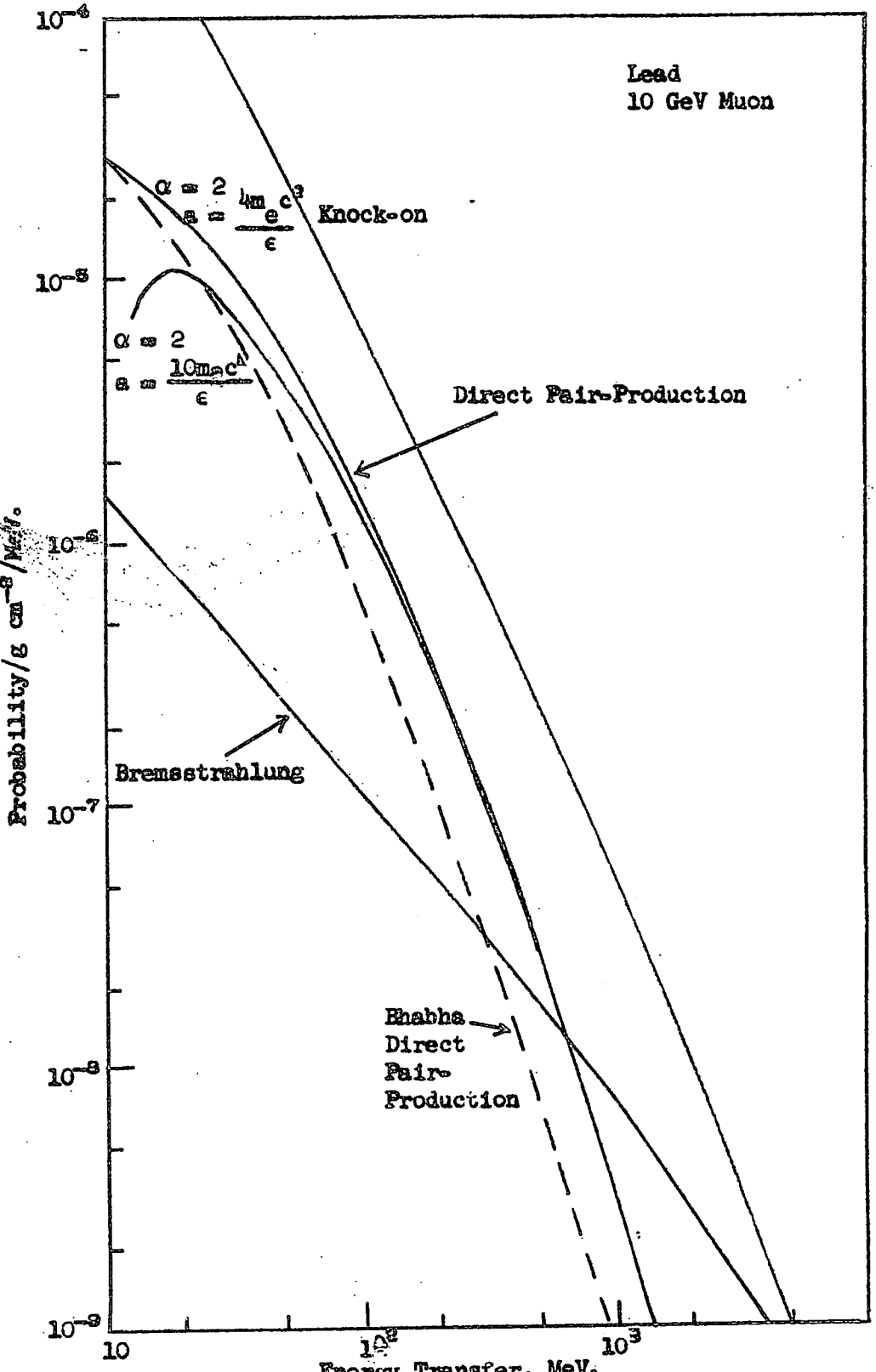

Differential Energy Transfer Curves for 10 GeV Muons in Lead.

Figure 2.5

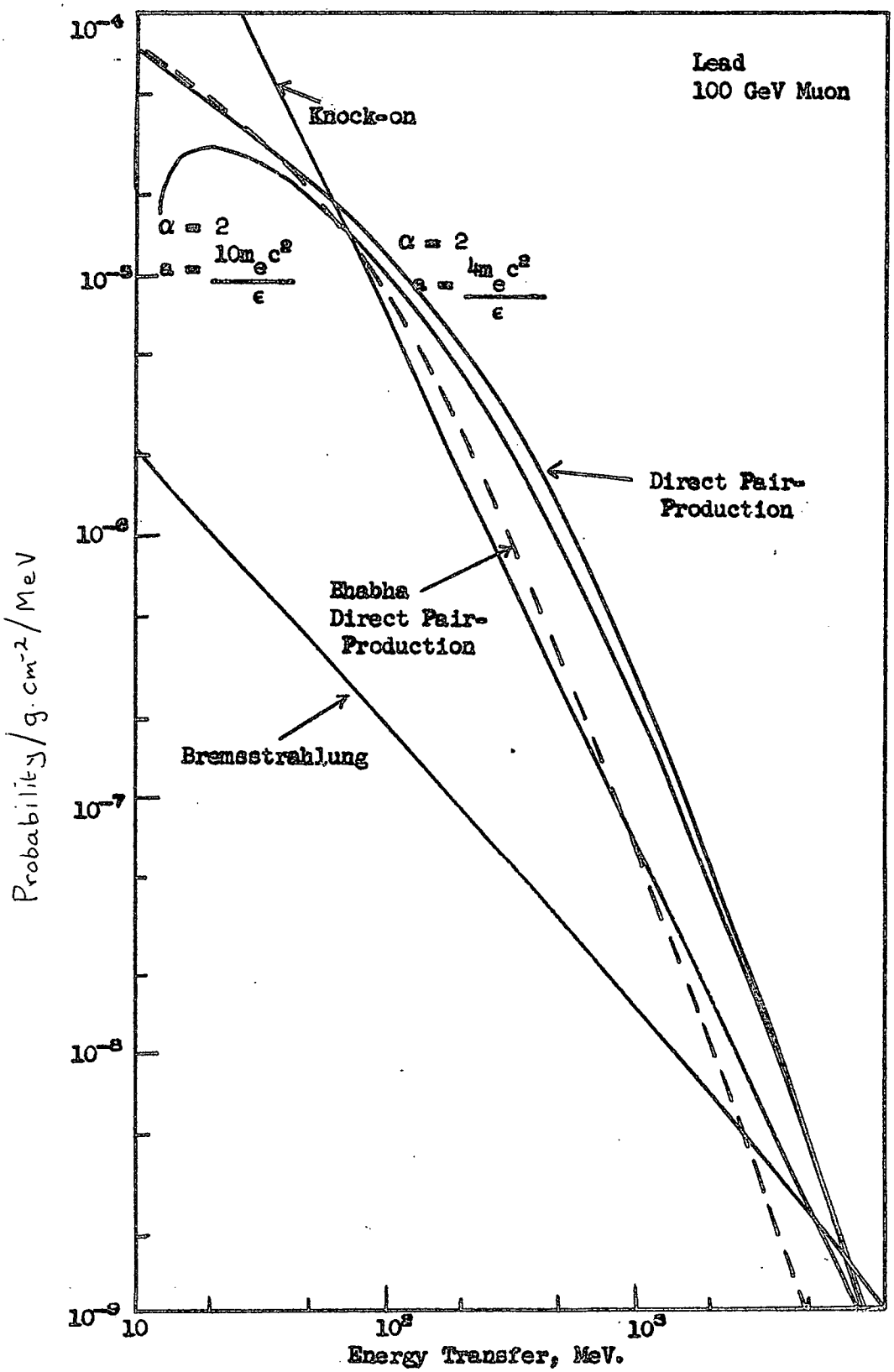

Differential Energy Transfer Curves for 100 GeV Muons in Le[6]d.

From these figures it is apparent that by a suitable choice of incident energy and absorber material one may investigate either direct pair production or the knock-on process over a large range of transferred energies with very little background due to the other two of the three electromagnetic interactions. It can also be seen that in order to study the Bremsstrahlung process one must go to very high incident energies and large energy transfers before knock-on and direct pair production events can be ignored.

2.6 Discussion

The theories of both the knock-on process and Bremsstrahlung were ~~calculated~~ derived on the basis of quantum electrodynamics and assume that the magnetic moment of the incident particle is normal. Thus any deviation from the theoretical values which might be obtained experimentally would be evidence for the breakdown of quantum electrodynamics or for the incident particle having an anomalous magnetic moment.

Whereas equations 2.1 and 2.2 lead to unique values for the cross-sections for the knock-on and Bremsstrahlung processes the direct pair production cross-section obtained from equation 2.9 contains the two indefinite parameters α and a and thus does not give a unique value for the cross-section. By a suitable choice of experimental technique, however, it is possible to ignore the effect of these parameters and obtain a direct comparison between theory and experiment. The following chapter is a review of past experimental

work on direct pair production, knock-on electron production and the Bremsstrahlung process.

CHAPTER 3

SURVEY OF PAST EXPERIMENTAL RESULTS

3.1 Introduction

Early investigations of the electromagnetic interactions of muons were carried out to determine the spin and magnetic moment of these particles. The results of work done before 1958 are contained in a review article by Fowler and Wolfendale (1958). These results showed that the measured cross-sections agreed with the theoretical predictions for energy transfers of up to 1 GeV in the case of the knock-on process and up to 100 GeV in the case of the bremsstrahlung process. From the results it was concluded that the muon has spin $\frac{1}{2}$ and an anomalous magnetic moment of less than 0.8 Bohr magnetons. It was also concluded that there is every reason to believe that, apart from its decay process, the muon is in all important respects simply a heavy electron.

For the past five or six years interest has centred on the investigation of the knock-on process for energy transfers of greater than 1 GeV in order to determine whether or not quantum electrodynamics is valid in this region. At the same time the direct production of electron-positron pairs has been studied in an attempt to check the theories which have been put forward for this process. The advantage of using muons in this work is that the background due to bremsstrahlung followed by the conversion of the photon into a pair is negligible (a factor of $\sim 10^4$ down on that found with incident electrons).

In the following paragraphs brief descriptions are given of some of the more recent experiments which have been carried out.

3.2 The Knock-on Process

3.2.1 Deery (1960)

Deery (see also Deery and Neddermeyer, 1961) used a cloud chamber to study the production of knock-on electrons with energies greater than 100 MeV by cosmic ray muons incident upon targets of carbon and paraffin.

The cloud chamber, which was divided into three sections one above the other, was placed in a magnetic field of 11,100 gauss. The target, consisting of 23.1 g cm^{-2} of carbon in one experiment and 17.0 g. cm^{-2} of paraffin in another, was placed above this chamber. The chamber was triggered whenever a coincidence occurred between two trays of geiger counters, one above the target and the second under 14 inches of lead below the cloud chamber, and a proportional counter, placed directly below the target, which was biassed at the level of $1\frac{1}{2}$ particles. In order to remove the electromagnetic component of the incident cosmic radiation a further 14 inches of lead was placed above the top geiger counter tray.

The momenta of the incident muon and the secondary electron were determined from the radius of curvature of the tracks in the magnetic field, the electron being identified by its catastrophic energy loss, or the production of a cascade shower, in $\frac{1}{2}$ inch lead plates at the bottom of the top section of the cloud chamber and between the centre and bottom sections.

Events were accepted in which the muon had an energy between 5 and 50 GeV and the secondary electron had energy greater than 100 MeV. Figure 3.1 shows a comparison between the theoretical curve, calculated using equation 2.1 and the Cornell vertical muon spectrum (Pine et al., 1959), and the experimental results obtained with the paraffin target, arbitrarily normalised to provide the best fit with the data in the energy range 0.3 to 0.9 GeV where uncertainty in the theory and corrections for efficiency were small. The upper and lower curves represent the limitations in normalisation possible within the uncertainty of an estimate of the absolute rate based on the Cornell spectrum.

Figure 3.2 shows the combined results for the carbon and paraffin targets, the results for carbon alone being very similar to those for paraffin. From this figure it can be seen that there is a discrepancy between theory and experiment for electron energies of greater than 1 GeV. Although this discrepancy is not statistically significant, as shown by the errors marked on the points, the experimental results are well fitted by a curve obtained by multiplying the theoretical values by a 'form factor' $F = 1 + |q^2| \lambda\!\!\!^{-2}_{\mu}$ where $|q^2|$ is the invariant of the four-momentum transfer in units of h and $\lambda\!\!\!^{-}_{\mu}$ is the Compton wavelength of the muon. This result gave the first indication of the possible breakdown of standard quantum electrodynamics at distances of the order of 10^{-13} cm.

Figure 3.1.

Integral knock-on energy spectrum

Paraffin Target

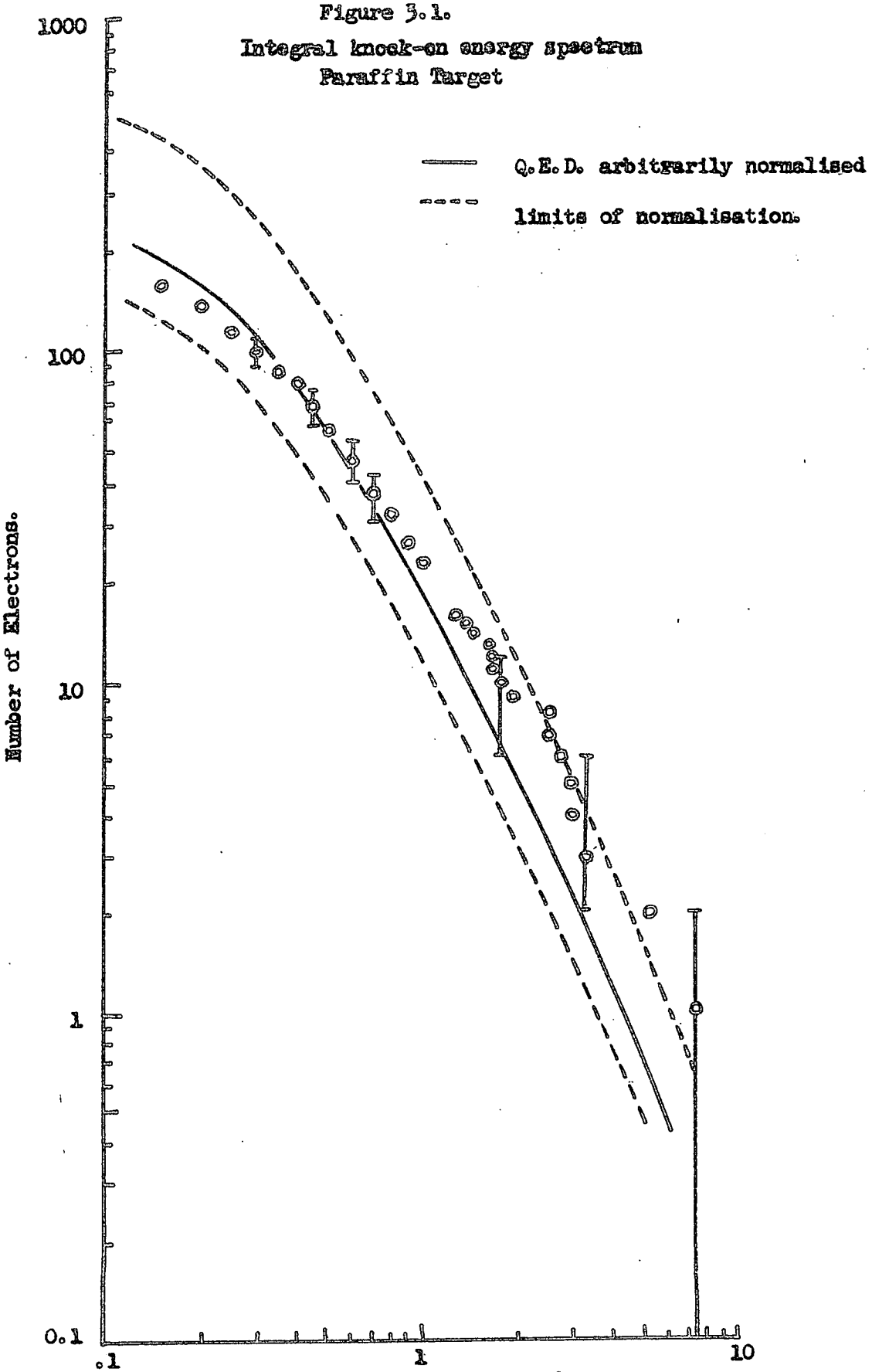

(from Deery, 1960).

Figure 3.2

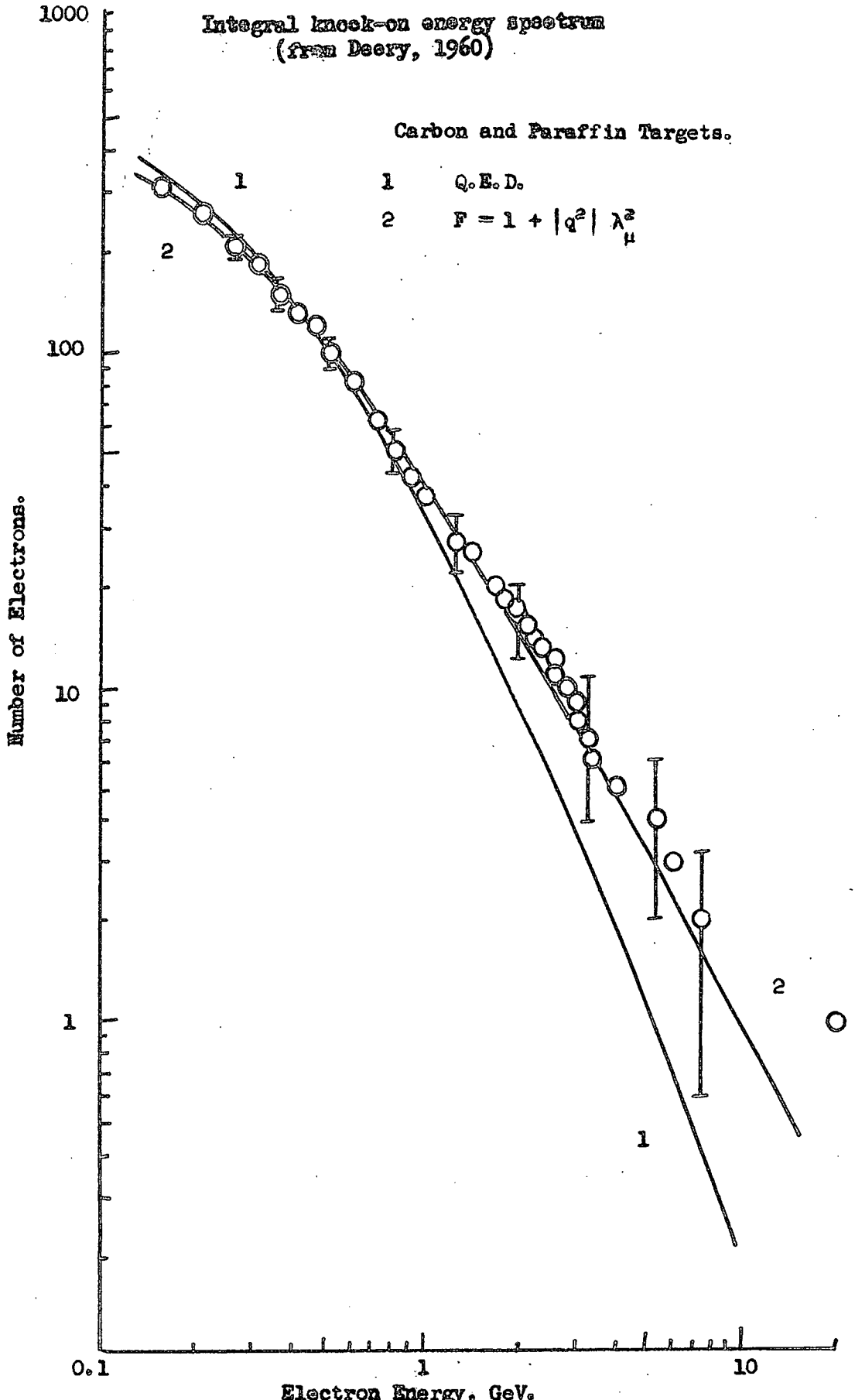
Integral knock-on energy spectrum
(from Deery, 1960)
Carbon and Paraffin Targets.
1 Q.E.D.
2 $F = 1 + |q^2| \lambda_\mu^2$
Number of Electrons.
1000
100
10
1
0.1
1
10
Electron Energy, GeV.

3.2.2 Stoker et al.

In 1961 Stoker et al. published the results of a cloud chamber investigation of the knock-on process. In this experiment they studied the knock-on electrons produced in lead plates of thickness 0.15 cm and 0.33 cm, contained in a multiplate cloud chamber, by muons in the energy ranges 450 to 1700 MeV and greater than 1700 MeV. Events were chosen in which a single electron accompanied the incident muon from one of the plates. The energies of the electrons were determined from a previously obtained empirical range-energy relationship when the electron did not interact. When the electron initiated a cascade shower its energy was estimated from the transition curves of Wilson (1951) which include multiple Coulomb scattering.

The energy spectrum of the knock-on electrons obtained in this experiment was compared with that calculated using equation 2.1 and the differential intensity spectrum of incident muons. In the incident energy range from 450 to 1700 MeV the spectrum used was that due to Rossi (1948), approximated by $(-0.0011E + 3.5)dE$. For energies above 1700 MeV the spectrum of incident muons was described by the power law $E^{-1.83}\,dE$ (Allkofer, 1960).

As a result of the comparison it was found that for the range of transferred energies from 1 to 1000 GeV there was good agreement between the theoretical and experimental results.

3.2.3 McDiarmid and Wilson

A third experiment on the production of high energy knock-on electrons was carried out by McDiarmid and Wilson (1962). These workers used a multiplate cloud chamber containing both lead and iron plates. Below the target plates were seven $\frac{1}{2}$" thick lead converter plates and at two positions in between these there was a plastic scintillation counter. Above the cloud chamber there were two trays of geiger counters separated by 30 inches of lead and with a further 5 inches of lead above the top tray. The chamber was triggered whenever a coincidence occurred between the top tray of geiger counters, one counter in the bottom tray and one of the scintillation counters, both of which were biassed to select ≥ 9 particles, i.e. cascade showers produced by incident muons were selected. The energy of the secondary particle was then determined from the total track length of the shower in the chamber, using a value of 30 MeV per radiation length for the average energy dissipated by an electron.

The energy spectrum of the cascade showers obtained was then compared with that predicted using the knock-on, bremsstrahlung and direct pair production theories and the differential muon energy spectrum.

The result of this comparison for the case of the iron target is given in figure 3.3. Although it is not possible to say which type of interaction has occurred it can be seen from the graph that either the knock-on or the bremsstrahlung process is dominant. From the figure it can be seen that there is reasonable agreement between

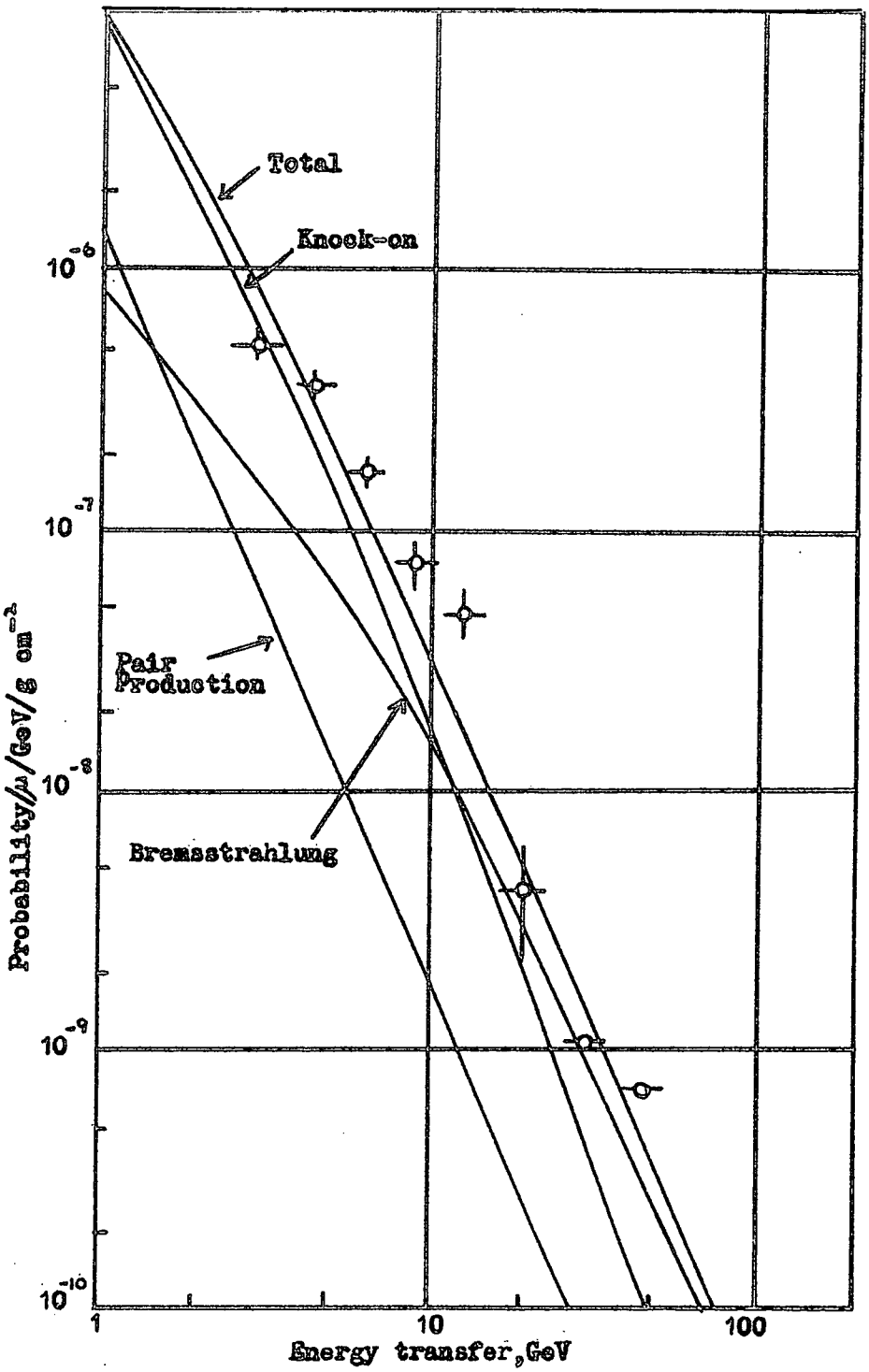

Figure 3.3 Differential energy transfer spectrum (from McDiarmid and Wilson, 1962)

experiment and theory for energy transfers up to 7 GeV but that over the remainder of the range in which the knock-on process is dominant there is an excess of experimental events. A similar discrepancy occurs for the case of the lead target. A possible explanation of the discrepancy is the fact that there may be systematic errors in the estimates of the shower energies. The results however do lend some support to those obtained by Deery (1960).

3.2.4 Backenstoss et al.

The most recent investigation of the knock-on process is that of Backenstoss et al. (1963b) who caused 8 GeV muons from the C.E.R.N. proton synchrotron to hit a total absorbtion spectrometer made up of twenty 1 cm thick sheets of iron interleaved with 1 cm sheets of plastic scintillator. The pulses from these scintillation counters were added to give a single pulse which was proportional to the total particle track length in the apparatus. Before the experiment was carried out the apparatus was calibrated using incident electrons of known energy (Backenstoss, et al. 1963a) and so the experimental pulse height distribution could be easily converted to an energy spectrum for the knock-on electrons.

The results of this experiment showed that for knock-on electron energies from 1 GeV to 3.4 GeV, the maximum transferrable energy, there was no deviation from the predictions of quantum electrodynamics within the experimental error of $\pm 5\%$. It is thus concluded that any small deviation from quantum electrodynamics must occur at distances of approach $\leq 0.64.10^{-13}$ cm.

3.3 Bremsstrahlung

As was mentioned in §3.1, investigation of bremsstrahlung production by muons which were carried out previous to 1958 showed good agreement between the measured and the predicted results.

A more recent study of the bremsstrahlung process was that of McDiarmid and Wilson (1962) who found that their results, although statistically rather weak, were in good agreement with the theoretical calculations for both the iron and lead targets (see §3.2). Their results for the iron target are shown in Figure 3.3.

Other recent measurements which have included effects due to bremsstrahlung i.e. those due to Backenstoss et al. (1963b) and Chaudhuri and Sinha, (1964), also gave good agreement with theory in the energy ranges where bremsstrahlung was important, so it can be concluded that there is no evidence up to now for any deviation from bremsstrahlung theory for energy transfers of up to 100 GeV.

3.4 Direct Pair Production

3.4.1 Introduction

By far the majority of recent work carried out to study the electromagnetic interactions of muons has been aimed at the determination of the cross-section for the direct production of electron-positron pairs in order to check the theory of this interaction.

One of the earliest experiments was that due to Avan and Avan (1957) who exposed nuclear emulsions at various depths underground. From a total of 61 direct pairs they obtained results which were in close agreement with those predicted by the formula of Block et al. (1954).

Since that experiment the results of measurements have been compared with the theoretical treatment of Murota et al. (1956).

3.4.2 Roe and Ozaki

The first of the post 1958 experiments was that due to Roe and Ozaki (1959) who used a multiplate cloud chamber containing nine 1.06 radiation lengths thick typemetal plates (essentially lead) below the Cornell magnetic spectrograph. The cloud chamber was expanded whenever a muon of energy greater than 8 GeV, as determined by trays of geiger counters in the spectrograph, traversed it. In order to remove the electromagnetic and strongly interacting components of the incident cosmic radiation a 1.5 inch thick lead block was placed directly above the cloud chamber.

Out of 6,046 cloud chamber photographs 451 contained showers initiated by single incoming particles. Of these only 98 were finally used in the analysis as for the others either the flash-tube trays used in the determination of the momentum of the incident particles did not function correctly or the energy transfers were so low that the data were difficult to interpret.

In order to determine the energies of the secondary particles from the cascade showers produced in the plates of the cloud chamber extrapolations were made of Wilson's Monte Carlo results (Wilson, 1950) to obtain theoretical shower curves for the energy region from 200 MeV to greater than 1 GeV. By using these shower curves, and assuming that the knock-on and Bremsstrahlung cross-sections were in agreement with theory, it was found that the ratio of the experimental direct pair

production cross-section to the theoretical value, calculated from the formula of Murota et al. with $\alpha = 2$ (Equation 2.9), was

$f = 0.48 \pm 0.11$ by one method of analysis

$f = 0.63 \pm 0.17$ by a second method.

3.4.3 Gaebler et al.

Following the work of Roe and Ozaki, Gaebler et al. (1961) used a multiplate cloud chamber at a depth of 1,032 ft underground to study the direct pair production interactions. This cloud chamber, which contained twelve $\frac{1}{8}$" lead plates, was triggered on vertical muons by means of a coincidence arrangement between trays of geiger counters above and below it and the pictures obtained were then scanned for cascade showers produced by energetic particles traversing the chamber. In this way 222 usable events were obtained.

The energies of the cascade showers were determined by comparing the showers with those obtained using a Monte Carlo method (Wilson, 1952). The energy spectrum of these showers was then compared with that calculated using equations 2.1 and 2.2 for the knock-on process and bremsstrahlung, equation 2.9 with $\alpha = 2$ and $a = 3m_e c^2/\epsilon$ for direct pair production and folding in a muon energy spectrum obtained from the results of Barrett, et al. (1952).

In order to differentiate between showers produced by knock-on electrons and those produced by direct pairs they took showers with only one electron accompanying the muon from the plate in which the interaction took place to be knock-on events and all others as being due to direct pair production (for the incident muon spectrum considered

bremsstrahlung was negligible for energy transfers up to 5 GeV). When these results, corrected for the cases in which a direct pair lost one electron in the first plate or a knock-on electron gave rise to two or more electrons leaving the first plate, were compared with the theoretical predictions it was found that the events which were taken as being knock-ons gave good agreement with theory while the pair production events agreed with the theoretical results up to 1 GeV when a cross-section of exactly half that given by equation 2.9 was used (see figure 3.4). Above 1 GeV the experimental points tended to lie above the theoretical curve and it was thought that this might have been due to a breakdown in quantum electrodynamics.

This experiment has since been repeated by Kearney (1962) who has obtained results which are in good agreement with those of Gaebler et al. up to 1 GeV but do not show any excess of experimental results above this energy.

3.4.4 Stoker et al.

In 1963 Stoker et al. carried out an experiment similar to those mentioned above using a multiplate cloud chamber containing four 0.15 cm thick lead plates as the target and a further five 0.33 cm thick lead plates which were used to estimate the energy of the produced pairs from the path lengths of the electrons or from the cascade showers produced by these electrons. This cloud chamber was triggered on vertical cosmic ray muons with energies greater than 1700 MeV using a three-fold geiger counter telescope with 1354 g cm^{-2} of lead between

Figure 3.4.

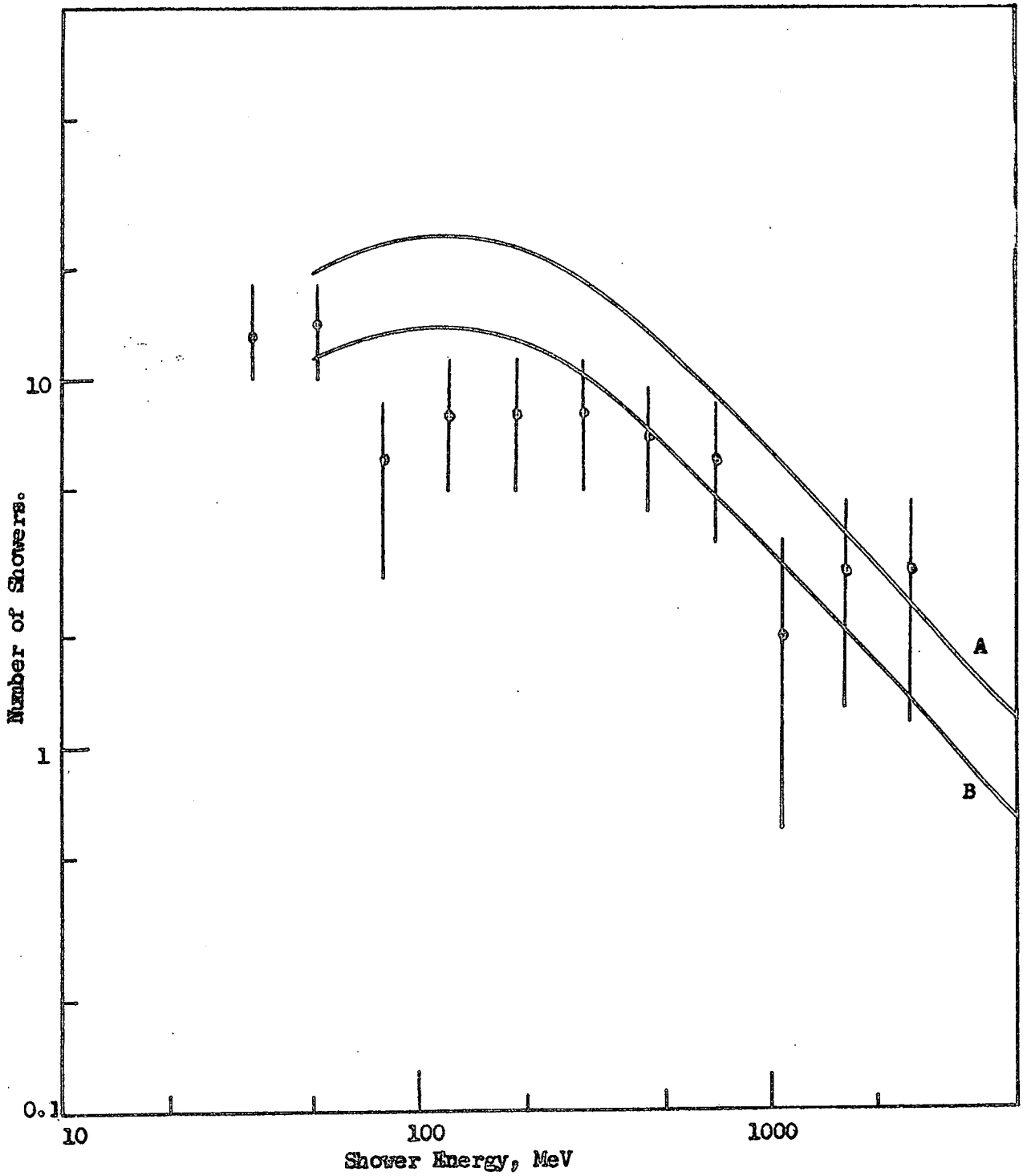

Number of showers with two or more tracks below the first plate vs. shower energy. Curve A was calculated from knock-on and pair production theories. Curve B assumes the number of direct pairs is $\frac{1}{2}$ that predicted. (Gaebler et al., 1961).

the bottom of the cloud chamber and the lowest geiger counter tray. From 12,082 traversals of the cloud chamber by muons of energy greater than 1700 MeV they obtained 274 usable events.

When the secondary particles from the interactions produced a cascade shower the energy of this shower was estimated using a semi-empirical formula due to Roe and Ozaki (1959). If this formula gave an energy of greater than 400 MeV then the shower energy was re-estimated by measuring thetotal track length, $T = \Sigma nt$ where n is the mean number of electrons entering and leaving a plate of thickness t radiation lengths, and then putting the energy $E_o = KT$ where $K = 29 \pm 3$ MeV per radiation length. In the cases where the secondary electrons did not produce cascade showers their energies were originally estimated from the multiple scattering which took place. The mean energies estimated in this way were found to fit on the absorbtion curve found by Wilson (1951), including the scattering correction, and thus the final estimates of the electron energies were determined from this curve.

As a check on the energy estimates for the electrons the knock-on energy spectrum was obtained from the 250 events in which only a single electron accompanied the muon from the target plate in which the interaction took place. When this spectrum was compared with that calculated using equation 2.1 and the Durham vertical muon spectrum (Brooke et al., 1962) it was found that there was good agreement between theory and experiment. It was thus concluded that the methods of estimating electron energies were correct.

The results obtained from the 24 pair production events are shown in Table 3.1 in which the observed number of events in a given energy range are compared with the predicted number calculated using the Durham vertical muon spectrum and a simplified version of the Murota et al. formula as given by Stoker and Haarhoff (1960). In this it is assumed that the energy of the produced pair is very much less than that of the incident muon and that each electron has a minimum energy of 10 $m_e c^2$ where $m_e c^2$ is the rest energy of the electron, with $\alpha = 1$, 2 and 3.

TABLE 3.1

Energy transfer (MeV)	Theoretical predictions $\alpha = 1$	$\alpha = 2$	$\alpha = 3$	Observed Numbers
25-60	9.5	13.1	16.4	13
60-150	5.7	7.6	8.4	6
150-350	2.2	2.8	3.1	3
350-800	0.81	0.95	1.15	2
800-2000	0.27	0.34	0.39	0
2000-10000	0.11	0.13	0.15	0

When a χ^2 test was carried out for the agreement between the experimental and theoretical numbers for $\alpha = 1,2$ and 3 the values obtained for $P(\chi^2)$ were 55%, 89% and 70% respectively when all events were considered and 66%, 76% and 71% when the transferred energy range from 25 to 60 MeV was neglected because of possible uncertainties in the energy estimations.

From this experiment it was concluded that the results were consistent with the theory for direct pair production obtained by a re-evaluation of the Murota, Ueda and Tanaka theory and that the best correspondance between theory and experiment was obtained for the indefinite constant $\alpha = 2$.

3.4.5 Chaudhuri and Sinha

The most recent investigation of the direct pair production process was that carried out by Chaudhuri and Sinha (1964) who used a multiplate cloud chamber containing, in one case, twelve 1.6 cm thick iron plates and one 1.25 cm thick lead plate, and in the second case nine 0.54 cm thick iron plates and one 1.25 cm thick lead plate. The chamber was triggered on vertical cosmic ray muons using a coincidence arrangement between four geiger counter trays above the cloud chamber in the first case and between three geiger counter trays, two above the cloud chamber and one under 5 cm of lead below the cloud chamber, in the second case.

Those events were chosen in which a single penetrating particle passed right through the chamber and in which this particle was accompanied by two or more electrons when it left one of the iron target plates. The energy transfer in the interaction was then estimated as follows:-

1) For energy transfers between 40 MeV and 1 GeV the energy was determined using the relationship found by Hazen (1955) for cascade showers in copper, i.e.

$$E_o = \frac{36}{20} \frac{E_c t}{\cos\theta} N$$

where E_o is the shower energy

E_c is the critical energy of the material

$\cos\theta$ is the inclination of the shower axis to the vertical

t is the thickness of material traversed, and

N is the total number of tracks seen in each gap.

2) For energy transfers greater than 1 GeV conventional shower theory as given by Bhabha and Chakrabarty (1948) was used.

3) Where the energy of the pair was less than 40 MeV the results of Wilson's Monte Carlo calculations (Wilson, 1951) were used.

The values of the cross-sections obtained from 13519 traversals of the 0.54 cm thick iron plates and 43623 traversals of the 1.6 cm thick iron plates are given in table 3.2 where they are compared with the values predicted by equation 2.9 with $\alpha = 2$ and $a = 3\, m_e c^2/\epsilon$, using an incident muon spectrum given by

$$N(E)dE = \frac{2.12.10^2}{(E + 32.6)^3} dE,$$

where E is in GeV and the mean energy of the muons was 32.6 GeV. In obtaining the measured cross-sections the experimental results were corrected for events in which an electron from the pair was absorbed in the target plate.

TABLE 3.2

Energy Range in MeV	Values of the cross section in barns/nucleus from set A and set B experiments		Theoretical values of cross section in barns/nucleus
	A (target thickness = 1.6 cm)	B(target thickness = 0.54 cm)	
35-100	0.0433 ± 0.0027	0.0377 ± 0.0074	0.0415
100-500	0.0195 ± 0.0018	0.0203 ± 0.0051	0.0196
500-1000	0.0015 ± 0.0005	0.0029 ± 0.002	0.0016

Experimental values of the cross-section for the direct pair production process at three energies (N.B. in the interval 500-1000 MeV the cross-sections given contain almost equal contributions from bremsstrahlung and direct pair production. The bremsstrahlung contribution was calculated from equation 2.2).

The conclusion drawn from this experiment was that in the range of transferred energies from 35-1000 MeV the results are satisfactorily explained by the theory of Murota et al.

3.5 Discussion

From the results quoted in the preceding paragraphs it can be seen that, except in the case of bremsstrahlung, there is conflicting evidence as regards the electromagnetic interactions of muons in which there are large energy transfers. In the case of the production of knock-on electrons the two most important experiments, those due to Deery (1960) and Backenstoss et al. (1963) are in complete disagreement, with Deery finding an excess of events at energy transfers of greater than 1 GeV

while Backenstoss et al. find complete agreement with theory. Of the two experiments that are due to Backenstoss et al. is more accurate, the quoted error being ±5%, and so it is probable that Deery's result is due to a statistical fluctuation. The other experimental results in the energy transfer region above 1 GeV are statistically so poor that it is not possible to take any excess of experimental results asbeing evidence in support of Deery's result.

As in the case of the knock-on process the experimental results for direct pair production are in conflict with each other. While Roe and Ozaki (1959) and Gaebler et al. (1961) find cross-sections which are a factor of 2 down on the predicted values, Chaudhuri and Sinha obtain good agreement between theory and experiment. (As Stoker et al. (1963) compared their experimental results with a modified version of the pair production theory the fact that they got good agreement between theory and experiment cannot be taken as evidence either for or against the unmodified theory). It is possible that the conflicting results are due to a difference in calculating the theoretical values since both Roe and Ozaki and Gaebler et al. used values for the theoretical direct pair production cross-section evaluated by Roe (1959) while Chaudhuri and Sinha (1964) did a separate calculation of the results.

In conclusion it is clear that much work remains to be done before the knock-on and direct pair production interactions can be said to be fully understood.

CHAPTER 4

THE DURHAM EXPERIMENT

ELECTROMAGNETIC INTERACTIONS OF MUONS IN IRON

4.1 Introduction

The electromagnetic interactions of muons in iron were investigated at Durham by selecting vertical cosmic ray muons which interacted in an iron target. The electrons or photons which were produced in these interactions then initiated cascade showers in a further amount of iron placed below the target. The energy of these secondary particles was estimated by comparing the cascade showers produced with experimental results for the development of such showers in iron.

In the experiment the vertical muons were selected by coincidences between two trays of geiger counters and events in which the muon interacted were selected by a further coincidence between the geiger counters and a scintillation counter.

The experiment was done in two parts. In the first the target consisted of two iron plates giving a total thickness of 22.04 g cm^{-2} of iron, see Figures 4.1 and 4.2, and the converter was made up of eight plates giving a total of 81.53 g cm^{-2} (5.91 radiation lengths) of iron in which the cascade shower could develop. In the second case the target was again made up of 22.04 g cm^{-2} of iron but the converter was increased in thickness by putting a further 2.545 radiation lengths of iron in place of one of the detecting levels, giving a total of 8.455 radiation lengths of iron for the converter.

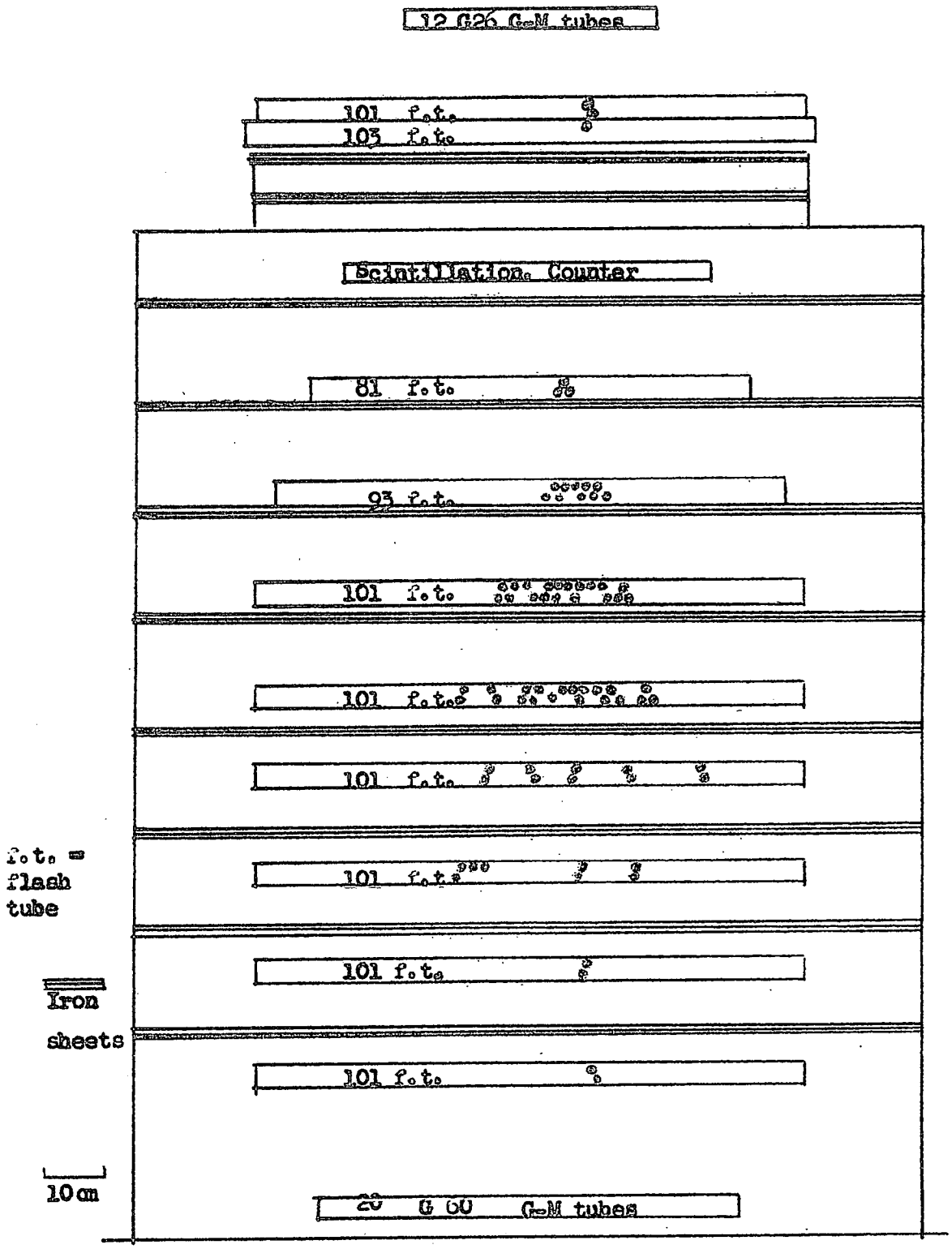

Figure 4.1. Face View of Durham Apparatus showing a typical cascade shower.

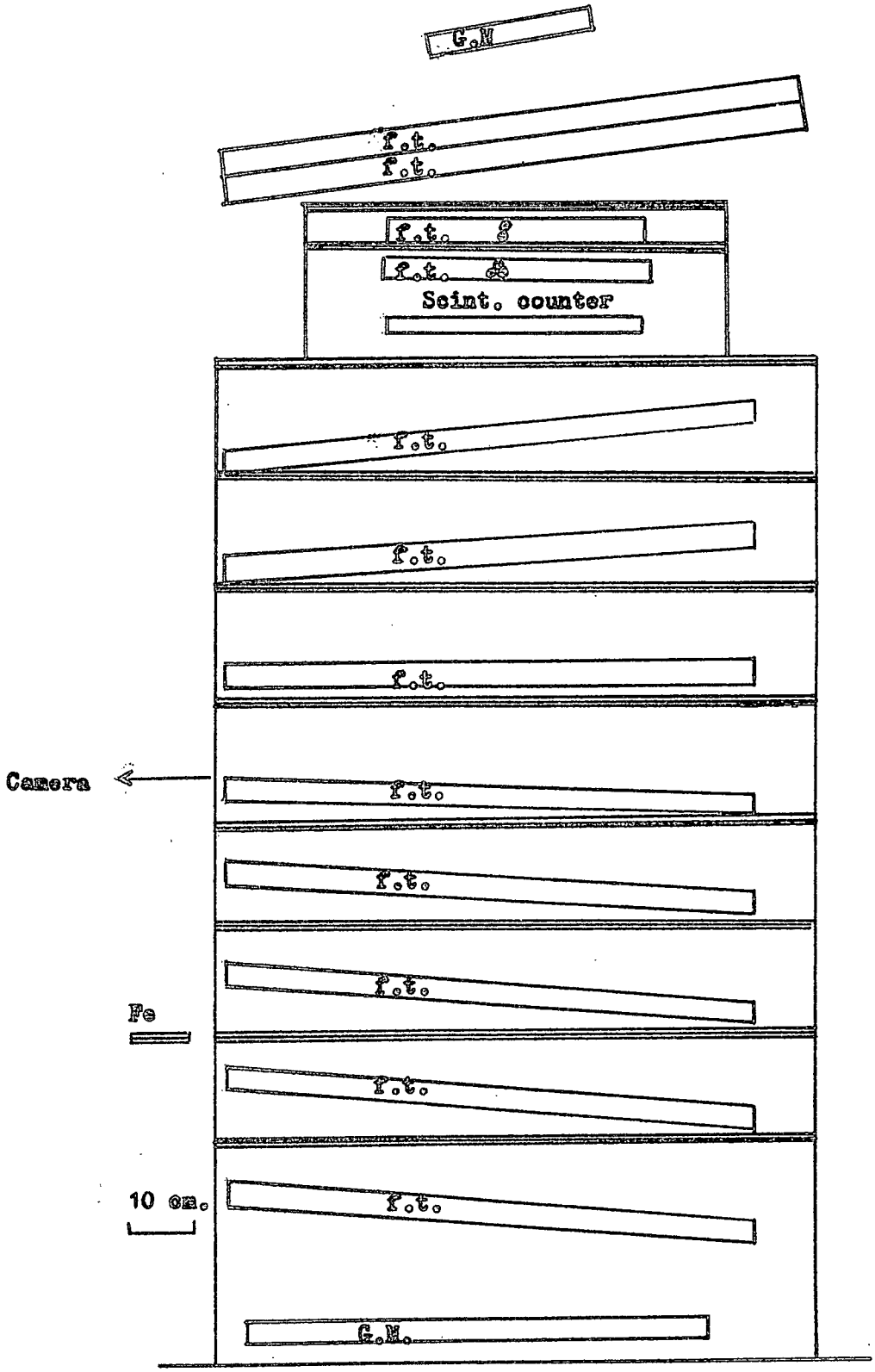

Figure 4.2 Side view of the Durham Apparatus.

In both parts of the experiment the incident muon and the shower electrons were detected visually using trays of neon flash tubes placed above the target and in between the iron plates.

4.2 The Selection System

4.2.1 The Geiger Counters

The two trays of geiger counters, one above the target and the other below the converter, see figures 4.1 and 4.2, were 192 cm apart and selected penetrating particles which traversed the apparatus at a small angle to the vertical ($16^{\circ}16'$ in one plane and $13^{\circ}12'$ in the other). The top tray consisted of twelve, 26 cm long counters (20th Century, G26) and the bottom tray of twenty, 60 cm long counters (20th Century, G60). The counters in the top tray were connected together in three groups of four counters each and those in the bottom tray were connected together in four groups of five. Each group of counters was connected to a single electronic quenching unit which reduced the dead time of the counters in the group.

The outputs from the quenching units in the top tray were mixed and fed into a two-fold Rossi coincidence circuit. Similarly the output pulses from the bottom tray were mixed and fed into the coincidence circuit. An output pulse was then obtained from this circuit whenever a coincidence was obtained between the pulses from the two geiger counter trays.

4.2.2 The Scintillation Counter

The scintillation counter, which was situated between the target and the converter, see figures 4.1 and 4.2, consisted of a rectangular slab of plastic scintillator, Nel02A (Nuclear Enterprises (G.B.) Ltd., Edinburgh) of area 24 x 15 inches^2 and thickness 1 inch. This had been coated, by Nuclear Enterprises (G.B.) Ltd., with a special white paint (Nuclear Enterprises type Ne560) on all except the two smallest faces. In optical contact with each of these two faces was a perspex light guide through which the counter was viewed by a single photomultiplier tube (Philips type AVP53). The whole of the scintillation counter was enclosed in thin aluminium foil to make it light tight while putting the minimum amount of absorbing material in the path of particles passing through the counter.

The output pulses from each of the photomultiplier tubes were fed, by way of head amplifiers with a gain of unity, to a linear adding circuit. The output pulses from this adding circuit were then attenuated before being fed into an amplifier with a gain of 10^4 (Dynatron type 1430A) from which they went into a discriminator (Dynatron type N101). The output pulses from this discriminator were then delayed for 2.5 μs before being taken into a second Rossi coincidence circuit. Pulses from the geiger counter coincidence circuit were also fed into this second coincidence circuit and an output pulse was obtained whenever a coincidence occurred between the delayed scintillation counter pulse and the two-fold geiger counter pulse.

4.2.3 Calibration of the Scintillation Counter

The scintillation counter was calibrated in its experimental position by feeding the output pulses from the adding circuit into a 100 channel pulse height analyser (Marshall, type H.S. 100) which was gated on the output pulses from the geiger counter coincidence circuit. In this way the differential pulse height distribution for single particles traversing the counter was obtained. Since the scintillation counter was below the target of 22.04 g cm^{-2} of iron some of the counts obtained in this single particle distribution were due to pairs of particles e.g. the muon plus a knock-on electron which had been produced in the target. In order to correct the distribution for this effect the pulse height distribution for pairs of particles was calculated from that for single particles. The two particle distribution was then normalised to be 5% of the single particle distribution and subtracted from this to obtain a good estimate of the true single particle distribution (5% being the value given by Lloyd and Wolfendale (1959) for the percentage of muons leaving a block of absorber accompanied by knock-on electrons). From this new distribution the final distribution for pairs of particles was calculated as before. This latter distribution did not differ noticeably from that obtained initially.

Finally curves were drawn of the percentage of events in the single and two particle distributions which gave pulses which would be registered by the pulse height analyser as being larger than those required to count in a certain channel as a function of channel number,

(Figure 4.3). These curves give the efficiencies for the detection of single particles and pairs of particles as a function of channel number.

Immediately after the pulse height distribution for single particles had been obtained the pulses from the adding circuit were fed into the pulse height analyser without the gate and thus the total counting rate of the scintillation counter was obtained. A curve, corrected for the dead time of the P.H.A., was then plotted of the counting rate of pulses which would give a count in a channel higher than a chosen one as a function of the chosen channel number (the integral counting rate), figure 4.3.

From figure 4.3 it can be seen that by measuring the counting rate of the scintillation counter with a given discriminator bias it is possible to determine the efficiency of the counter for the detection of single particles and of pairs of particles.

4.2.4 The Anticoincidence Tray

In order to reject some of the events in which a shower of particles was incident upon the apparatus a tray of eight 60 cm long geiger counters was placed one metreaway from the tray of 26 cm long counters. These counters were connected in pairs, each pair having its own quenching unit. The output pulses from the four quenching units were mixed and then fed into an anticoincidence circuit together with the output pulse from the second Rossi coincidence circuit. This anticoincidence circuit only transmitted the pulse from the second Rossi coincidence circuit when there was no coincident pulse from the anticoincidence tray of geiger counters.

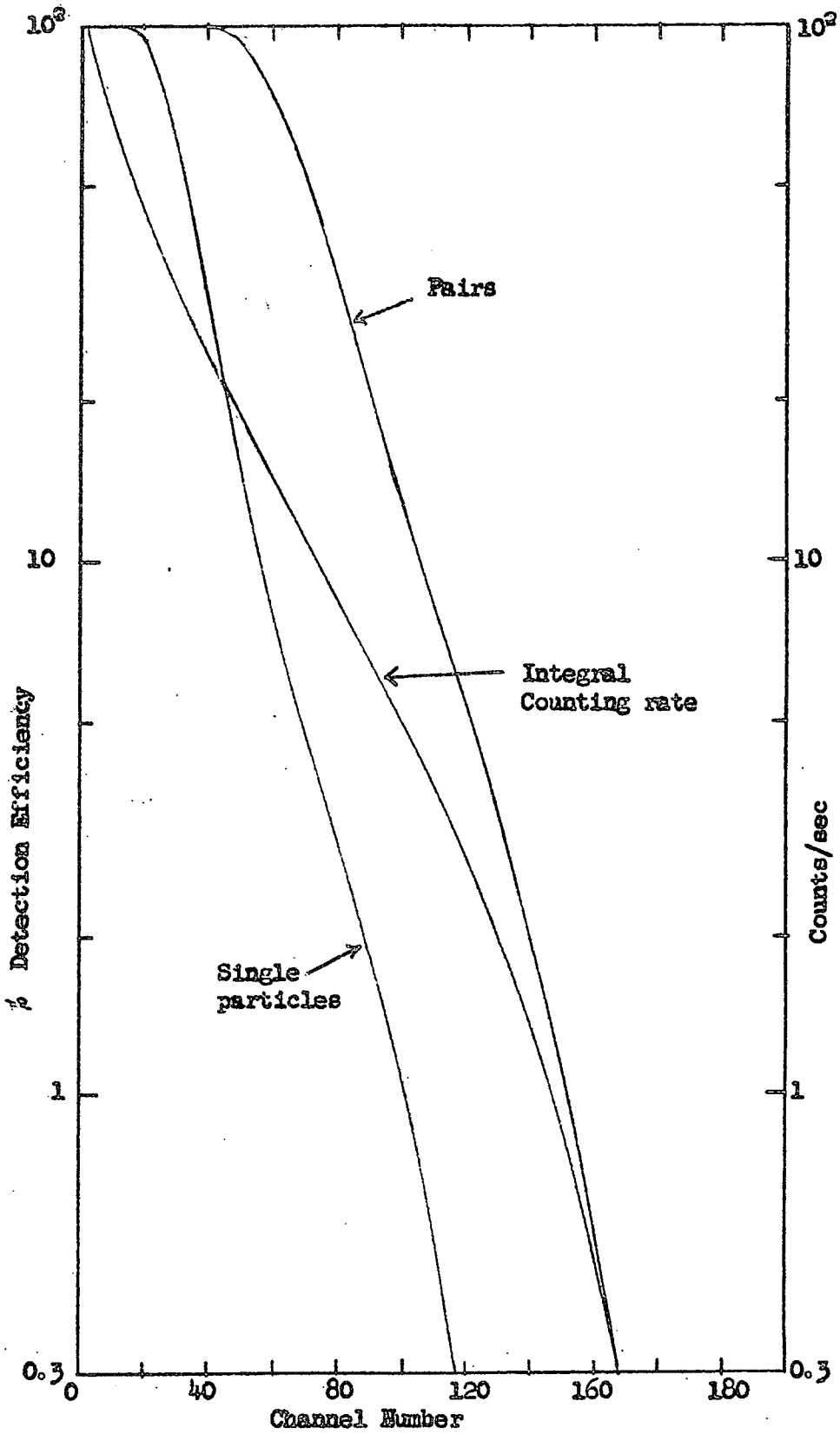

Figure 4.3. Calibration curves for scintillation counter.

4.2.5 Summary of Selection Criteria

For an event to be selected there had to be a coincidence between the geiger counter trays above and below the apparatus and the scintillation counter, and no coincidence between these counters and the anticoincidence tray.

4.3 The Flash Tube Trays

The neon flash tube, originally developed by Conversi et al. (1955), consists of a glass tube filled with neon. When a high voltage pulse is applied across the tube a short time after the passage of an ionising particle the gas in the tube glows sufficiently brightly to be photographed. In order to prevent the photoionisation of adjacent tubes by the discharge, which would cause these tubes to glow spuriously, the tubes are painted black over the whole of their surfaces apart from a plane window at one end through which the discharge is viewed.

The flash tubes used in this experiment were of the type developed by Coxell (Ph.D. thesis - 1961) for the investigation of Extensive Air Showers. These tubes have an internal diameter of 1.5 cm, external diameter 1.8 cm, and are greater than 80 cm long. They are filled with Commercial Neon (98% Ne, 2% He, <200 v.p.m. A, O_2 and N_2) to a pressure of 60 cm Hg and have a sensitive time (the time between the passage of the particle and the application of the high voltage pulse in which the efficiency drops to 60%) of 120 μs with no applied d.c. clearing field.

Each of the twelve trays of flash tubes used in the experiment consisted of two layers of tubes placed one on top of the other, see Fig. 4.4. The bottom layer of tubes rested upon a sheet of thin aluminium which acted as one electrode and the second electrode, also a sheet of thin aluminium, was placed on top of the upper layer.

Since the sensitive region of a flash tube is dependent upon the length of the tube covered by the smaller of the two electrodes the top electrode of each tray was made 80 cm long. Thus the sensitive area of any one layer of tubes is given by N x 1.5 x 80 cm^2, where N is the number of flash tubes in the layer.

Of the twelve flash tube trays ten were placed with the axes of the tubes parallel to the axes of the geiger counters while the tubes in the other two, namely those between the target plates and above the scintillation counter, had their axes perpendicular to the axes of the geiger counters. These latter two trays were used to give an indication as to whether a shower might have left the front or back of the apparatus.

Since the light output from flash tubes is highly collimated along the axis of the tube, see Coxell et al. (1961), the flash tube trays were tilted in such a way that the camera used to record the events looked along the axes of the tubes, Fig. 4.2.

The high voltage pulse for the flash tubes was obtained by triggering a small hydrogen thyratron, CV797, with the output pulse from the anticoincidence circuit. The output pulse from this thyratron was then applied, through a Ferrox cube pulse transformer, to the grid

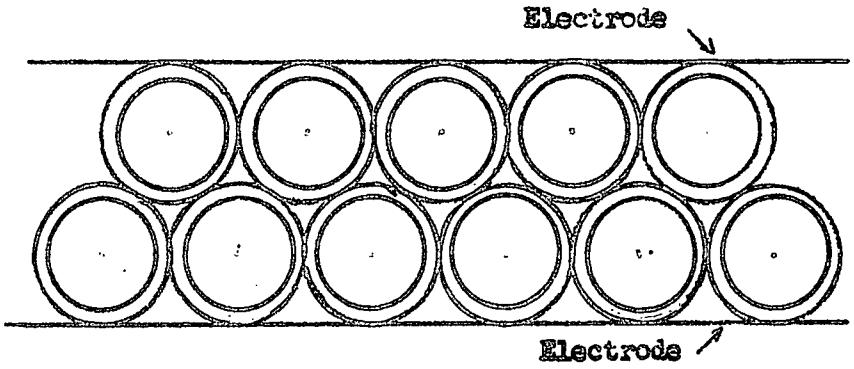

The Flash tube tray

Fig. 4.4

of a large hydrogen thyratron, XH8-100, which in turn was used to trigger a trigatron, CV85 (see Fig. 4.5). The output pulse from the trigatron was then applied, by way of a pulse transformer and resistance chain, across the electrodes of each of the flash tube trays. The values of the trigatron anode voltage and the tapping on the resistance chain for maximum tray efficiency, with the minimum of spurious flashes, were determined emperically and are shown in Fig. 4.5.

4.4 The Recording System

The selected events were recorded photographically on Ilford HPS film using a camera with an f/1.9 lens situated at a distance of 14 feet from the front of the apparatus. This camera viewed the ten main trays directly and the two trays at right angles to these through a mirror which was inclined so that the camera looked along the axes of the tubes. Since it was not practicable to open a camera shutter in the time, 5 μs, between the selection of an event and the application of the high voltage pulse, the laboratory in which the apparatus was situated was blacked out and the camera operated without a shutter.

As well as recording the tubes which flashed the camera also recorded the positions of three fiducial lamps and the time at which the event occurred.

When an event was selected the high voltage pulse was applied to the flash tube trays and then the Rossi coincidence circuit was paralysed for three seconds while the fiducial lamps and clock were illuminated and the camera was wound on.

A schematic diagram of the experimental arrangement is shown in Fig. 4.6.

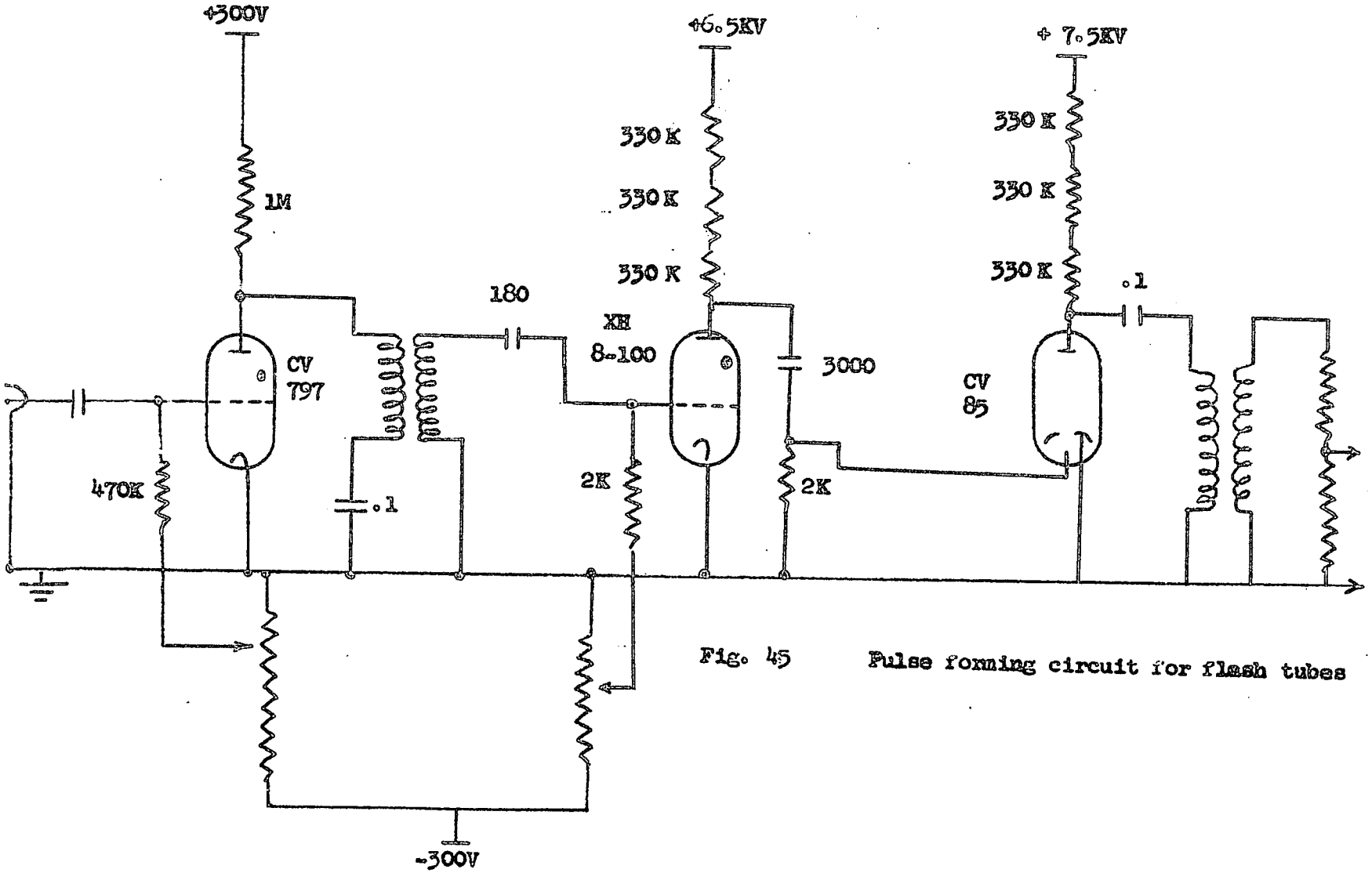

Fig. 45 Pulse forming circuit for flash tubes

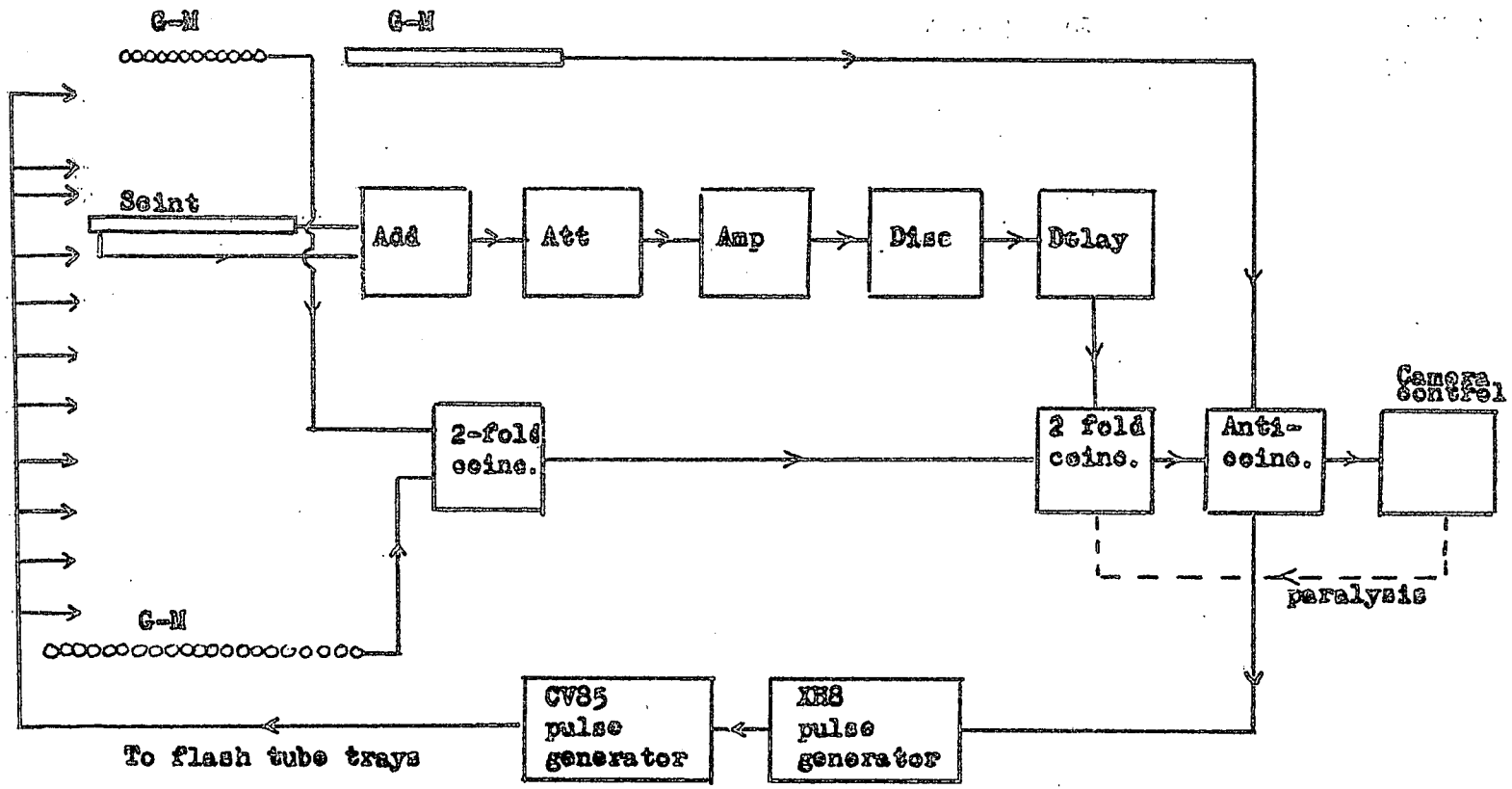

Figure 4.6 Schematic Diagram of Durham Apparatus.

4.5 Running Time

The apparatus was run during the period June 10th, 1964 to July 30th, 1964, in which time a total of 54 hours 39 mins. of film was obtained. Of this 33 hours 4 minutes were obtained with the apparatus as shown in figures 3.1 and 3.2 and the remaining 21 hours 35 minutes were obtained with the eighth flash tube tray replaced by 2.545 radiation lengths of iron. In what follows the initial run will be known as experiment A and the second run as experiment B.

CHAPTER 5

THE ANALYSIS OF THE DURHAM DATA

5.1 Introduction

In order to estimate the energies of the secondary particles produced in interactions which took place in the iron target, the cascade showers produced in the converter plates were compared with a set of standard shower curves. The following paragraphs contain a description of the standard curves and details of the methods used in comparing the showers obtained experimentally with these.

5.2 The Standard Shower Curves

The choice of the standard shower curves was made on the basis of the following requirements:

i) The material in which the shower developed must have been either iron or some material with values of the radiation length and critical energy similar to those of iron.

ii) The cut-off energy of the shower electrons i.e. the minimum energy at which the electrons are considered as contributing to the measured, or predicted, shower, must have been of the order of 1 MeV or less. This requirement was necessary since in the Durham experiment electrons required very little energy to cross the gaps between the converter plates and be detected by the flash tubes.

After studying the theoretical results due to Butcher and Messel (1960) and Crawford and Messel (1962), and the experimental results of Backenstoss et al. (1963a) it was decided that the last

were most amenable to use in the present analysis. These results, which were obtained using a total absorption spectrometer, consisting of twenty sheets of 1 cm thick plastic scintillator interleaved with iron plates, in an electron beam from the C.E.R.N. proton synchrotron, are shown in the form of average shower curves in figure 5.1. Since all electrons were included in these curves which had sufficient energy to traverse one of the scintillator sheets (~2 MeV) these results fulfil the second of the two requirements stated above. The first requirement is fulfilled by the fact that the showers were allowed to develop in the iron plates of the absorption spectrometer.

Once this choice of standard showers had been made, shower curves were constructed for incident electron energies of 1, 2, 3, 4 and 5 GeV by interpolation and extrapolation of the curves of figure 5.1. These new shower curves, which include the incident muon, are shown in figure 5.2 and are the curves which were used as standards in the analysis of the experimental results.

5.3 Estimation of Shower Energies. Method 1

5.3.1 Introduction

The first method adopted for estimating the energies of the experimentally observed cascade showers consisted of comparing the total electron track lengths in these with the total electron track lengths of the standard showers.

Figure 5.1.

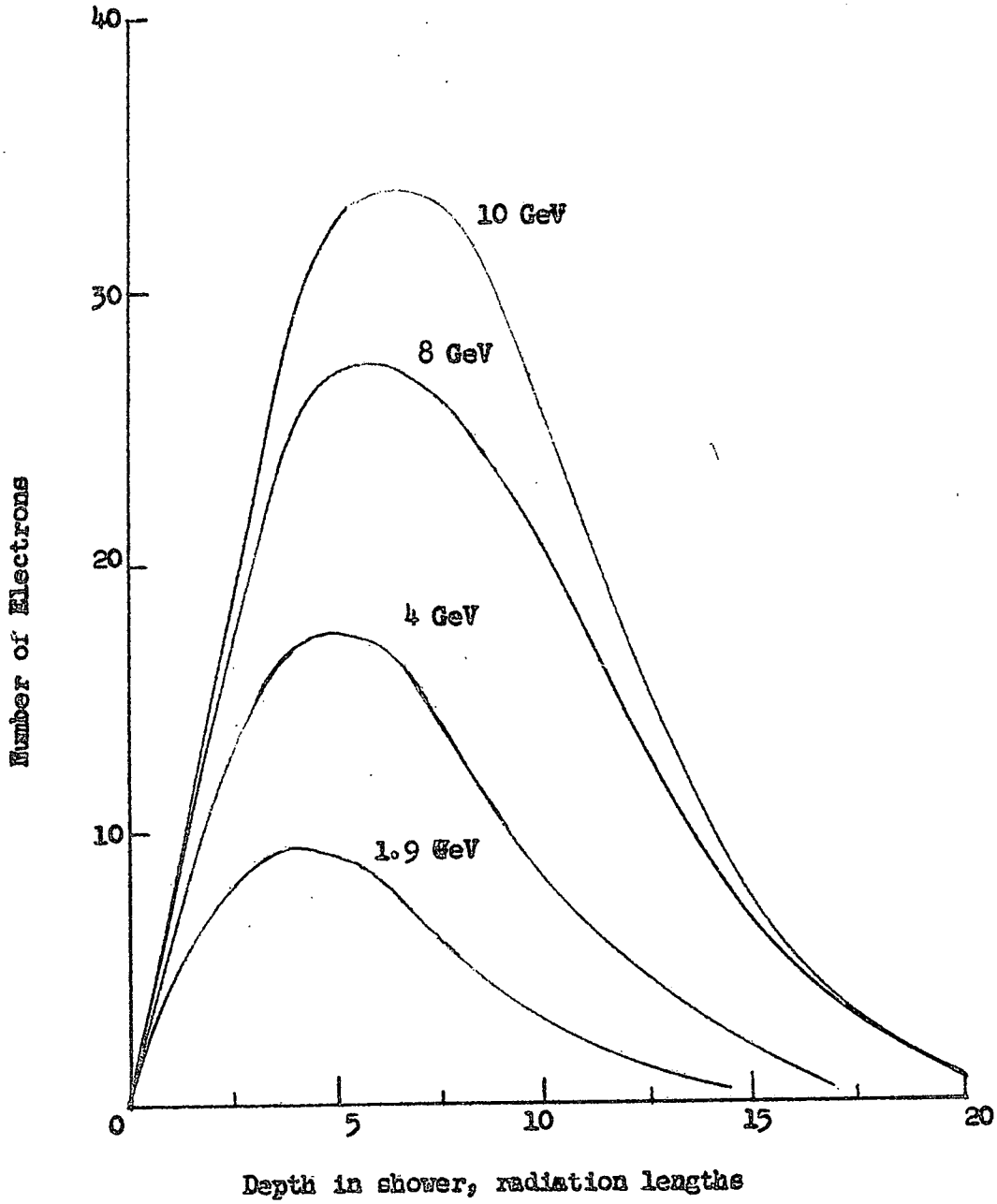

Average cascade shower curves (Backenstoss et al., 1963a).

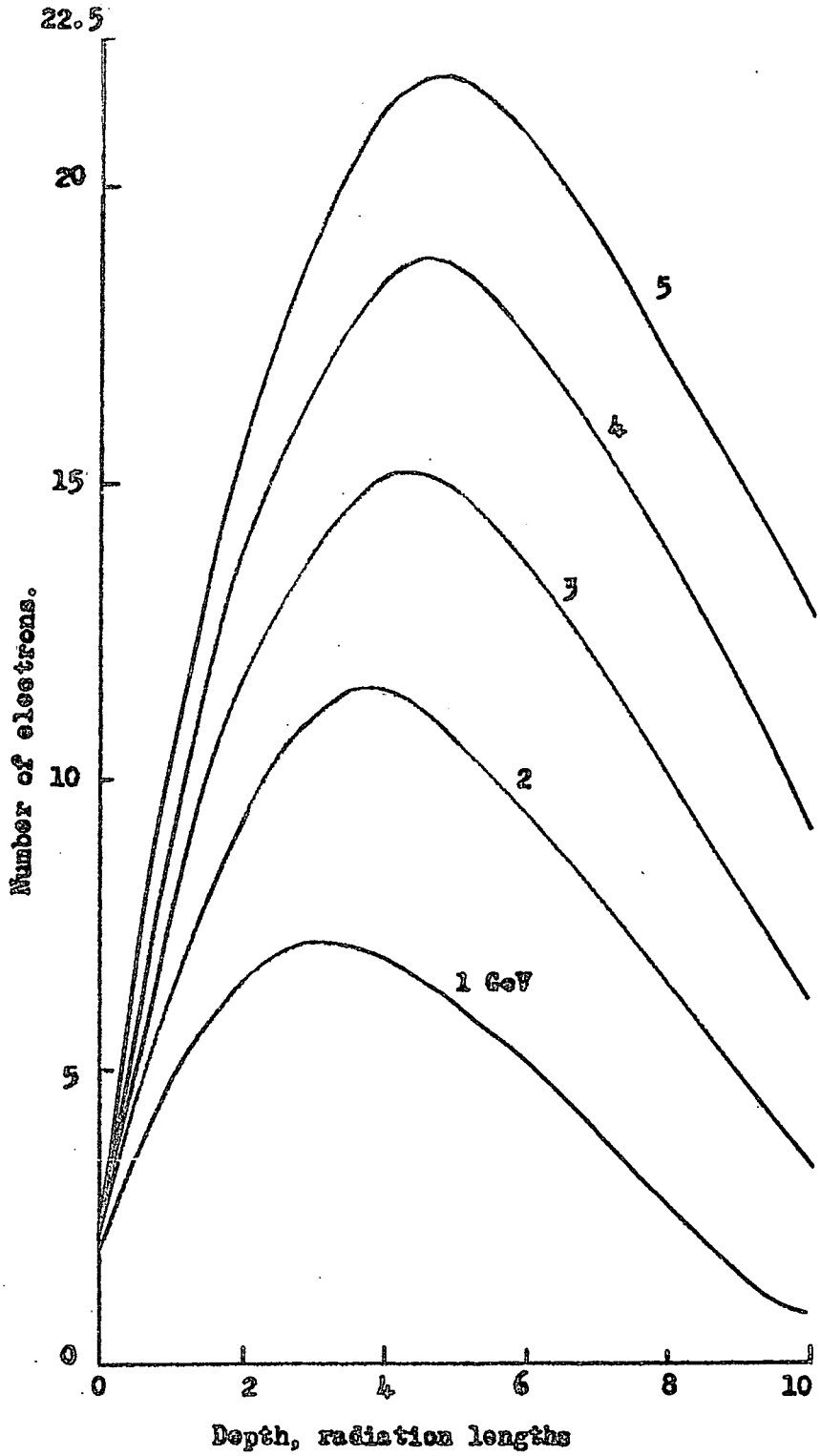

Figure 5.2 Standard shower curves obtained from the experimental curves of Backenstoss et al. (1963a)

Because the method of determining the track length of an observed shower contained assumptions with regard to the number of particles and the thickness of the converter plates, §5.3.4, method 1 was only used for low energy, completely developed, showers obtained in experiment A.

5.3.2 The Total Electron Track Length

The total track length of a cascade shower is defined by

$$T = \sum_{1}^{m} nt \text{ radiation lengths} \qquad 5.1$$

where T is the total track length,

n is the mean number of electrons entering and leaving a converter plate of thickness t radiation lengths, and

m is the total number of converter plates which the shower traverses.

From the theory of cascade showers using Approximation B it can be shown that the total track length of a cascade shower is related to the energy of the electron producing the shower by the expression (Rossi, 1952)

$$T = KE_o \text{ radiation lengths} \qquad 5.2$$

where E_o is the energy of the incident electron in MeV, and

$1/K$ is the critical energy in the material of the converter.

For iron converter plates, one should then expect that

$$T = 41.7\ E_o \text{ radiation lengths,}$$

where E_o is in GeV.

5.3.3 Total Track Length from Standard Shower Curves

Rather than use the theoretical relationship when converting from total track length to energy it was decided to construct a calibration curve using the standard shower curves of figures 5.1 and 5.2 (without the incident muon). The total track lengths for the various shower energies were obtained directly by measuring the areas under the shower curves. The calibration curve obtained in this way is shown in figure 5.3.

It is of interest to note that a least squares fit to the points used in constructing this curve gave

$$\tilde{T} = 39.3\ E_o^{0.96}, \qquad 5.3$$

which is in fairly good agreement with the theoretically predicted curve, §5.3.2.

5.3.4 Determination of Total Track Lengths and Energies for Observed Showers

In determining the total track lengths of showers observed experimentally the following assumptions were made:

i) All of the iron plates, both in the target and the converter, were of equal thickness. This was true in the case of experiment A but not for experiment B where the eighth flash tube tray was replaced by an extra amount of iron, thus increasing the thickness of the converter 'plate' at that level.

ii) When the number of particles traversing a flash tube tray was determined it was assumed that only one particle had traversed each flash tube which had fired. It was also assumed that when two tubes,

Figure 5.3

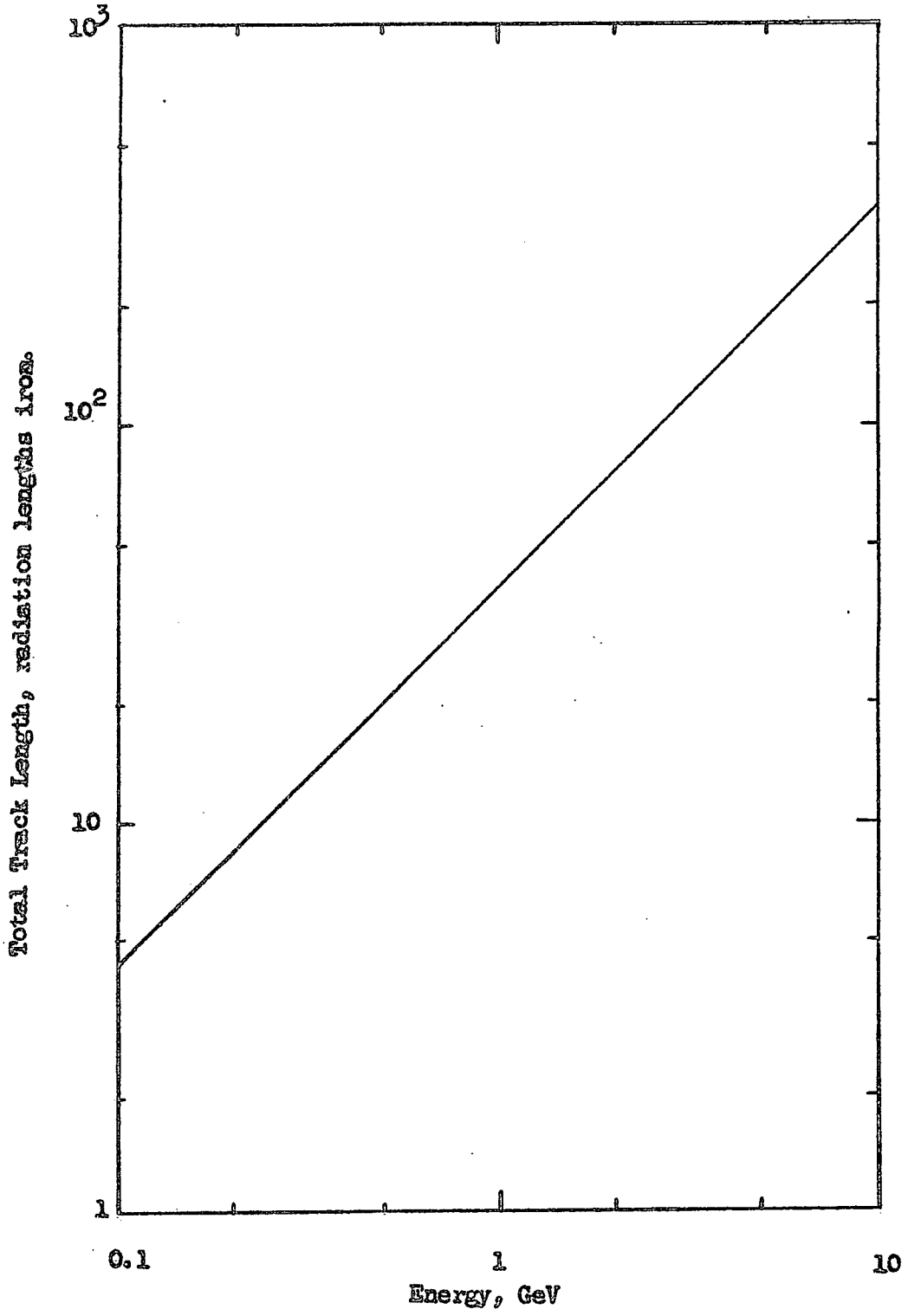

Calibration curve for energy estimation from total electron track length.

one below the other, had fired a single particle had traversed both and that when two tubes either in the same layer or in different layers, but separated laterally by at least one tube, had fired then two particles had been present. These assumptions are correct for low energy showers in which there are few shower electrons and these are widely spread laterally. As the shower energy, and thus the number of electrons at any one depth in the shower, increases the accuracy of these assumptions falls. For this reason only showers which had developed completely in the apparatus, and were thus of relatively low energy, were analysed using the total track length.

Using these assumptions the total track length of a shower was determined by taking the product of the number of shower particles traversing a flash tube tray and the thickness, in radiation lengths, of the converter plate immediately above this tray, and then summing over all flash tube trays. The energy of the shower was then obtained from the calibration curve, figure 5.3.

5.3.5 Accuracy of the Energy Estimates

The main error on the estimate of the shower energy from the total track length was the statistical error on the sum of the products of the number of particles in a flash tube tray and the converter thickness i.e. on $\sum nt$. Since all the converter plates were of equal thickness (0.738 radiation lengths), then

$$T = t \sum n$$

Putting $\sum n = N$ then the statistical error on T is given by

$$\frac{dT}{T} = \frac{dN}{N} = 1/\sqrt{N}$$

Now, from equation 5.3,

$$T = 39.3\ E_o^{0.96}, \quad \therefore\ dT = 39.3 \times 0.96\ E_o^{(0.96-1)}\ dE_o$$

$$\therefore\ \frac{dT}{T} = 0.96\ \frac{dE_o}{E_o} \text{ and } \frac{dE_o}{E_o} = 1.04\ \frac{dT}{T} = 1.04/\sqrt{N}.$$

From this it can be seen that as the energy, and thus N, increases the fractional error on the energy due to statistical fluctuations decreases e.g. $\frac{dE_o}{E_o}$ goes from 43% at 0.1 GeV to 20% at 0.5 GeV.

Apart from the statistical error on the energy estimate the only other source of error lay in the second of the two assumptions made in §5.3.4 i.e. the assumption that only one particle had traversed any flash tube which had fired. For showers in which the shower particles were reasonably well separated laterally the error in determining the value of N is unlikely to have been greater than 20% and in the majority of cases would be less than this.

It is therefore reasonable to assume that the errors on the energy estimates in no case exceeded 43% and were probably of the order of 30%.

5.4 Estimation of Shower Energies. Method II

5.4.1 Introduction

The second method used for estimating the energies of the observed showers consisted of making a more accurate estimate of the number of particles traversing a flash tube tray than was done in method I. This was done by determining the most probable number of particles required to trigger the flash tubes observed to have fired in a given flash tube tray. The energy of the shower was then estimated by comparing this

number with a calibration curve showing the number of particles at a given depth, as a function of the shower energy.

This method of analysis was used to estimate the energies of those showers in experiment A which had not developed completely in the stack and all of the showers obtained in experiment B.

5.4.2 The Calibration Curves

The calibration curves were obtained directly from the standard shower curves of figures 5.1 and 5.2, including the incident muon in both cases, by reading off the mean number of particles found at any one depth in the shower for each of the incident energies. Examples of the calibration curves obtained in this way are shown, for three different depths in the shower, in figure 5.4.

5.4.3 Estimation of the Number of Particles Traversing a Flash Tube Tray

The method used to estimate the number of particles traversing a flash tube tray and triggering those tubes which were seen to have fired was based on Poisson statistics. It was assumed that the density of shower particles was uniform over the whole of the area of the shower.

If one considers ℓ counters, each of area s square metres, then the probability that k of these counters would be triggered by a shower of particles with a uniform density of Δ particles per square metre is given by

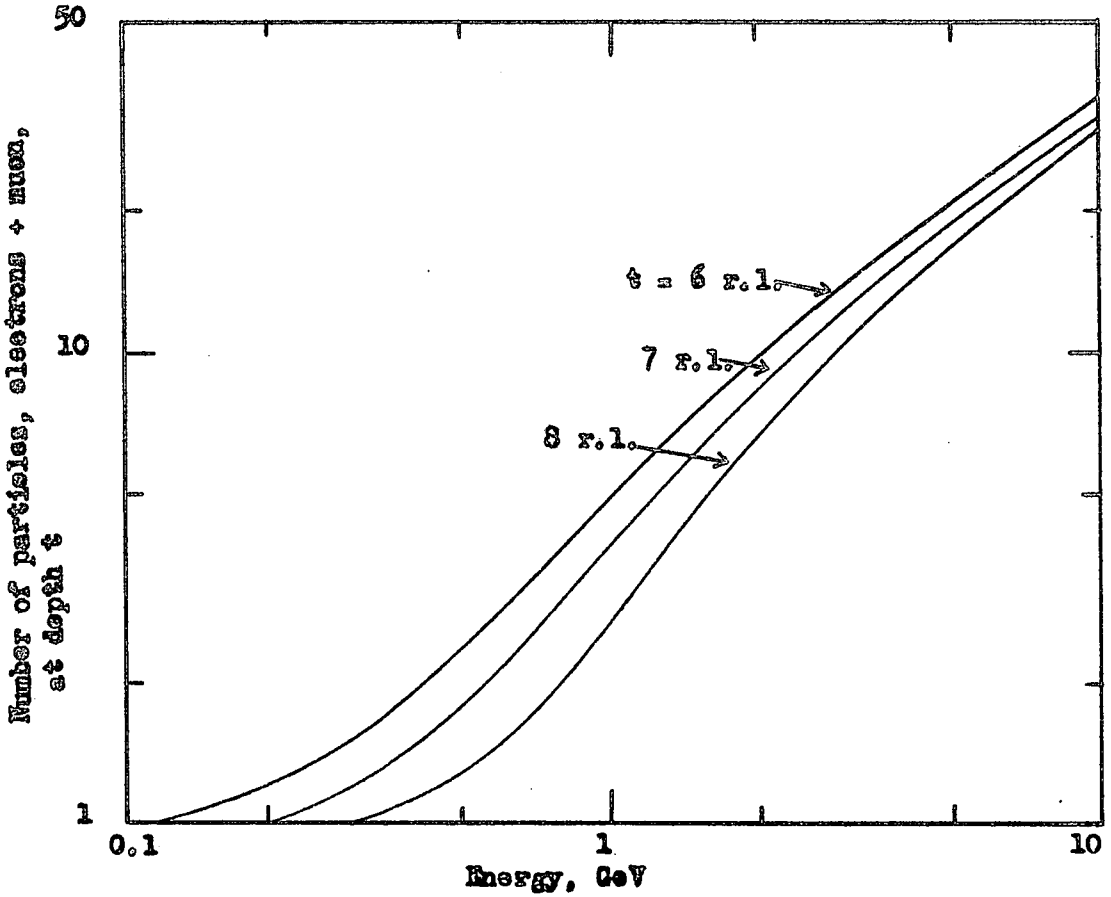

Figure 5.4 Calibration curves for analysis by Method II.

$$P(k,\Delta) = \left(\frac{\ell!}{k!(\ell-k)!}\right)\left(1 - e^{-\Delta s}\right)^{k}\left(e^{-\Delta s}\right)^{\ell-k} \qquad 5.4$$

By differentiating this equation with respect to Δ and then putting $\frac{dP}{d\Delta} = 0$ one obtains an expression for the most probable particle density which will trigger the k out of ℓ counters, namely:

$$\Delta = \frac{1}{s}\log_e\left(\frac{\ell}{\ell-k}\right) \text{ particles/m}^2 \qquad 5.5$$

In analysing the results from the present experiment it was decided to calculate the number of particles present at the centre of a converter plate rather than the number traversing a flash tube tray. To do this the values used for s, ℓ and k were determined as follows:

s was the sensitive area of a flash tube. This was taken to be the length of the smaller electrode multiplied by the internal diameter of the flash tube. From the dimensions quoted in §4.3 one obtains $s = 1.2 \times 10^{-2}$ m^2.

It is to be noted here that this value of s assumes that the flash tube was ~100% efficient over the whole of its internal diameter, an assumption which was borne out by measurements of the layer efficiency.

If the distribution of flash tubes which had fired in the trays above and below a converter plate was as shown in figure 5.5 then the value of ℓ was taken as being

$$\ell = (\ell_1 + \ell_2)/2$$

where ℓ_1 was the maximum lateral distance between any two flash tubes which had fired in the upper flash tube tray, expressed as a number of

Figure 5.5

Example of an event for which

$l = (l_1 + l_2)/2 = 7$ tube diameters

$k = 16/4 = 4$

Number of particles = 7.1

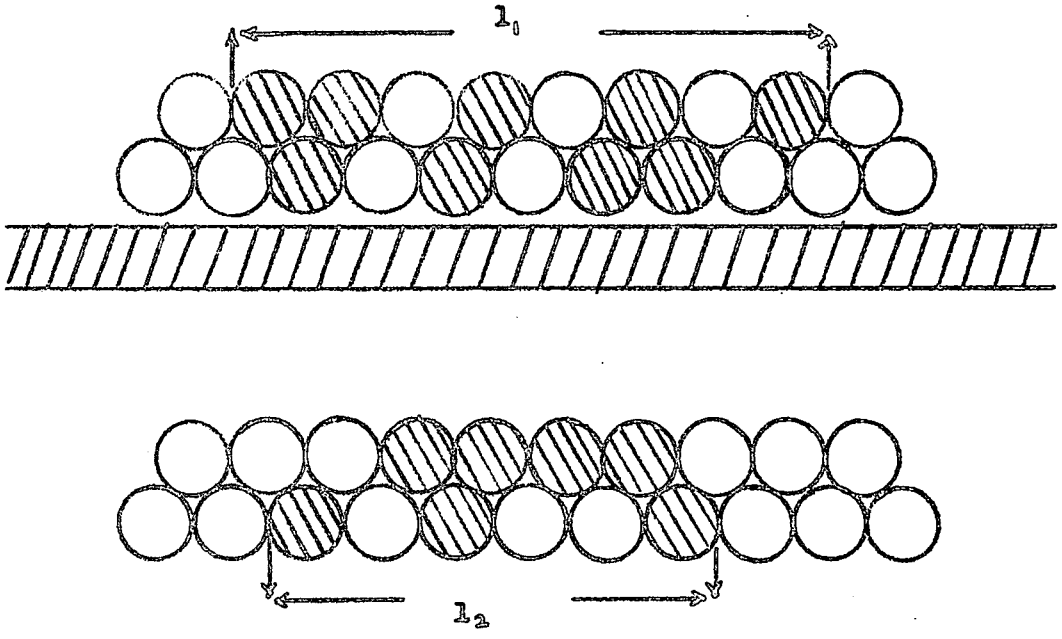

flash tubes, and ℓ_2 was the same value for the lower flash tube tray. The value of k was taken as being N/4 where N is the total number of flash tubes which had fired in the two trays together.

Using the values of s, ℓ and k obtained in this way the most probable particle density was then calculated using equation 5.5. To obtain the number of particles present at the centre of the converter plate the value of Δ was multiplied by the area of the shower, given by 1.2 ℓs, where the factor 1.2 allows for particles which passed through the glass walls of the flash tubes and did not cause the tubes to fire.

The energy of the shower was then estimated by comparing the calculated number of particles present at the given depth with a calibration curve similar to those shown in figure 5.4.

5.4.4 Accuracy of the Energy Estimates

The estimates of the shower energies obtained by using method II to analyse the experimental data are subject to three types of error, namely:

i) The statistical error. Equation 5.5 contains the two measured variables, ℓ and k, both of which are subject to statistical errors. If the standard errors are represented by their differentials it can be shown that

$$\frac{d\Delta}{\Delta} = \frac{1}{k}\left[\frac{dk}{k} - \frac{d\ell}{\ell}\right] / (\ell - k) \log_e \left(\frac{\ell}{\ell - k}\right) \qquad 5.6$$

Now, §5.4.3, $\ell = (\ell_1 + \ell_2)/2$ and hence $\frac{d\ell}{\ell} = \frac{1}{2\sqrt{\ell}}$.

Similarly $k = N/4$, hence $\frac{dk}{k} = \frac{1}{2\sqrt{k}}$.

By putting these values into equation 5.6 one obtains

$$\frac{d\Delta}{\Delta} = \frac{1}{2k}\left[\frac{1}{\sqrt{k}} - \frac{1}{\sqrt{\ell}}\right] \Big/ (\ell - k)\log_e\left(\frac{\ell}{\ell - k}\right) \qquad 5.7$$

Since the number of particles, N_e, was given by

$$N_e = C \quad \text{where } C = 1.2\,\ell s, \text{ then}$$

$$dN_e = \Delta dC + C d\Delta$$

$$\frac{dN_e}{N_e} = \frac{dC}{C} + \frac{d\Delta}{\Delta} = \frac{1}{2\sqrt{\ell}} + \frac{d\Delta}{\Delta} \qquad 5.8$$

It can thus be seen that the fractional error in the calculated number of particles is a fairly complex function of the measured variables ℓ and k. However it can be shown that, except for very small values of k, the fractional error in N_e is made up almost entirely by the fractional error in ℓ and decreases as ℓ increases.

The error in the value of the shower energy could then be obtained using the value obtained for dN_e/N_e and the calibration curve. For example, for a shower in which $k = 8$, $\ell = 17.5$ and hence $N_e = 16.4$ the energy is found to be $(3.85 \pm^{0.95}_{0.75})$ GeV i.e. a fractional error of approximately 20%.

ii) The second error to which this method of analysis is subject is due to the fact that in using equation 5.4 it is assumed, a priori, that all particle densities are equally probable. However, since low energy showers, and thus low particle densities, were more probable then high energy showers, see figures 2.1 and 2.3, this assumption is

not correct. Thus, instead of using equation 5.4 to determine the most probable density an equation of the form

$$P(k,\Delta)d\Delta = \left(\frac{\ell!}{k!(\ell-k)!}\right)\left(1-e^{-\Delta s}\right)^{k}\left(e^{-\Delta}\right)^{\ell-k} A\Delta^{-\gamma}\, d\Delta$$

should have been used, where $A\Delta^{-\gamma}\, d\Delta$ is the shower density spectrum.

Because of the fact that the values taken for k and ℓ could be non-integral, it was not ~~possible~~ convenient to use such an expression to determine the most probable density.

In carrying out the analysis of the results, Chapter 6, the error due to the use of equation 5.4 has been allowed for by taking into account the fluctuations of the energies allotted to a single shower by considering a number of depths in the shower.

iii) The final source of error in the energy estimates obtained by method II is due to the assumption, §5.4.3, that the density of the shower particles was uniform at any one depth in the shower. It can be seen from an examination of cloud chamber photographs of cascade showers that this assumption is incorrect, the particle density being higher near the axis of the shower. It is not possible, however, to calculate the effect of this assumption on the energy estimates since no details are available for the radial distribution of shower particles in showers which develop in an inhomogenous medium i.e. iron and air.

An indication that the uncertainty introduced by this assumption was not very great is given by the fact that for low energy showers the number of particles found using equation 5.5 is not very different from N', the number which would be expected if only one particle had

gone through each tube which had fired, e.g. in figure 5.4

$$N^1 = {}^{11}/_2 = 5.5, \quad N = 7.1 .$$

5.5 Conclusions

From the arguments put forward in the preceding paragraphs it is concluded that the energies of the cascade showers obtained experimentally can be estimated with an uncertainty of 30% in method I and with an uncertainty of 25% in method II.

CHAPTER 6

RESULTS AND CONCLUSIONS FROM THE DURHAM EXPERIMENT

6.1 Introduction

It has already been stated, §4.4, that events which fulfilled the requirements of the selection system were recorded photographically. The films were then projected and scanned and the events divided into four groups, namely:

1) Single particles

2) Incident showers

3) Interactions

4) Random coincidences

The events which were classified as interactions were then re-examined and those which showed more than one penetrating particle leaving the interaction were rejected as being nuclear interactions. These were either interactions of incident protons in the target or 'nuclear' interactions of incident muons, as defined in Chapter 1. The remainder of the interactions, the electromagnetic interactions, were then analysed using the methods described in Chapter 5 and the energy spectrum of the secondary particles from the interactions was compared with that predicted theoretically.

The following paragraphs contain details of the criteria used to classify the events, the results of the analysis, a discussion of the results and the conclusions.

6.2 Selection Criteria

The criteria used in the division of the events were as follows:

1) Single particles

These events contained a single particle track in at least eleven out of the twelve flash tube trays in experiment A, and in at least ten out of the eleven trays in experiment B. Also classed as single particles were events in which, as well as the single particle track, the track of a low energy knock-on electron was visible in one or more of the third, fourth and fifth flash tube trays but stopped before it reached the sixth tray, or in which a knock-on electron track or cascade shower was seen to start in any flash tube tray other than the third, fourth or fifth.

2) Incident showers

All events in which two or more particle tracks were visible in the top two flash tube trays, and in which at least one of these particles left the bottom of the apparatus, were classed as incident showers.

3) Interactions

For an event to be classed as an interaction it had to satisfy the following criteria:

a) Only a single particle track was visible in the top two flash tube trays.

b) Two or more particle tracks were visible in the third, fourth or fifth flash tube trays.

c) Two or more particle tracks were visible in the sixth flash tube tray, and

d) At least one particle track was seen leaving the bottom of the apparatus within the area defined by the bottom tray of geiger counters, figure 4.1.

4) Random coincidences

These were events in which the apparatus had been triggered by one or more particles traversing the scintillation counter and one of the geiger counter trays in coincidence with a particle traversing the second geiger counter tray. Such events appeared as a single track, or a shower, passing through the scintillation counter and one geiger counter tray and then leaving the side of the apparatus.

Examples of events in classes 1), 2) and 3) are shown in plates 2, 3 and 4.

6.3 Experimental Conditions and Running Times

A summary of the experimental conditions and the running times for experiments A and B are given in table 6.1. This table also includes the results of the initial analysis of the films.

In constructing this table the value for the total sensitive time, 14, was obtained from the total running time, 7, by subtracting from the latter the total time for which the apparatus was paralysed. The calculated number of incident muons was obtained from the total sensitive time, 14, and the two-fold geiger counting rate, 3.

PLATE 2

A SINGLE MUON

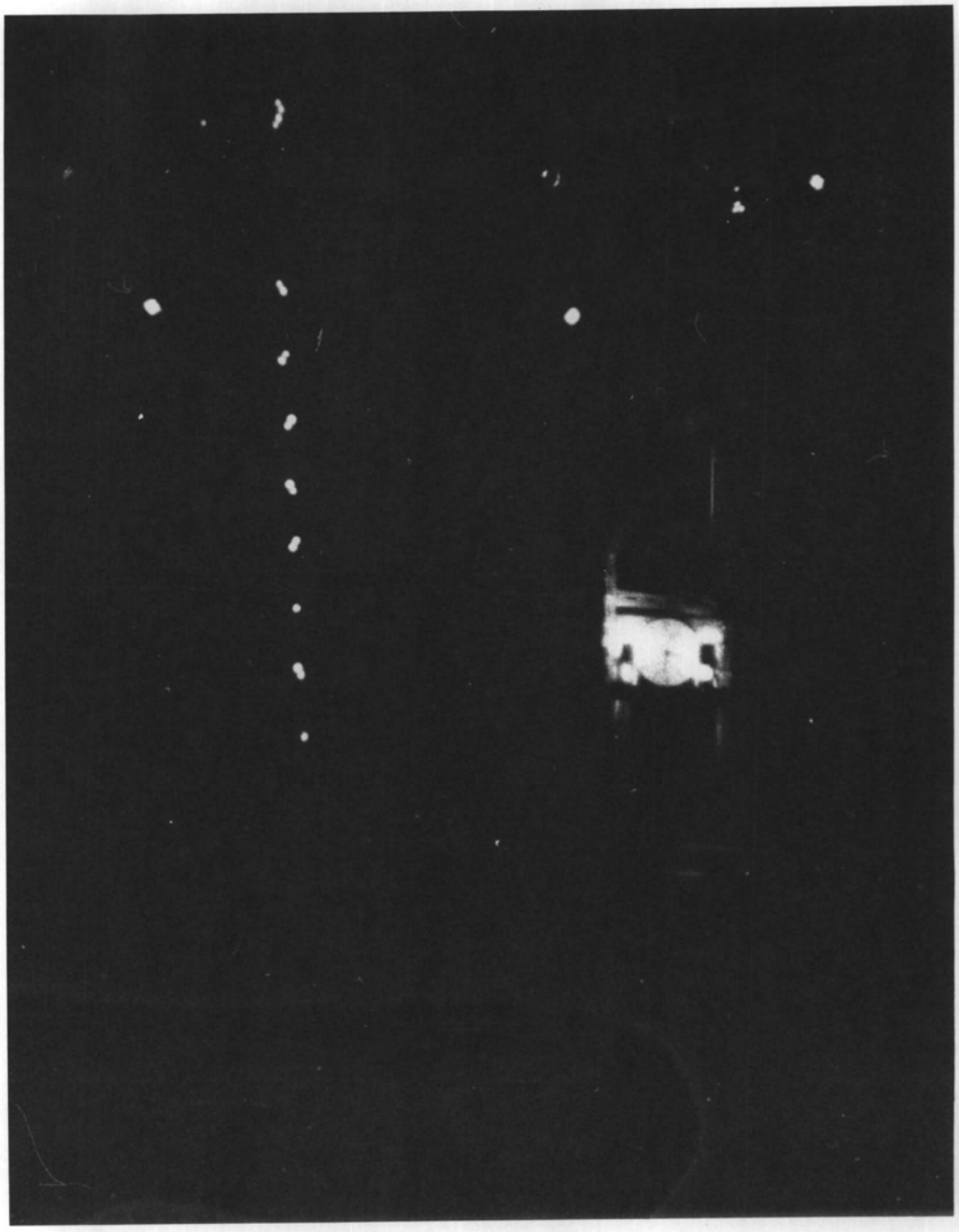

PLATE 3

AN INCIDENT SHOWER

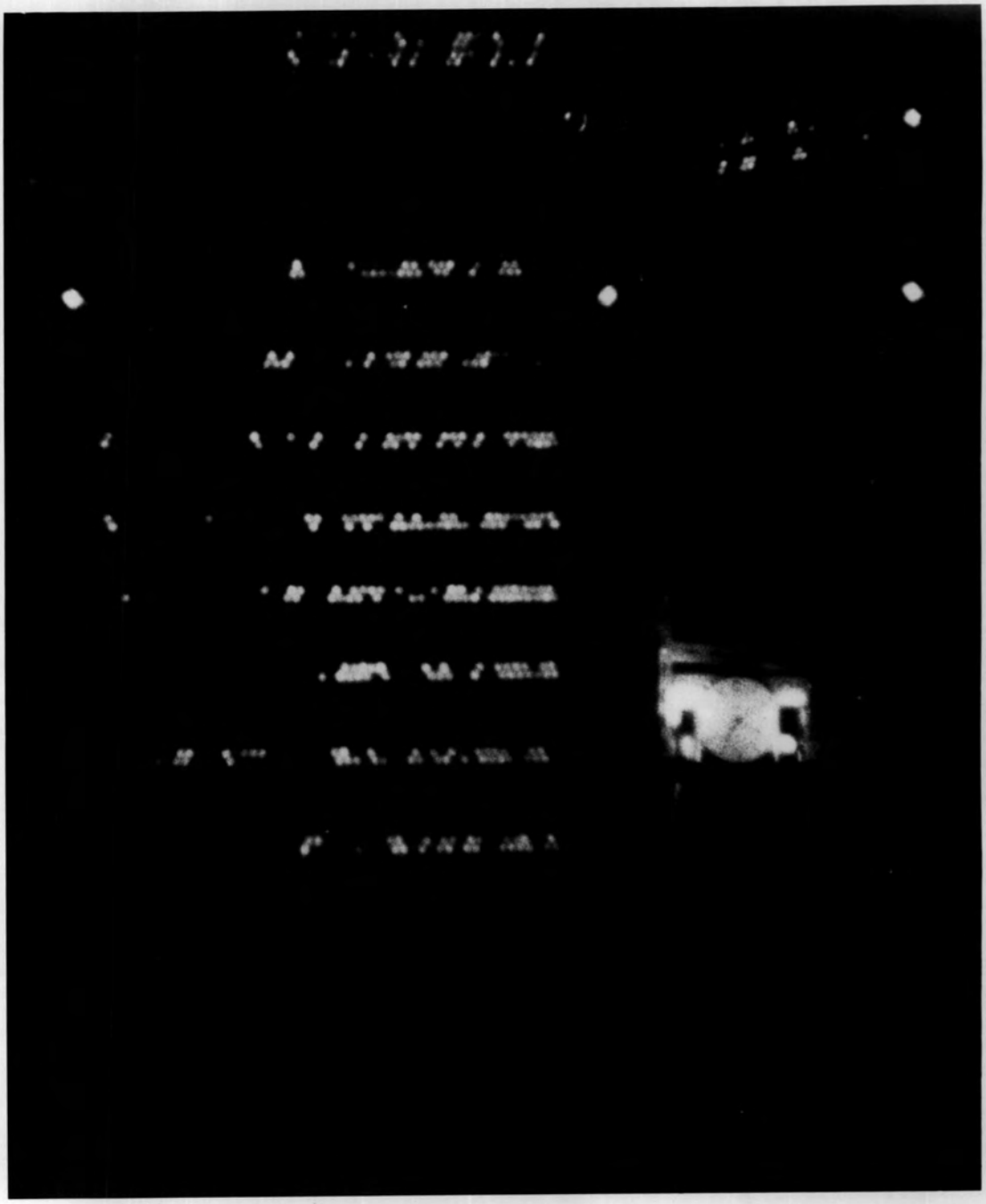

PLATE 4

AN ELECTROMAGNETIC INTERACTION

ESTIMATED ENERGY 1.6 GeV

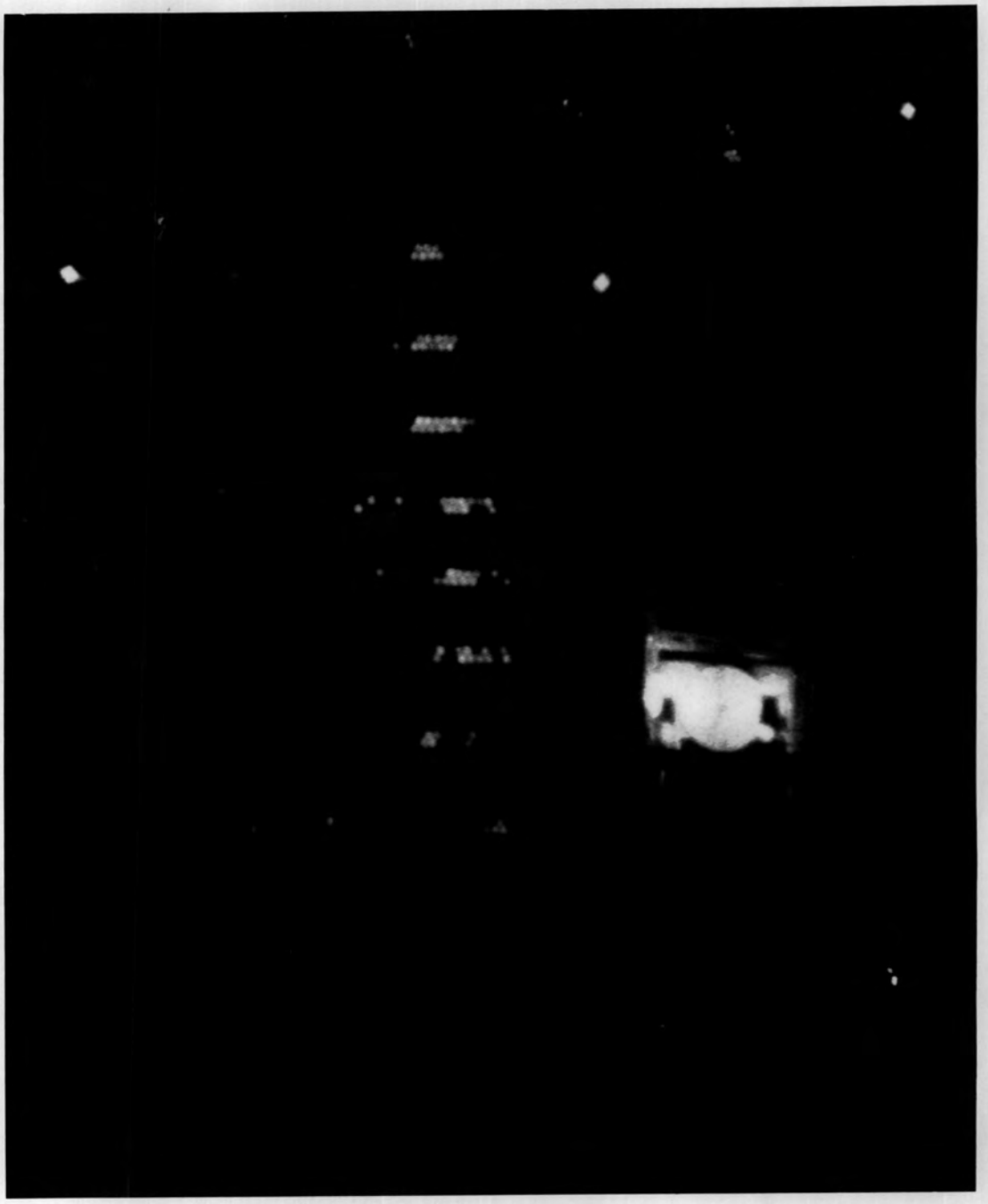

TABLE 6.1

	Experiment A	Experiment B
1. Target	22.04 g cm^{-2} Fe	22.04 g cm^{-2} Fe
2. Converter	5.90 radiation lengths Fe	8.45 radiation lengths Fe
3. 2-fold geiger counting rate, corrected for random coincidences	(1.01 ± 0.09) counts/sec	(0.83 ± 0.02) counts/sec
4. Scintillation counter bias level	30 volts	45 volts
5. Attenuation of scintillation counter pulses	50 db	50 db
6. Mean counting rate of scintillation counter	(9.22 ± 0.15) counts/sec	(4.35 ± 0.26) counts/sec
7. Total running time	33 hours 4 minutes	21 hours 35 minutes
8. Mean counting rate of selection system	(2.50 ± 0.06) counts/min	(1.08 ± 0.05) counts/min
9. Number of single particles selected	2408	431
10. Number of incident showers selected	1426	468
11. Number of interactions selected	312	108
12. Number of random coincidences	701	420
13. Total number of events selected	4847	1427
14. Total sensitive time	1.045 10^5 secs	7.342 10^4 secs
15. Calculated number of incident muons	(1.1 ± 0.1) 10^5	(6.1 ± 0.1) 10^4

6.4 The theoretical curves

The theoretical curves, with which the results from the two experiments were compared, were calculated using equations 2.1, 2.2 and 2.9 (with $\alpha = 2$, $a = 10\ m_e c^2/\epsilon$) and folding in the sea level vertical muon momentum spectrum, for muon momenta above 400 MeV/c, as measured at Durham (Hayman and Wolfendale, 1962). The calculation was carried out using the Durham University Elliott 803 computer and the curves obtained are shown in figures 6.1. From figure 6.1 it can be seen that for energy transfers up to 15 GeV the dominant process is knock-on production and that above 15 GeV bremsstrahlung becomes dominant.

6.5 Experiment A

6.5.1 Final classification of events

The 312 interactions found in the initial analysis of experiment A were analysed further and divided into groups as follows:

a) Nuclear interactions - these events have already been described, §6.1, as those in which two or more penetrating particles were seen to leave the target plate in which the interaction took place.

b) Doubtful events - these were events in which, although only a single particle track was visible in the top two flash tube trays the distribution of flash tubes which had fired in the third and fourth trays was such that the event could possibly have been an incident shower.

c) Electromagnetic interactions - this group, which contained all events except those described in a) and b) was further sub-divided into i) events in which the cascade shower was completely developed in

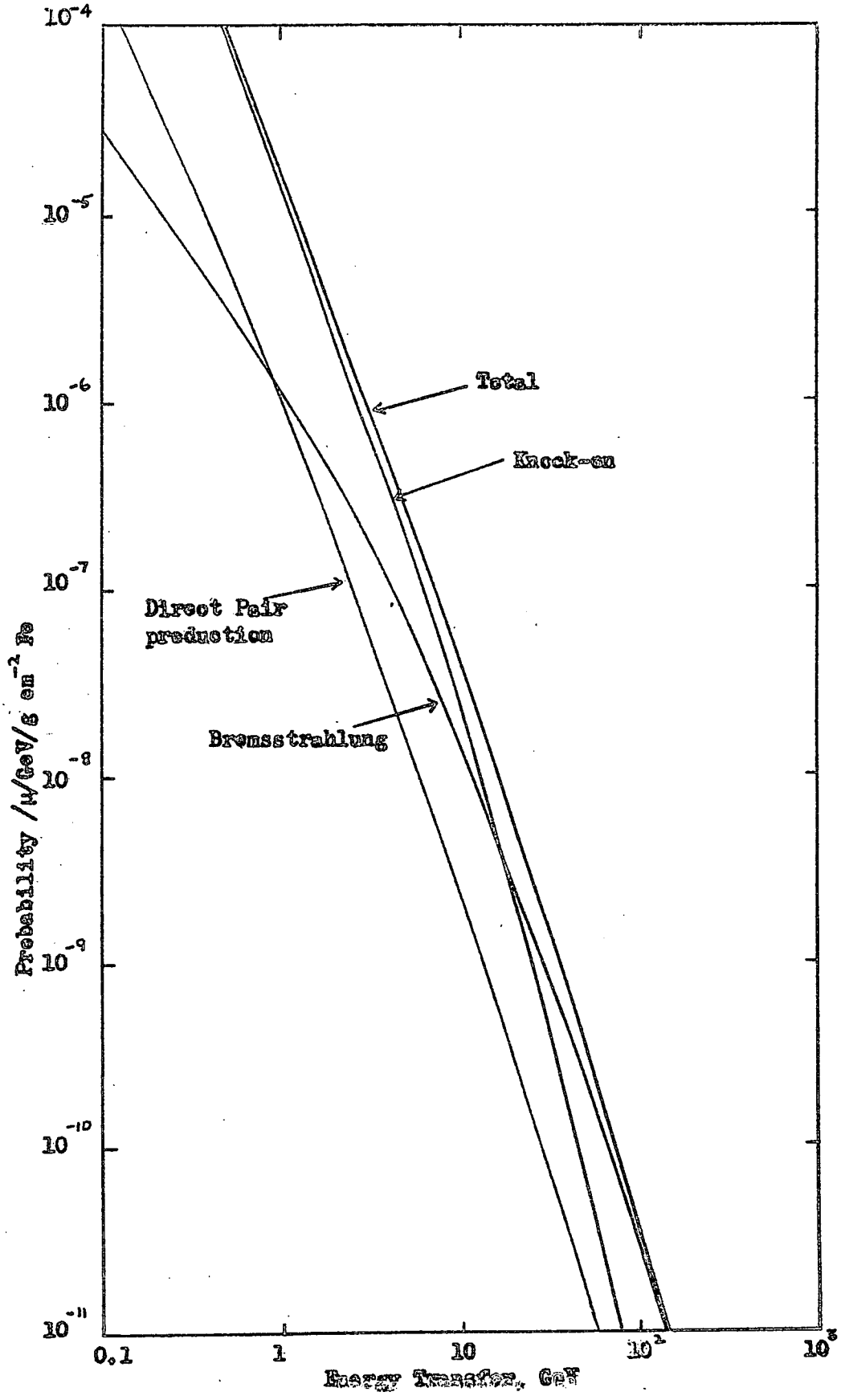

Figure 6.1 Differential energy transfer probabilities in iron at sea level

the apparatus, and ii) events in which the shower left the bottom of the apparatus.

After consideration it was decided that, in the final analysis only those electromagnetic interactions should be used which appeared to start above the third or fourth flash tube trays, and not those starting above the fifth flash tube tray.

The numbers of events which were put in the different classes are shown in table 6.2.

TABLE 6.2

Class of event	Number of events
a) Nuclear Interactions	12
b) Doubtful events	33
c) Electromagnetic interactions	
i) Complete	88
ii) Incomplete	91
iii) Starting above tray 5	88

6.5.2 The transferred energy spectrum

To determine the spectrum of transferred energies the energies of the secondary particles in the case of the complete events were determined using method I, §5.3. For the incomplete showers the energy of the secondary particle from the interaction was taken as being the median value of five energy estimates. These estimates were obtained by applying method II, §5.4, to the centre points of the five lowest absorber plates, figure 4.1.

The final spectrum of secondary particle energies is given in table 6.3. The comparison between this spectrum and that predicted theoretically is described in §6.7.

TABLE 6.3

Energy range, GeV	Number of Events	Number of Events/GeV
0.1 - 0.3	$37^{+7.5}_{-6.1}$	$185^{+37.5}_{-30.5}$
0.3 - 0.5	$30^{+7.0}_{-5.7}$	$150^{+35}_{-28.5}$
0.5 - 1.0	$34^{+7.0}_{-6.0}$	68^{+14}_{-12}
1.0 - 2.0	44^{+8}_{-7}	44^{+8}_{-7}
2.0 - 3.0	$7^{+3.9}_{-2.45}$	$7^{+3.9}_{-2.45}$
3.0 - 5.0	$10^{+4.3}_{-3.0}$	$5^{+2.15}_{-1.5}$
5.0 - 8.0	$2^{+2.6}_{-1.29}$	$0.67^{+0.87}_{-0.43}$
8.0 - 15.0	$1^{+2.3}_{-0.83}$	$0.14^{+0.33}_{-0.12}$

Experiment A

The differential transferred energy spectrum obtained from 165 events with secondary energies greater than 0.1 GeV.

6.6 Experiment B

6.6.1 Final classification of events

The 108 interactions selected from the experiment B films were subdivided in the same way as the interactions from experiment A but with the complete and incomplete events grouped together. The result of this subdivision is given in table 6.4.

TABLE 6.4

Class of event	Number of events
a) Nuclear interactions	1
b) Doubtful events	12
c) Electromagnetic interactions	
i) Starting in trays 3 and 4	82
ii) Starting in tray 5	13

6.6.2 The transferred energy spectrum

In determining the transferred energy spectrum from experiment B the energies of the secondary particles in class c i) events were determined using method II, §5.4. For incomplete showers the energy was taken as the median value of four energies, these being obtained by determining the number of shower particles at the centres of the bottom four converter plates. For complete showers the energies were determined from the number of particles at the mid points of the last one or two converter plates traversed by the shower.

The transferred energy spectrum obtained from experiment B is given in table 6.5 and is compared with the predicted spectrum in §6.7.

6.7 Comparison between predicted and experimental results

6.7.1 Introduction

Before comparing the experimental results with those predicted by theory it was first necessary to make certain corrections to the latter. These corrections were made to allow for a) the fluctuations

TABLE 6.5

Energy range, GeV	Number of events	Number of events/GeV
0.1 - 0.3	$7^{+3.9}_{-2.45}$	$35^{+19.5}_{-12.2}$
0.3 - 0.5	$5^{+3.3}_{-2.1}$	$25^{+16.5}_{-10.5}$
0.5 - 0.1	$23^{+6.5}_{-4.5}$	46^{+13}_{-9}
1.0 - 2.0	$19^{+5.8}_{-4.1}$	$19^{+5.8}_{-4.1}$
2.0 - 3.0	$13^{+5}_{-3.4}$	$13^{+5}_{-3.4}$
3.0 - 5.0	$7^{+3.9}_{-2.45}$	$3.5^{+1.95}_{-1.27}$
5.0 - 8.0	$3^{+2.45}_{-1.63}$	$1^{+0.98}_{-0.54}$

Experiment B

Differential transferred energy spectrum obtained from 77 interactions with secondary energy greater than 0.1 GeV.

---

in the energies allotted to the experimental cascade showers, due to the fluctuations in the number of shower particles at a given depth in the shower, and b) the efficiency of the scintillation counter for the detection of 1, 2 and 3 particles and the overall detection efficiency for low energy showers.

6.7.2 Correction for fluctuations

The correction of the predicted transferred energy spectrum for fluctuations was carried out using the method due to Lloyd and Wolfendale (1955). These workers show that if the uncorrected differential distribution is represented by $f(E)dE$ and the experimental errors in E are normally distributed with standard deviation σ then

$$\frac{g(E_o)}{f(E_o)} = \tfrac{1}{2} \exp\,(m^2\sigma^2/2) \left\{1 + \operatorname{erf}\left(\frac{E_o - m\sigma^2}{\sigma\sqrt{2}}\right) + \exp\,(2mE_o)\left[1 + \operatorname{erf}\left(\frac{E_o + m\sigma^2}{\sigma\sqrt{2}}\right)\right]\right\} \quad 6.1$$

where $g(E_o)dE_o$ is the corrected differential distribution,

$f(E_o)dE_o$ is the uncorrected differential distribution,

and $f(E)dE = A \exp(-mE)dE$.

Since the term in the brackets is almost 2 for $E_o \gg m\sigma^2$ then the ratio of the corrected to the uncorrected distribution is, to a good approximation,

$$g(E_o)/f(E_o) = \exp\,(m^2\sigma^2/2). \quad 6.2$$

In calculating this ratio for the two experiments the value of σ was taken as being the standard deviation of the curve of log N versus log F, where 1/F is the ratio of the median energy allotted to a shower, method II, to the energies allotted to this shower from measurements at different depths in the shower, and N is the frequency with which the values of F occurred.

m was the slope of the differential transferred energy spectrum, figure 6.1.

The values used and the correction factors obtained for the two experiments are given in table 6.6.

TABLE 6.6

	Experiment A	Experiment B
m	2.65	2.65
σ	0.18	0.15
$g(E_o)/f(E_o)$	1.12	1.08

6.7.3 Correction for detection efficiency

In correcting the theoretical curve for the detection efficiency for showers of various energies it was assumed that the fluctuations in the number of particles at any one depth in a shower could be described by Poisson statistics. Since the particles in the shower are not independent this assumption is not strictly correct. It is believed, however, that the difference in the results obtained using Poisson statistics and those using Pólya statistics, as proposed by Bertanza and Martelli (1954), is not very great.

In the experiments two types of selection operated, namely:

i) The selection of events by the scintillation counter, i.e. instrumental selection, and

ii) The selection of events from the film by requiring two or more particles in flash tube trays three or four plus two or more particles in flash tube trays five and six (figure 4.1).

Knowing the efficiency of the scintillation counter for the detection of n particles, n = 1, 2, 3 etc., the overall detection efficiency for interactions was obtained as follows:

Consider a shower of energy E_o starting in the target at a height

of t g cm^{-2} above the scintillation counter. Let this shower contain an average of n_1 particles at depth t from the start of the shower, n_2 particles at depth t + T and n_3 particles at depth t + 2T, where T is the thickness of the converter plates above the fifth and sixth flash tube trays.

Now, from Poisson statistics, if the mean number of particles is n the probability of getting m is $(e^{-n}\, m^n)/m!$

If the efficiency of the scintillation counter for the detection of k particles is $\epsilon(k)$ it can now be shown that the efficiency for the detection of a shower starting t g cm^{-2} above the scintillation counter is:

$$\epsilon_f = [1-e^{-n_2}]\,[1-e^{-n_3}]\left\{1-e^{-n_1}\sum_{m=0}^{2}\left(\frac{m^{n_1}}{m!}\right) + e^{-n_1}\,\epsilon(2) + e^{-n_2}\,\epsilon(3)\right\}$$

N.B. In determining this expression it must be remembered that the incident muon was present at all points in the shower.

To determine the total detection efficiency for a shower of energy E_o the values of n_1, n_2 and n_3 were then found for different values of t and the average value of ϵ_f was determined for showers starting at all points in the target. The results obtained for the two experiments are given in table 6.7, as are the values of $\epsilon(k)$ used in the calculations. These values were obtained from the curves of figure 4.3, and a curve for the detection efficiency for three particles, using the counting rates given in table 6.1 (6). The values of n_1, n_2 and n_3 were obtained from the standard shower curves, figure 5.2, without the incident muon.

TABLE 6.7

	Experiment A	Experiment B
$\epsilon(2)$	0.35	0.11
$\epsilon(3)$	0.99	0.39
Detection efficiency for 0.15 GeV shower	0.22	0.11
0.24 GeV "	0.39	0.24
0.5 GeV "	0.65	0.47
1.0 GeV "	1.00	0.65

The theoretical curves, corrected for fluctuations and detection efficiency, are shown in figures 6.2 and 6.3, where the number of events/GeV energy transfer expected in the two experiments are plotted as a function of the energy transfer. Also plotted are the experimental results, tables 6.3 and 6.5.

6.7.4 Discussion of the Experimental Results

From a comparison of the experimental and the theoretical results it can be seen that the results from both experiment A and experiment B follow the same pattern. Below energy transfers of 1 GeV there are less events than predicted while above this energy there is an excess particularly in the case of experiment B. Since the only differences between the two experiments were i) the converter in experiment B contained 2.55 more radiation lengths of iron than in experiment A, and ii) the scintillation counter bias level was higher in experiment B than in experiment A, the difference between the two sets of results must be due to one of the following:

Figure 6.2

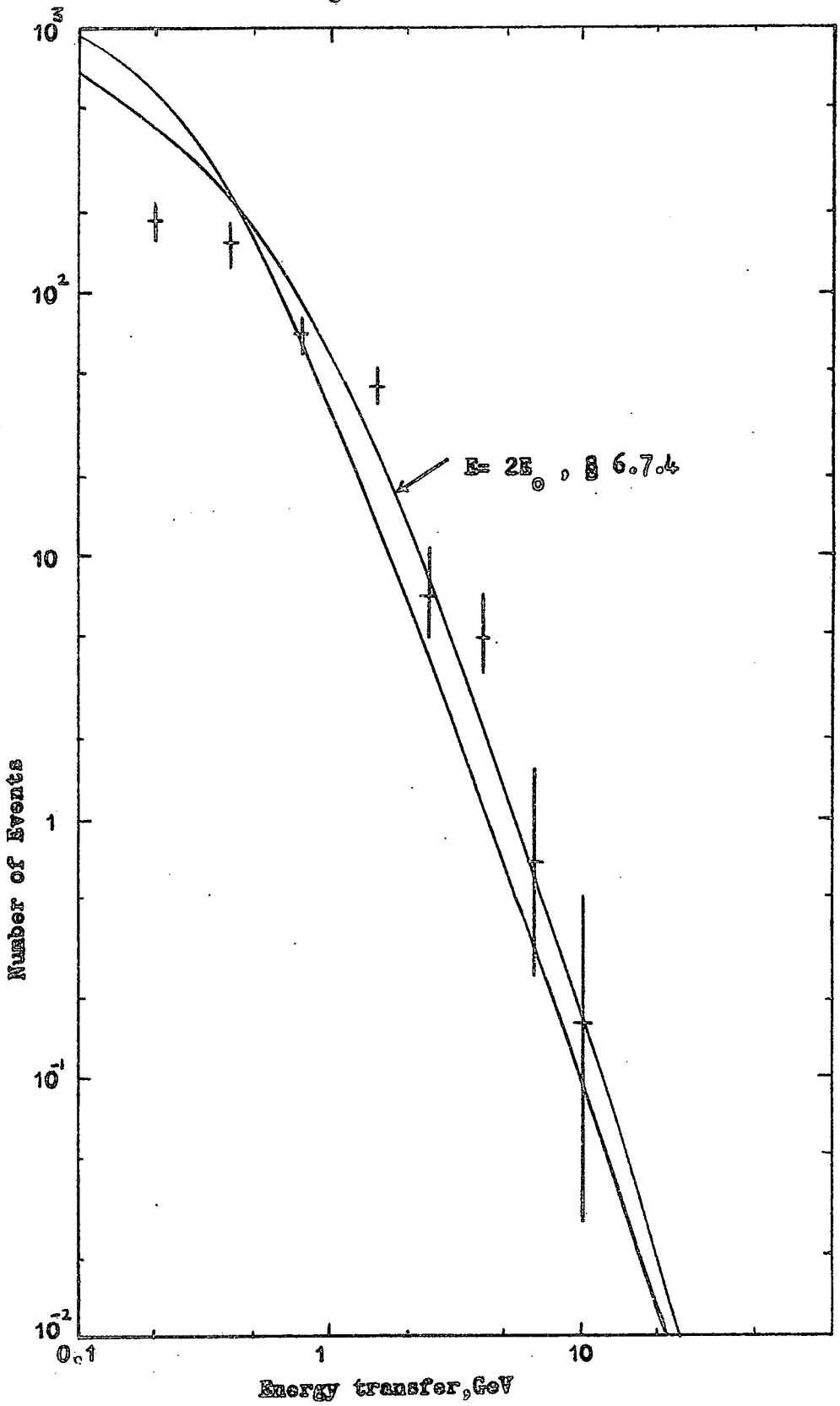

Differential transferred energy spectrum - Experiment A

Figure 6.3

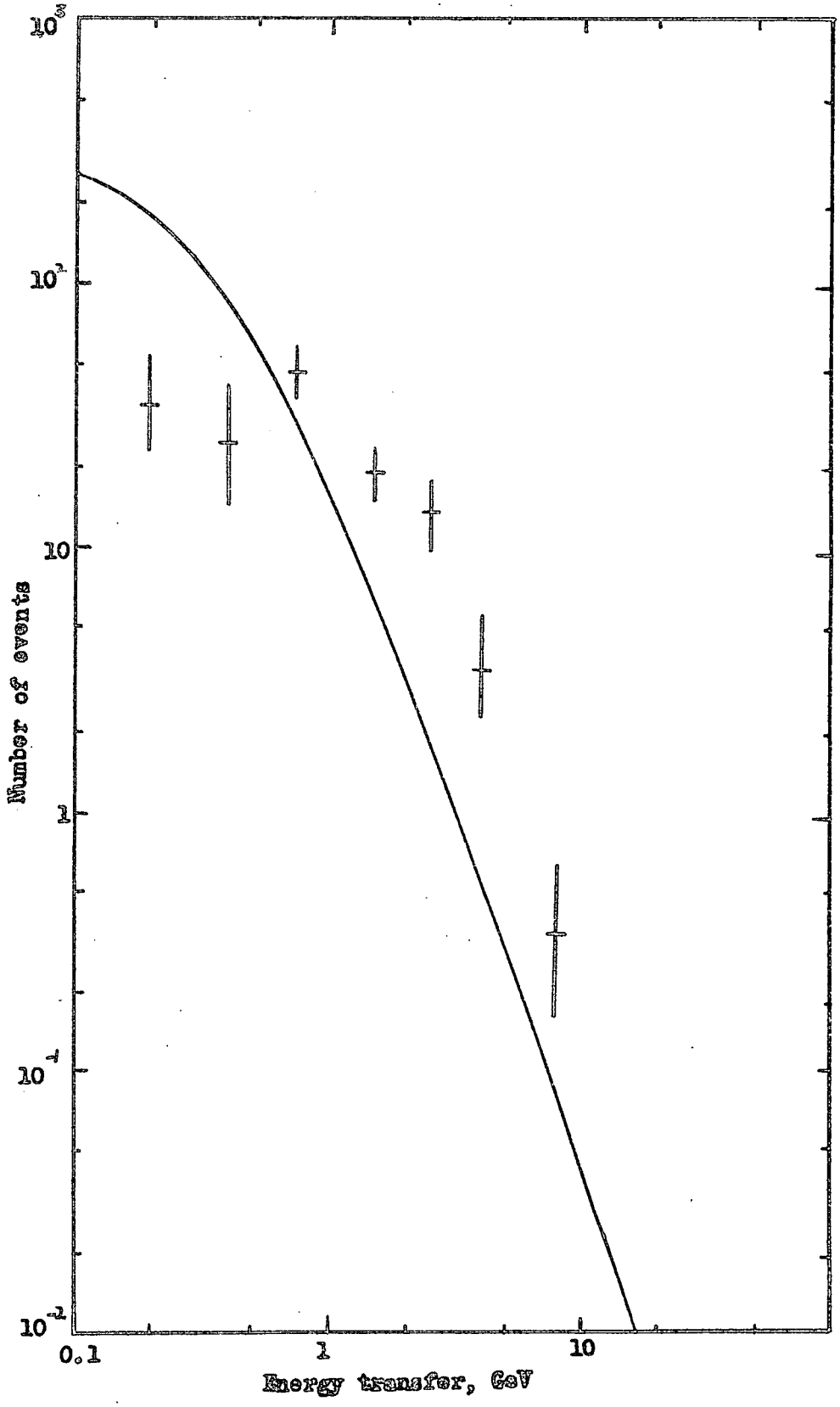

Differential transferred energy spectrum
Experiment B

a) A difference in the incident muonspectrum in the two experiments - by introducing the further amount of iron into the converter in experiment B the minimum momentum required by a vertical muon to traverse the apparatus was raised from 280 MeV/c to 335 MeV/c. Since the theoretical curves were calculated using the momentum spectrum of muons above 400 MeV/c such a change in the minimum required momentum should make no difference to the theoretical curves. However, it can be seen from the values of the two-fold geiger counting rates quoted in table 6.1 that the counting rate in experiment B was 83% of that in experiment A. Thus it would appear that by introducing the extra iron in experiment B 17% of the incident muons were stopped. Since the stopped muons would have had too little energy to produce 0.1 GeV knock-on electrons the probability per muon of getting an event should have been increased by approximately 20% as compared with that for experiment A. This would have the effect of reducing the discrepancies between the two sets of results.

b) An error in the energy estimates - the most probable error in estimating the energies of the cascade showers is due to the fact that the standard shower curves, §5.2, give the apparent number of electrons with energies greater than 2 MeV at any point in the shower. Since, in a scintillation counter, two, 1 MeV electrons would appear as a single electron in constructing the shower curve the actual number of electrons present at that point in the shower would be underestimated. Also, because the energy required by an electron for it to traverse the gap between two converter plates and trigger a flash tube was less than 1 MeV

it follows that the energies obtained using the standard shower curves would be overestimates of the true energy.

By examining figures 6.3 and 6.4 it can be shown that, if the true energy of the shower was E_o and the estimated energy was E, then the experimental points are a good fit to the theoretical line above 1 GeV if $E \simeq 2E_o$ for experiment A and $E \simeq 4E_o$ for experiment B. Since the energies in experiment B were estimated at depths 2.55 radiation lengths further down the shower than in experiment A, and since the average energy of the electrons in the shower decreases with depth, the difference in the two ratios E/E_o is probably due to the effect of electrons with less than 2 MeV, there being more of these at the depths considered in experiment B than at those in experiment A.

Because of the discrepancies between the experimental and predicted number of events in the different energy ranges, and the fact that these were possibly due to the choice of standard shower curves, the ratio of observed number of events to predicted number was calculated as a function of the transferred energy as estimated from three sets of shower curves.

The sets of shower curves used were:

a) The results of Backenstoss et al. (1963a).

b) Approximation B as given by Rossi (1952).

c) The results due to Buja (1963).

These results, which apply to showers produced in lead were converted to showers in iron using the expression

$$\frac{E_{Fe}}{E_{Pb}} = \frac{\epsilon_{Fe}}{\epsilon_{Pb}}$$

where E_{Fe} is the energy of the shower in iron, E_{Pb} is the shower energy in lead, and ϵ_{Fe} and ϵ_{Pb} are the critical energies in iron and lead respectively.

The results of these calculations, for the mean depths at which the shower energies were determined, are shown in figure 6.4 in the case of experiment A.

6.8 Conclusions

From figure 6.4 it can be seen that, although the results calculated from the three sets of shower curves give widely differing values for the ratios, the ratios calculated from each set do not show any tendency to increase with increasing energy above 1.5 GeV. Below this energy the ratios decrease with decreasing energy. This is probably due to an underestimation of the correction for the detection efficiency of the apparatus. Also contributing to this effect is the fact that, due to the assumptions used, the energies estimated using method I may have been underestimates of the true energies.

The results obtained from experiment B follow the same pattern as those from experiment A.

The final conclusion which can be drawn from the two experiments, A and B, is that there is no evidence from an increasing discrepancy between the experimental and theoretical cross-sections for the electromagnetic interactions of muons with increasing energy. This result is in contradiction to that of Deery (1960), §3.2.1 and figures 3.1 and 3.2.

Figure 6.4 Comparison of experimental and theoretical numbers for different cascade shower curves - experiment A

∘ Backenstoss et al. (1963a)

+ Approximation B (Rossi, 1952)

◎ Buja, 1963

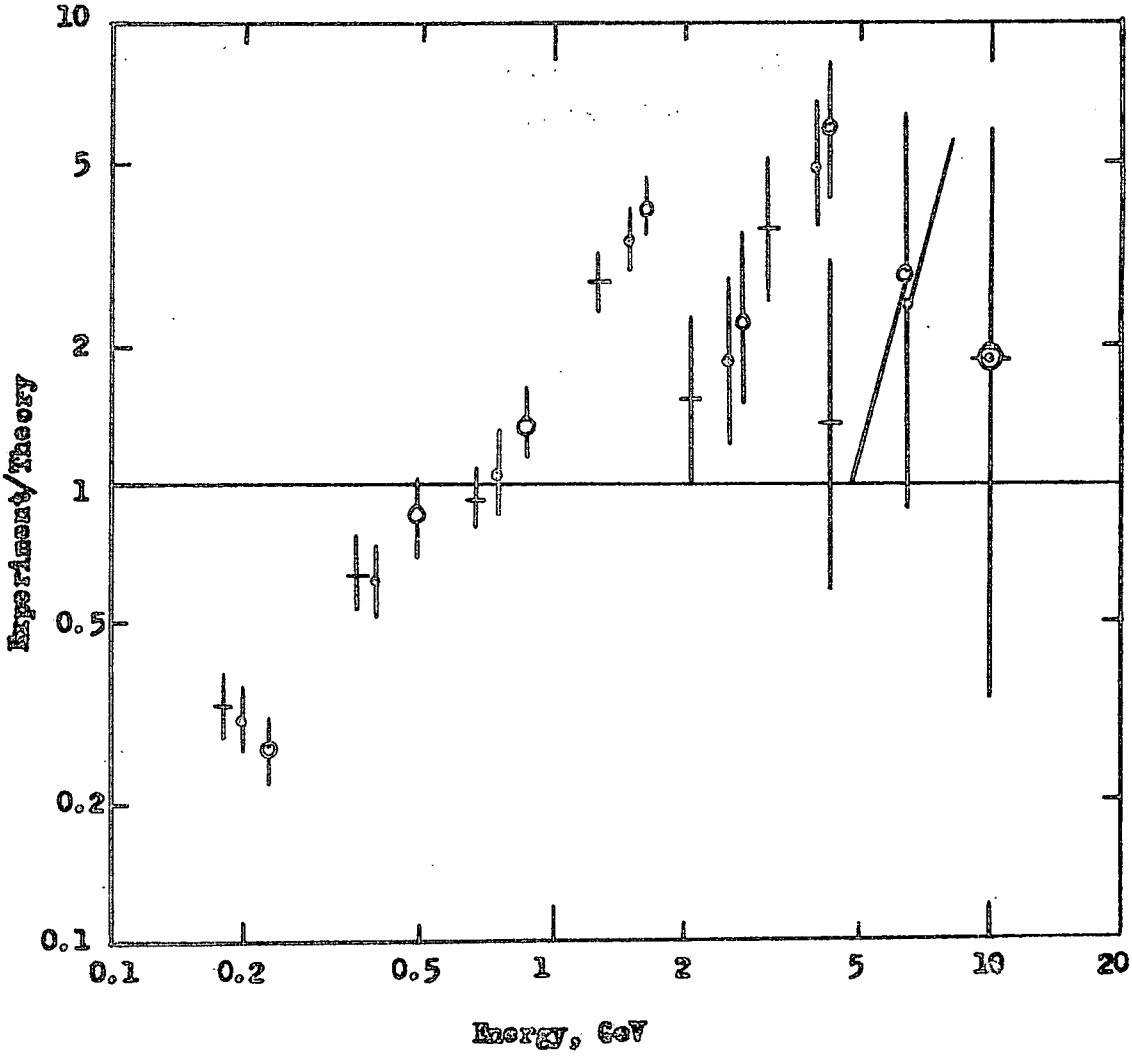

CHAPTER 7

THE LONDON EXPERIMENT

ELECTROMAGNETIC INTERACTIONS OF MUONS IN LEAD

7.1 Introduction

The electromagnetic interactions of muons in lead were studied using data provided by Dr. J.C. Barton of the Northern Polytechnic, London, from an experiment carried out at a depth of 60 m.w.e. in the laboratory on Holborn Underground Railway Station. In this experiment events were selected in which incident cosmic ray muons interacted in sheets of lead to produce secondary electrons and photons. The energies of these particles were determined by comparing the cascade showers produced by them in further sheets of lead with a set of standard shower curves.

7.2 General Description of Apparatus

The apparatus used in this experiment consisted of six large liquid scintillation counters interleaved with sheets of lead. Each of these lead sheets was 14.4 g cm^{-2} thick and was supported by 2.7 g cm^{-2} of aluminium, see figure 7.1.

Both above and below the stack there was a set of five index trays. Those above the stack were trays of geiger counters while those below were small liquid scintillation counters, figure 7.1.

Events were selected by requiring a coincidence between one or more of the top index trays, the fourth scintillation counter and one or more of the bottom index trays. The logarithms of the pulse heights from each of the scintillation counters were then converted

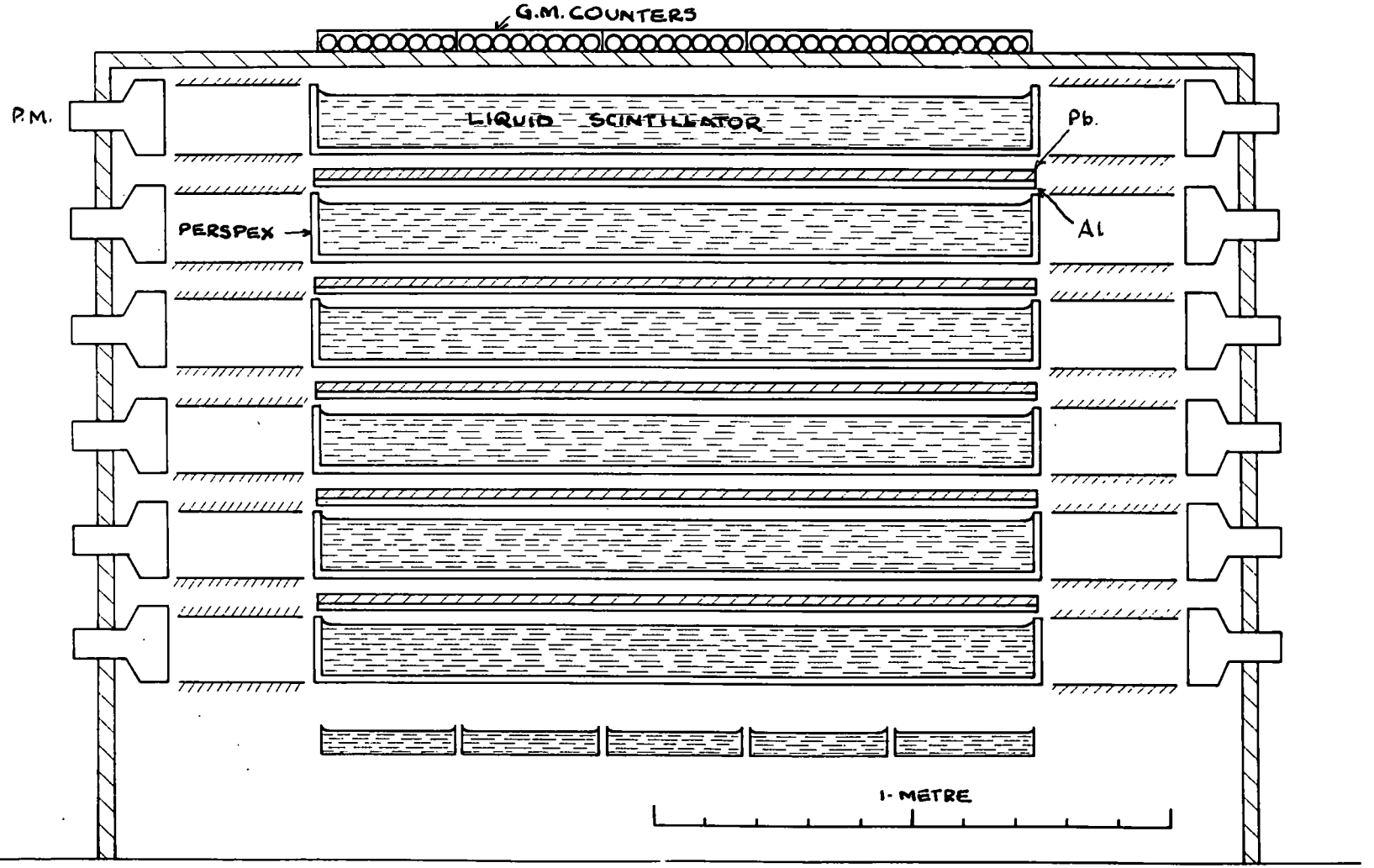

FIGURE 7.1 THE LONDON APPARATUS

into digital form and recorded on punched paper tape. Also recorded on this tape was information as to which of the index trays had been triggered.

7.3 The Scintillation Counters

7.3.1 Construction

The six large liquid scintillation counters used in this experiment were similar to that described by Barton et al. (1962). Each counter consisted of a tank of area 150 x 75 cm^2 and depth 10 cm constructed of $\frac{3}{8}$ in. thick Perspex. This was filled to a depth of 9.4 cm with liquid scintillator (medicinal paraffin (liquid paraffin, B.P.) + 0.8 g ℓ^{-1} p-terphenyl + 0.008 g ℓ^{-1} POPOP).

The tank was viewed through each of its two smallest faces by a five inch photomultiplier tube (E.M.I. type 9579b) with its photocathode at a distance of 22 cm from the tank. In order to improve the light collection efficiency of the counter the space between the tank and the photomultiplier tube was made into a rectangular light guide, with the same cross-section as the smallest face of the tank, by surrounding it with plane mirrors, figure 7.1.

7.3.2 Measurement of Output Pulse Heights

For each of the six scintillation counters the output pulses from the two photomultiplier tubes were added in a simple mixing circuit. The output pulses from this circuit were then fed into a logarithmic pulse height analyser (Barton and Crispin, 1962). This converted the logarithm of the pulse height into a train of pulses, the number of

pulses in the train being directly proportional to the logarithm of the pulse height.

Whenever a sufficiently large pulse was obtained from the fourth scintillation counter, §7.3.3, the number of pulses in the pulse train was recorded, in digital form, by a 64-channel register.

7.3.3 The Fourth Scintillation Counter as part of the Selection System

As well as being fed into the pulse height analyser the pulse from the fourth scintillation counter was also used to control both the recording of the pulse heights from all six scintillation counters and the selection of events.

To control the recording of the pulse heights the pulse from the fourth scintillation counter was fed into a variable attenuator. The output pulse from this attenuator, which was used in the same way as the variable bias in a discriminator circuit, was then fed into a fast amplifier with a fixed gain and a resolving time of 0.1 μsec. The pulse from this was then fed into a master circuit with a fixed trigger level. If the output pulse from the amplifier was of sufficient size to trigger this master circuit the latter carried out two operations:

i) It opened a 200 μs long gate between the pulse height analysers and the 64-channel registers, and

ii) It quenched the photomultiplier tubes of the six scintillation counters by connecting together two of the dynodes in each of the photomultiplier tubes, thus reducing the gains by a factor of between

15 and 20. The length of time for which the photomultiplier tubes were quenched was 800 μsec if no event was selected and 700 msec if an event was selected.

In its role as part of the selection system the output pulse from the fourth scintillation counter was fed into a tunnel diode fast coincidence circuit which gave an output pulse whenever a coincidence was obtained between this pulse and a pulse from the bottom index trays. This coincidence circuit had a measured resolving time of 150 ns.

7.4 The Index Trays

7.4.1 Introduction

It has already been mentioned, §7.2, that both above and below the scintillation counter - lead stack there were five index trays. These were incorporated into the apparatus for three reasons, namely:

i) They indicated the number of particles incident upon, and leaving, the stack.

ii) They indicated the direction, in one plane, of incident single particles which traversed the apparatus, and

iii) They acted as part of the selection system.

7.4.2 The Geiger Counter Index Trays

Each of the five upper index trays consisted of a tray of eight, 60 cm long geiger counters (20th Century, type G.60) connected in parallel. From these trays of counters the output pulses were used in two ways:

i) The output pulses from each tray were fed into a register which recorded whether or not a particle had passed through that tray. In this way an indication of the number of particles incident upon the stack, in terms of the number of index trays which had been triggered, and the positions at which these had arrived, was obtained.

ii) The output pulses from all five of the index trays were fed into a Rossi coincidence circuit which was part of the selection system.

7.4.3. The Scintillation Counter Index Trays

Each of the five lower index trays consisted of a liquid scintillation counter, of area 27 x 11 in.^{2} and depth 2 inches. These counters were constructed in a way similar to the large scintillation counters except that instead of using two photomultiplier tubes the scintillator was viewed by a single 2 inch photomultiplier tube (E.M.I. type 9584b).

In the same way as the upper index trays were used as part of the selection system and also to indicate the number and positions of particles incident upon the stack, the lower trays were used as part of the selection system and indicated the number and positions of particles leaving the stack. The method used to indicate which of the trays had been traversed by particles was identical with that for the upper trays. At the same time the pulses from all five trays were mixed and fed into the tunnel diode coincidence circuit, §7.3.3. This circuit then gave an output pulse whenever a coincidence occurred

between a pulse from one of the scintillation counter trays and a pulse from the fourth large scintillation counter.

The output pulses from the tunnel diode coincidence circuit were then fed into the Rossi coincidence circuit, §7.4.2, which gave an output pulse whenever a coincidence occurred between one of these pulses and a pulse from the geiger counter index trays.

7.5 The Selection and Recording of Events

Both the selection and the recording of events were controlled by the fourth large scintillation counter. The selection was carried out by requiring a fast coincidence between the output pulse from this scintillation counter and the lower set of index trays. This coincidence was selected using a tunnel diode coincidence circuit which gave an output pulse whenever a coincidence occurred. The output pulse from this coincidence circuit was then fed into a Rossi coincidence circuit. This gave an output pulse whenever a coincidence occurred between a pulse from the upper index trays and the tunnel diode coincidence circuit. Hence events were selected by requiring a coincidence between both sets of index trays and the fourth large scintillation counter.

In controlling the recording of events the output pulse from the fourth large scintillation counter was used to trigger a master circuit, the size of pulse required to trigger this circuit being set by a variable attenuator. The master circuit then carried out three operations:

1) It quenched the photomultiplier tubes of the six large scintillation counters, §7.3.3.
2) It opened a gate between the pulse height analysers, §7.3.2, and allowed the pulse heights from each of the large scintillation counters to be recorded by the 64-channel registers.
3) It opened a gate between the output of the Rossi coincidence circuit and the circuit controlling the read out of the description of the event onto punched paper tape.

If the master circuit had been triggered but no coincidence had occurred at the Rossi coincidence circuit then a pulse was sent to each of the registers to reset them. When a coincidence occurred at the same time as the master circuit was triggered the read out circuit caused the information contained in the registers to be recorded on punched paper tape. Thus a description of the event, in terms of the index trays which had been triggered and the pulse heights from each of the large scintillation counters, was obtained.

7.6 The Dead Time of the Apparatus

The dead time of the apparatus was controlled by the master circuit. In the case where the master circuit was triggered but no event was obtained the imposed dead time was 800 μs during which the photomultiplier tubes were quenched. When an event was selected and the master circuit had been triggered the dead time was 700 msecs during which the tape punch was operated.

7.7 The Resolving Time

In carrying out a purely counter experiment, such as this one, an important parameter is the resolving time of the apparatus, which controls the number of random coincidence events which could be expected. Since the selection of events in this experiment was carried out using a fast-slow coincidence system, i.e. a fast coincidence is required between the fourth large scintillation counter and the lower index trays, followed by a slow coincidence between the upper set of index trays and the coincidence pulse from the fast coincidence circuit, it is not possible to give a definite value for the resolving time. An estimate of the expected rate of random coincidences can be obtained, however, by comparing the components of the selection system separately i.e.

1) The amplifier into the master circuit - this amplifier had a resolving time of 0.1 μs. Since the counting rate of the fourth large scintillation counter was 10-15 counts/sec the probability of two pulses arriving within 0.1 μs of each other was negligible.

2) The tunnel diode coincidence circuit - this had a resolving time of 150 ns. Since the lower index trays counted at a rate of 200 counts/sec and the fourth large scintillation counter at 10-15 counts/sec the expected rate of random coincidences was $(4 \rightarrow 6).\ 10^{-4}$/sec.

3) The Rossi coincidence circuit - as no attempt was made to measure the counting rate of the tunnel diode coincidence circuit it was not possible to put a value on the rate of random coincidences from the Rossi circuit.

A further possible source of error is present in the pulse height analysers. If two scintillation counter pulses arrive at the ringing circuit within 200 μs of each other than, depending upon their relative times of arrival, the pulse height would be greater or smaller than either of these two pulses. Since the counting rates of the large scintillation counters were 10-15 counts/sec the probability of this happening was $\sim e^{-500}$ and was thus negligible.

7.8 Running Times

The data obtained from this experiment was in two parts. In the first of these the fourth large scintillation counter was biassed to accept single particles and the total sensitive time, corrected for the dead time, was 422 minutes.

In the second run the fourth large scintillation counter was biassed to accept four or more particles. The total sensitive time was 6760 minutes.

CHAPTER 8

ANALYSIS OF THE LONDON DATA

8.1 Introduction

It has already been mentioned, §7.5, that a description of each event selected by the apparatus was recorded on punched paper tape. A preliminary analysis of this tape was then carried out, using the London Atlas computer, in which the events were sorted into four groups, namely:

1) Incomplete events

2) Incident muons

3) Incident showers

4) Interactions

The descriptions of the interactions were then converted into a more convenient form than the original and re-recorded on punched paper tape.

A copy of this tape was sent to Durham where the interactions were grouped according to the maximum pulse height obtained from one of the six large scintillation counters and the direction of incidence of the muon undergoing the interaction.

By comparing the number of particles at the maximum of the cascade shower, determined from the maximum pulse height registered, with the number predicted by theory the energy of the secondary particle from the interaction was estimated.

This chapter contains descriptions of the London analysis, the Durham analysis and the theoretical shower curves used in the energy estimation.

8.2 The London Analysis

8.2.1. The Original Form of the Data

The description of an event was recorded in the form of two numbers, one containing five digits and the second twelve digits. The first of these numbers indicated which of the index trays had been triggered. In order to do this each digit represented one pair of index trays, an upper tray and the one vertically below it (figure 7.1). Depending upon which of the pair of index trays had triggered this digit could take one of four values, i.e. 0, 1, 2, or 3. The meaning of each of these values is given in table 8.1

TABLE 8.1

Value of digit	Event
0	Neither of the index trays triggered.
1	The top index tray triggered.
2	The bottom index tray triggered.
3	Both index trays triggered.

The twelve digit number contained the information obtained from the six large scintillation counters. Each of these counters was represented by a two digit number which represented the pulse height obtained from the counter. These two digit numbers were actually the number of pulses from the logarithmic pulse height analysers, §7.3.2, which had been recorded by the 64-channel registers and will be known as the 'channel numbers'.

Thus it can be seen that between them the two numbers, the five digit and the twelve digit number, contained information about the number of particles incident upon, and leaving, the apparatus, their angles of incidence and the number of particles, represented by the pulse height, passing through each of the six large scintillation counters.

8.2.2 The Division of the Events

In dividing the events into the groups named in §8.1 the following selection criteria were used:

1) Incomplete events - events in which one or both of the numbers describing them contained more or less than the required number of digits, and those events in which no pulse was recorded from either of the sets of index trays or from one or more of the large scintillation counters.

2) Incident muons - those events in which only one upper and one lower index tray had triggered and in which the pulse height from each of the large scintillation counters was within the limits for single particles, as determined from a calibration run.

3) Incident showers - events in which more than one of the upper index trays had triggered and events in which the pulse height from the first large scintillation counter was greater than that for a single particle.

4) Interactions - this group contained those events in which only one of the top index trays had triggered, the pulse height from the first large scintillation counter was that for a single particle, the

pulse height from at least one of the remaining five large counters was equivalent to more than one particle, and one or more of the lower index trays had triggered.

Once the events had been sorted into these groups the interactions were given a category number, in place of the five digit number, which represented the pattern of index trays which had triggered. The descriptions of the interactions were then recorded on punched paper tape.

8.3 The Durham Analysis

8.3.1 Introduction

To determine the energy of an electron or photon from the cascade shower which this particle produces in an absorber one may use one or more of the following parameters of the shower:

1) The total electron track length in the shower (§5.3).

2) The number of particles at a depth t in the shower (§5.4).

3) The number of particles present at the maximum of the shower. This is a special case of (2).

In the present experiment it was only possible to use the last of these three parameters. The reasons for rejecting the first two were:-

1) Since the lead plates in which the showers developed were each 2.47 radiation lengths thick (14.4 g cm^{-2}), §7.2, the uncertainty in determining the total track length in the shower would be large.

2) The determination of the depth in the shower at which the measurement of the number of particles was made would be subject to an uncertainty

of the order of the thickness of one of the lead plates. Although this also applies to the determination of the number of particles at the shower maximum it will be shown in §8.3.5 that, at least for high energy showers, the uncertainty in the position of the shower maximum is relatively unimportant.

A third reason for using the number of particles at the shower maximum, rather than the number at a depth t, to estimate the shower energy is that it has been shown experimentally (Nichiparuk and Stugal'skii, 1964) that the fluctuations on the number of particles at shower maximum are smaller than at any other depth in the shower.

8.3.2 Grouping of the Events

The interactions contained on the paper tapes from the London analysis were grouped according to a) the category of the interaction, §8.2.3, b) the maximum channel number in the interaction, and c) the large scintillation counter in which this maximum occurred.

The reasons for carrying out this grouping procedure were:

1) to determine the angle of the incident muon (a)

2) to reject events which had an apparent maximum in the sixth large scintillation counter. Such events could not be used in the analysis

3) to obtain the differential spectrum of maximum channel numbers.

8.3.3 Conversion from Channel Number to Number of Particles

The logarithmic pulse height analyser, §7.3.2, gave a cycle of 16 channels for an increase in the pulse height recorded of a factor of 10. Thus it can be seen that if the mean channel number for a single particle is $\bar{c}$ and the recorded channel number for a shower is c then

the number of particles present in the scintillation counter is

$$N = \exp\left(\frac{c - \bar{c}}{16} \log_e 10\right) \qquad 8.1$$

From this expression it can be shown that the width of a channel is 14.5%.

8.3.4 The Calibration Curve

In predicting the number of particles present at the maximum of a cascade shower which develops in a sandwich of lead and scintillation counters and is seen in a scintillator it is necessary to take into account the following factors.

a) The effect of electrons with energy less than that required to traverse the counter. Each of these electrons can be taken as contributing an amount to the pulse height from the counter proportional to its track lengths in the counter.

b) The interactions of photons in the counter which give rise to electrons which are seen by the counter.

c) The angular spread of the shower particles. This causes each particle traversing the counter to have a greater track length than a vertical particle and thus appear as more than one particle.

Using the Monte Carlo results of Crawford and Messel (1962) and Messel et al. (1962) shower curves were constructed taking the above effects into account.

Since these results only applied for shower energies up to 1 GeV the shower curves obtained in this way were compared with those due to

Buja (1963), Belen'kii and Ivanenko (1959) and Approximation B (Rossi, 1952). As a result of good agreement in the overlap energy region it was decided to use the results of Buja which cover shower energies from 0.3 to 10^5 GeV.

The calibration curve obtained from Buja's results is shown in figure 8.1. From this curve it is found that the number of particles at the shower maximum, N, and the energy of the incident electron, E_o, are related by the expression

$$N = 13.60\ E_o^{0.912} \qquad 8.2$$

which is in fair agreement with elementary cascade theory (Rossi, 1952) which gives

$$N = K\ E_o$$

By combining equations 8.1 and 8.2, and taking into account the incident muon, it is possible to determine the energy of a shower with a maximum channel number, C.

8.3.5 Discussion of Analysis

In taking the maximum channel number to determine the shower energy it is assumed that the shower maximum always occurs in a scintillation counter. Although this is obviously not correct the errors in the energy estimates can be shown to be small, particularly at high energies, by consideration of figure 8.2. From this figure it can be seen that if one considers depths $1\frac{1}{4}$ radiation lengths on either side of the shower maximum then in the case of a 0.3 GeV shower the number of particles is 3.5 as compared with 4.6 at the maximum. Thus the

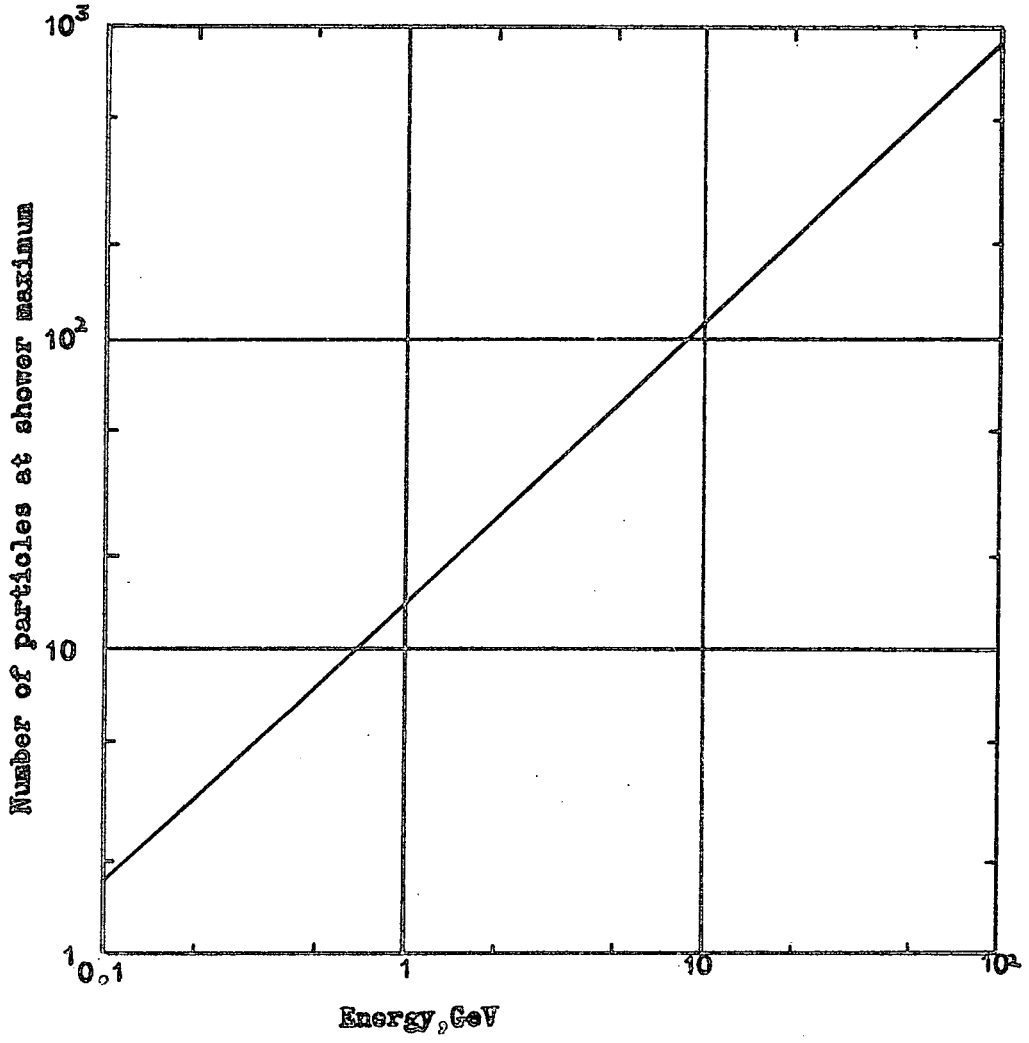

Figure 8.1 Calibration curve for the London Experiment

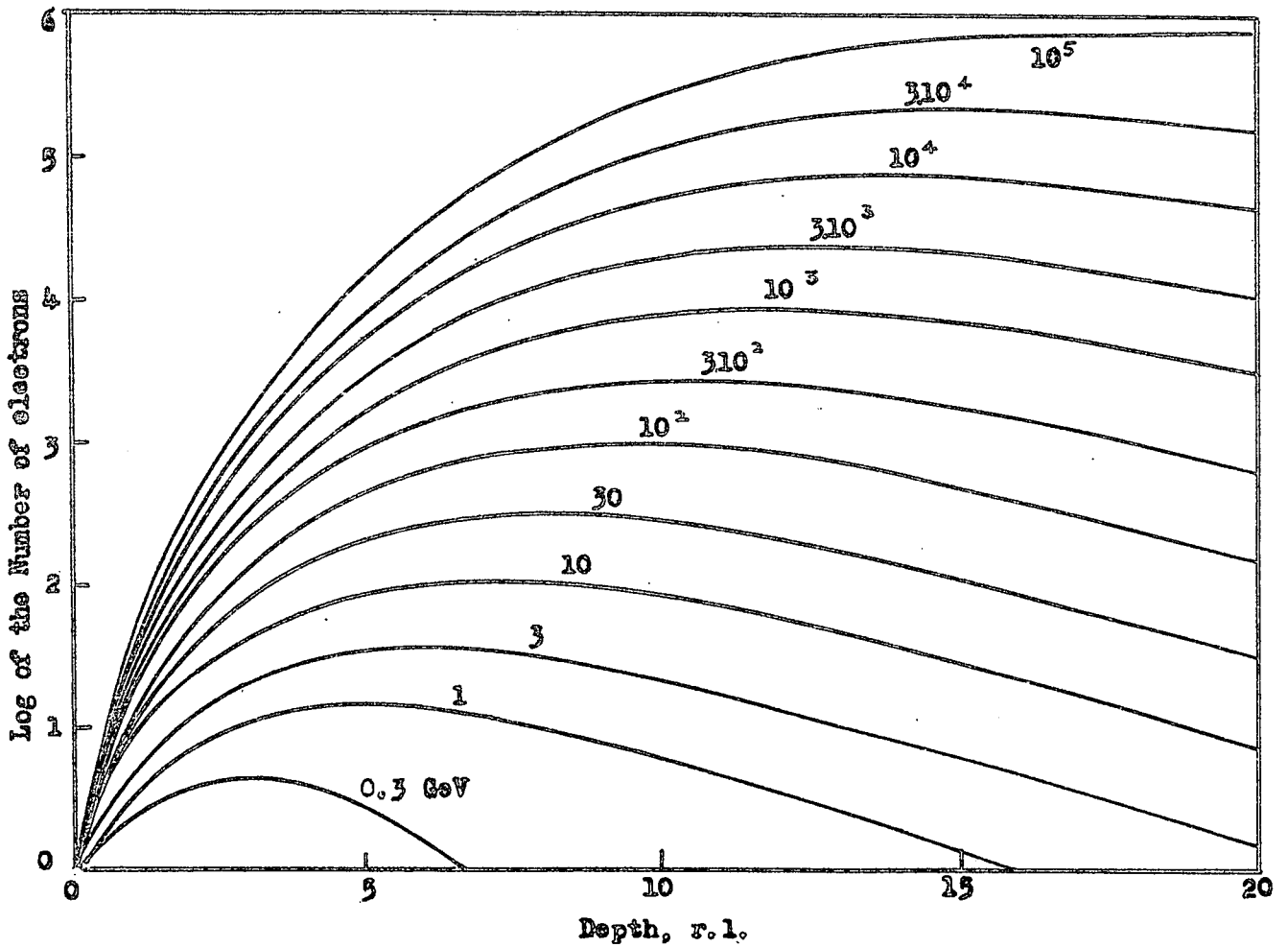

Figure 8.2 Average cascade shower curves for showers initiated by electrons (Buja, 1963)

shower energy would be underestimated by 24%. This factor by which the energy is underestimated decreases with increasing energy, being 7% at 10 GeV and 5% at 100 GeV.

Apart from the above uncertainty, which always gives rise to underestimates of the shower energies, the major uncertainty is due to the statistical fluctuations in the number of particles at the shower maximum. While the calculations due to Buja (1963) do not give estimates for these fluctuations the Monte Carlo calculations of Messel (private communication), in which he considers shower electrons with energy greater than 10 MeV, and the experimental results of Nichiparuk and Strugal'skii (1964) and Backenstoss et al. (1963a) contain details of the fluctuations. Table 8.2 shows the value of the standard deviation of the number of particles at shower maximum according to these workers.

TABLE 8.2

Workers	Standard deviation on N particles at shower maximum
Messel (private communication, 1964)	$\simeq \sqrt{N}$
Nichiparuk and Strugal'skii, (1964)	$\simeq 0.25\sqrt{N}$
Backenstoss et al. (1963a)	$\simeq 0.50\sqrt{N}$

Hence $\frac{dE_o}{E_o} = \frac{1}{k\sqrt{N}}$, where E_o is the shower energy, N is the number of particles at the maximum and k is a constant of value greater than 1. As the value of N, and thus E_o, increases the uncertainty upon the energy estimate decreases until it becomes less than the uncertainty due to the channel width, §8.3.3. This point is reached at different

channel numbers, depending upon the value of k taken.

It is of interest to note here that the uncertainty due to statistical fluctuation is in all cases greater than that in determining the shower maximum.

CHAPTER 9

RESULTS AND CONCLUSIONS FROM THE LONDON EXPERIMENT

9.1 Introduction

This chapter contains details of the results obtained when the interactions selected by the apparatus were analysed by the method described in Chapter 8. These results, in the form of a differential transferred energy spectrum, are then compared with the predicted spectrum and the result of this comparison discussed.

In carrying out the comparison between experiment and theory the experimental results are considered in two sets, namely:
1) The unbiassed set i.e. those results which were obtained with the fourth large scintillation counter biassed to accept all pulse heights equal to, and greater than, the pulse height for a single particle.
2) The biassed set i.e. the results which were obtained with the fourth large scintillation counter biassed to accept only those events which gave a channel number equal to, or greater than, 20.

9.2 The Predicted Results

9.2.1 Introduction

In the calculation of the predicted transferred energy spectrum a basic spectrum, in the form of the probability/muon/GeV/g cm^{-2} Pb that an incident muon, at a depth of 60 m.w.e. underground, would undergo an electromagnetic interaction giving rise to secondary particles with energy E as a function of E, was obtained. For each of the two parts of the experiment this spectrum was then multiplied by the number of

muons incident upon the apparatus, and the target thickness seen by these muons, to give the predicted differential energy spectrum.

9.2.2 The Basic Spectrum

The basic transferred energy spectrum was obtained using the probabilities for the electromagnetic interactions given by equations 2.1, 2.2 and 2.9 (with $\alpha = 2$, $a = 10\ m_e c^2/\epsilon$) and folding in the incident muon energy spectrum. This spectrum, which is shown in figure 9.1, was derived from the sea level muon momentum spectrum due to Hayman and Wolfendale (1962). In the derivation the depth of the apparatus, 60 m.w.e., was divided into 1 m.w.e. intervals and then the energy of an incident muon upon leaving one of these intervals was determined from its incident energy using the energy loss equation due to Hayman et al. (1963). This was repeated for all muon energies for each of the sixty intervals to give the final energy spectrum at 60 m.w.e.

The basic transferred energy spectrum obtained from these calculations, which were carried out on the University of Durham Elliott 803 computer, is shown in figure 9.2.

9.2.3 The Target Thickness

The target thickness to be used in the calculation of the energy spectrum depends upon a) the type of interaction considered, and b) the development of the cascade shower produced in the interaction, and thus the method of selecting events. The reasons for the dependence upon these factors and the way in which this was allowed for are as follows:

Figure 9.1.

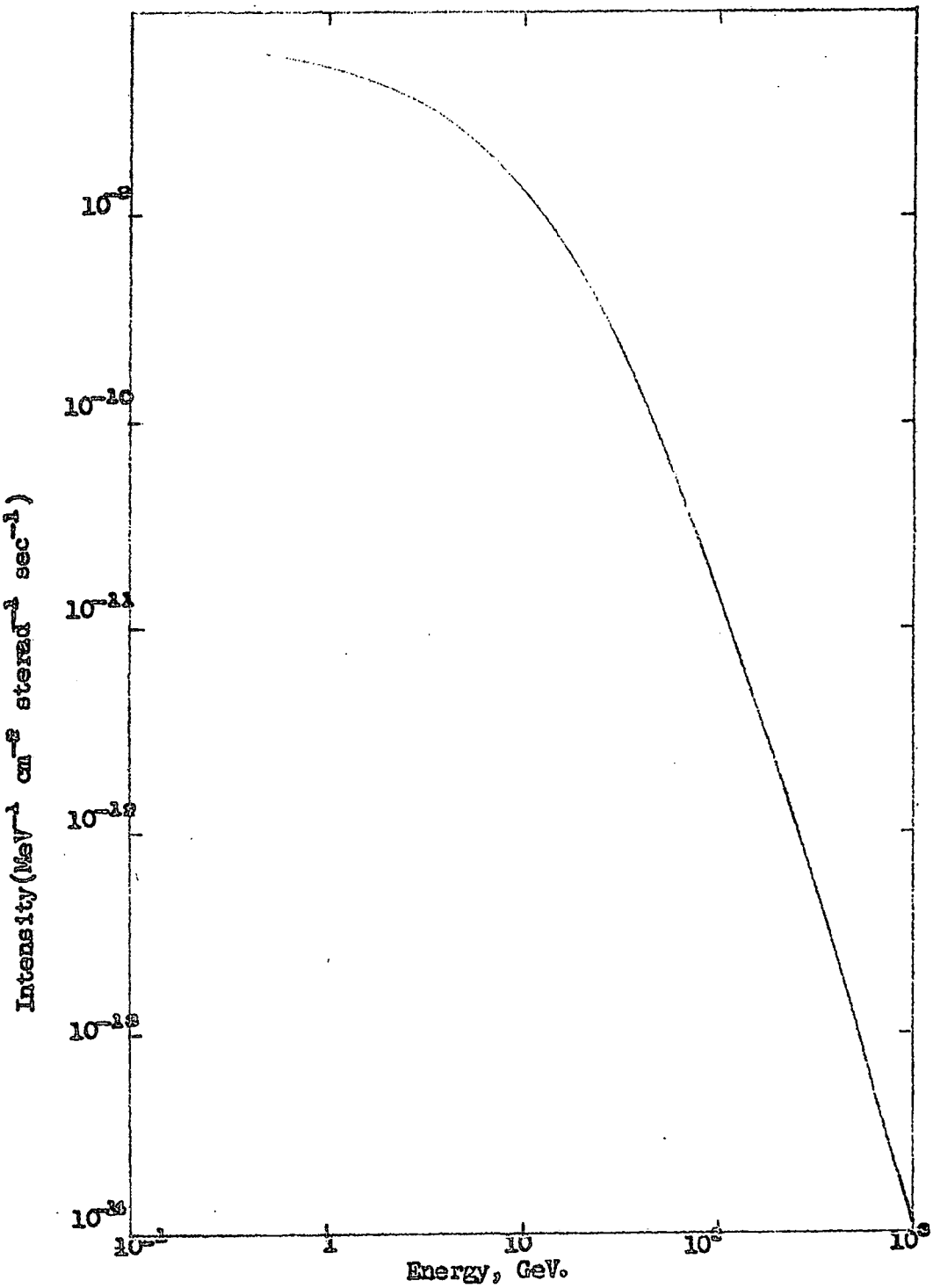

The differential incident Muon energy spectrum at 60 m.w.e. calculated from the sea level spectrum of Hayman and Wolfendale (1962) using the energy loss equation due to Hayman et al., (1963).

Figure 9.2

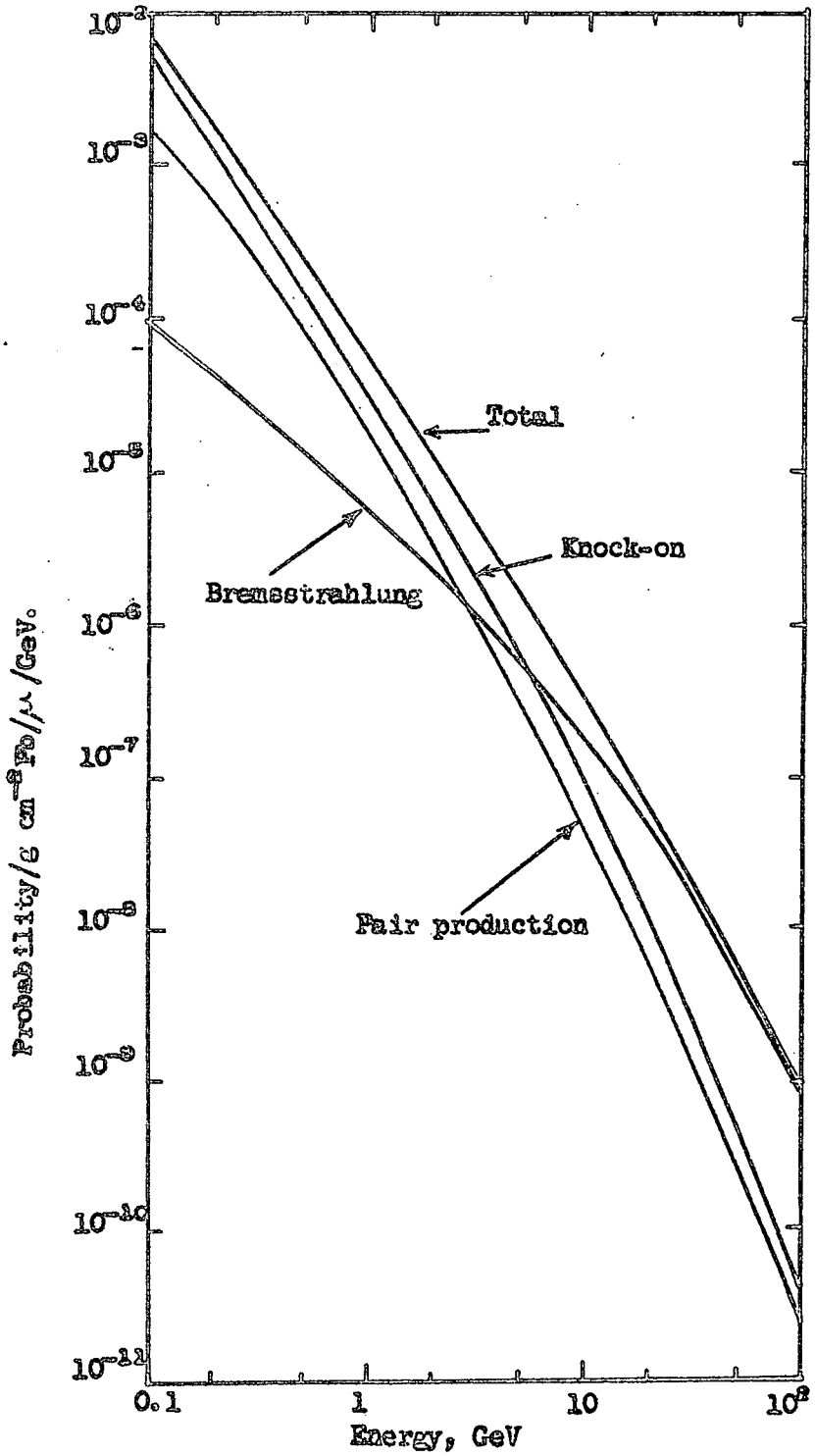

Differential Probabilities for the Electromagnetic Interactions of Muons in Lead at 60m.w.e.

a) The type of interaction considered - since the apparatus contained, as well as the lead, a relatively large amount of liquid scintillator, perspex and aluminium (Chapter 7) these materials must be considered when calculating thetarget thickness. To do this account is taken of the fact that the probability per g cm^{-2} of a muon undergoing knock-on production is proportional to Z/A, where Z is the atomic number of the target material and A is its atomic weight. For bremsstrahlung and pair production, on the other hand, the probabilities are proportional to Z^2/A. For one unit of the apparatus, consisting of one scintillation counter, one lead sheet and one aluminium sheet, the target thicknesses for the various interactions are as given in table 9.1.

TABLE 9.1

Material	g cm^{-2}	Z	A	Effective Target thickness g cm^{-2} K.O.	Br.	P.P.
Scintillator and perspex (C)	9.2	6	12	11.6	0.85	0.85
Lead	14.4	82	207.2	14.4	14.40	14.40
Al	2.7	13	27	3.3	0.52	0.52
		Totals		29.3	15.77	15.77

From this table it can be seen that by taking into account all of the material in one unit the amount of target present for knock-on production is almost twice that for both bremsstrahlung and pair-production. It will be shown later that this fact has quite an effect upon the energy range over which knock-on production is dominant.

b) The cascade shower development - Because only those events were used in the analysis which had a maximum in or before the fifth large scintillation counter, §8.3.2, and because a cascade shower requires a finite thickness of absorber to reach its maximum the amount of target available for the interaction depends, in the unbiassed case, upon the rate of development of the shower. In the biassed case account has also to be taken of the fact that a certain minimum number of particles must be present in the fourth large scintillation counter. To allow for these facts it was assumed that the development of a cascade shower was simply proportional to the amount of absorber, independent of the type of absorber, in radiation lengths that was present between the point of interaction of the muon and the large scintillation counter in which the maximum was expected to occur.

Using this assumption the amount of target available for different shower energies was calculated, in the unbiassed case, by assuming that the shower started at the top of the apparatus and finding the scintillation counter in which the number of particles would be a maximum, using the cascade shower curves due to Buja (1963) (figure 8.2). By moving the point of interaction of the shower down through the apparatus, at intervals of 0.1 units for 0.3 GeV showers and 0.2 units for greater energy showers, until the maximum fell in the sixth large scintillation counter the target thickness, in units, for each shower energy was determined. To convert from units to g cm^{-2} account was taken of the fraction of a unit made up of C(scintillator and perspex), Pb and Al (Table 9.2) to determine the amount of each of these materials present in the target.

TABLE 9.2

Material	g cm^{-2}/ unit	Fraction of unit
C	9.2	0.074
Pb	14.4	0.886
Al	2.7	0.040

For the biassed set of results the calculation was carried out in exactly the same way as for the unbiassed set with the added proviso that the number of particles in the fourth large scintillation counter was greater than, or equal to, 3.5. In the case of showers of low energy, of the order of 1 GeV or less, this had the effect of making the first point at which the interaction producing the shower could occur part of the way through the apparatus and not at the top as in the unbiassed case.

For both knock-on production and direct pair production the cascade shower curves used were those for electron induced showers while for bremsstrahlung, photon induced shower curves were used (Buja, 1963).

9.2.4 The Effect of the Incident Angle of the Muon

Since themuons incident upon the apparatus did not allarrive in the vertical direction it was necessary to take into account the increase of target thickness due to the angle of incidence of the muons. To do this the mean angles of incidence of muons in different categories of events, §8.2.2, were determined from the ratio of the mean pulse height for vertically incident single muons and the mean pulse height for muons in the category considered. The results of this calculation are shown in table 9.3.

TABLE 9.3

Category Vertical	Mean Angle $\bar{\theta}$ 0	Descriptions of events (§8.2.1)
6,7	10° 9'	30000, 03000, 00300, 00030, 00003
8	$26^{\circ}15'$	12000, 21000, 01200, 02100, etc.
9	39° 4'	10200, 20100, 01020, 02010, etc. 10020, 20010, 01002, 02001
10	$48^{\circ}28'$	10002, 20001

To allow for these angles in calculating the target thickness it was simply necessary to increase the thickness of each unit by $\cos \theta^{-1}$ when carrying out the calculations described in §9.2.3.

9.2.5 The Effect of the Point of Interaction on the Estimated Energy of the Shower

It was stated in §8.3.1 that one reason for determining the energy of showers obtained experimentally from the maximum number of particles at any point in the shower was that the inaccuracy in determining the position of this maximum point, due to the thickness of the lead sheets, was less than for any other point in the shower. However, as a check of this assumption and in order to correct for any error which may be introduced in this way for electron induced showers, and to allow for the fact that photon induced showers contain less particles at their maxima than do showers due to incident electrons, the mean value of the maximum which would be seen for a shower of a certain energy was determinedas follows.

At the same time as the target thickness was being calculated,

§9.2.3, the maximum number of particles in any one large scintillation counter was determined for each point of interaction of the muons. The arithmetic mean value was then calculated for this particular shower energy and the equivalent energy which would be allotted to such a shower was determined from the calibration curve, figure 8.5.4. Examples of the results of this calculation are given in table 9.4.

TABLE 9.4

Incident Energy, GeV	Equivalent Energy, GeV, e induced	Equivalent Energy, GeV, γ induced
1	0.97	0.76
10	9.73	7.86
100	97.60	80.76

From this table, which applies to showers produced by vertically incident muons in the unbiassed run, it can be seen that for electron induced showers the error which would have occurred if it had been assumed that the maximum seen was the true maximum of the shower is, for energies greater than 1 GeV, less than 3%.

§9.2.6 The Predicted Energy Spectra

To obtain the final predicted energy spectrum for the unbiassed and biassed sets of results the basic probabilities of figure 9.2 were multiplied by the calculated target thickness and the number of muons traversing the apparatus. This was done for each of the angles of incidence given in table 9.3, the values of the probability from figure 9.2 being that for the incident electron or gamma energy

and the result being plotted at the equivalent energy (table 9.4).

The number of muons selected in each category is given in table 9.5 for both the unbiassed and biassed runs and the resultant curves, obtained by summing the curves for all of the categories are shown in figure 9.3 for the unbiassed run and figure 9.5 for the biassed run.

TABLE 9.5

Category	Measured Number of Muons (unbiassed)	Estimated Number of Muons (biassed)
Vertical	$1.445\ 10^{4}$	$2.303\ 10^{5}$
6,7	$1.930\ 10^{4}$	$3.076\ 10^{5}$
8	$9.402\ 10^{3}$	$1.499\ 10^{5}$
9	$3.472\ 10^{3}$	$5.534\ 10^{4}$
10	$8.30\ 10^{2}$	$1.323\ 10^{4}$

From an examination of figure 9.3, and a comparison of these curves with the basic probability curves of figure 9.2, it can be seen that, due mainly to the difference in target thickness contained in one unit of the apparatus for knock-on production, as against bremsstrahlung and direct pair production, knock-on production is more truly the dominant process than if only lead had been the target. Also, for the same reason, plus the fact that the equivalent energy for a bremsstrahlung shower is approximately 80% of the incident energy, table 9.4, the knock-on process is dominant over a much larger range of energy than in the case of a lead target alone, i.e. up to 15 GeV as against 5 GeV.

Figure 9.3

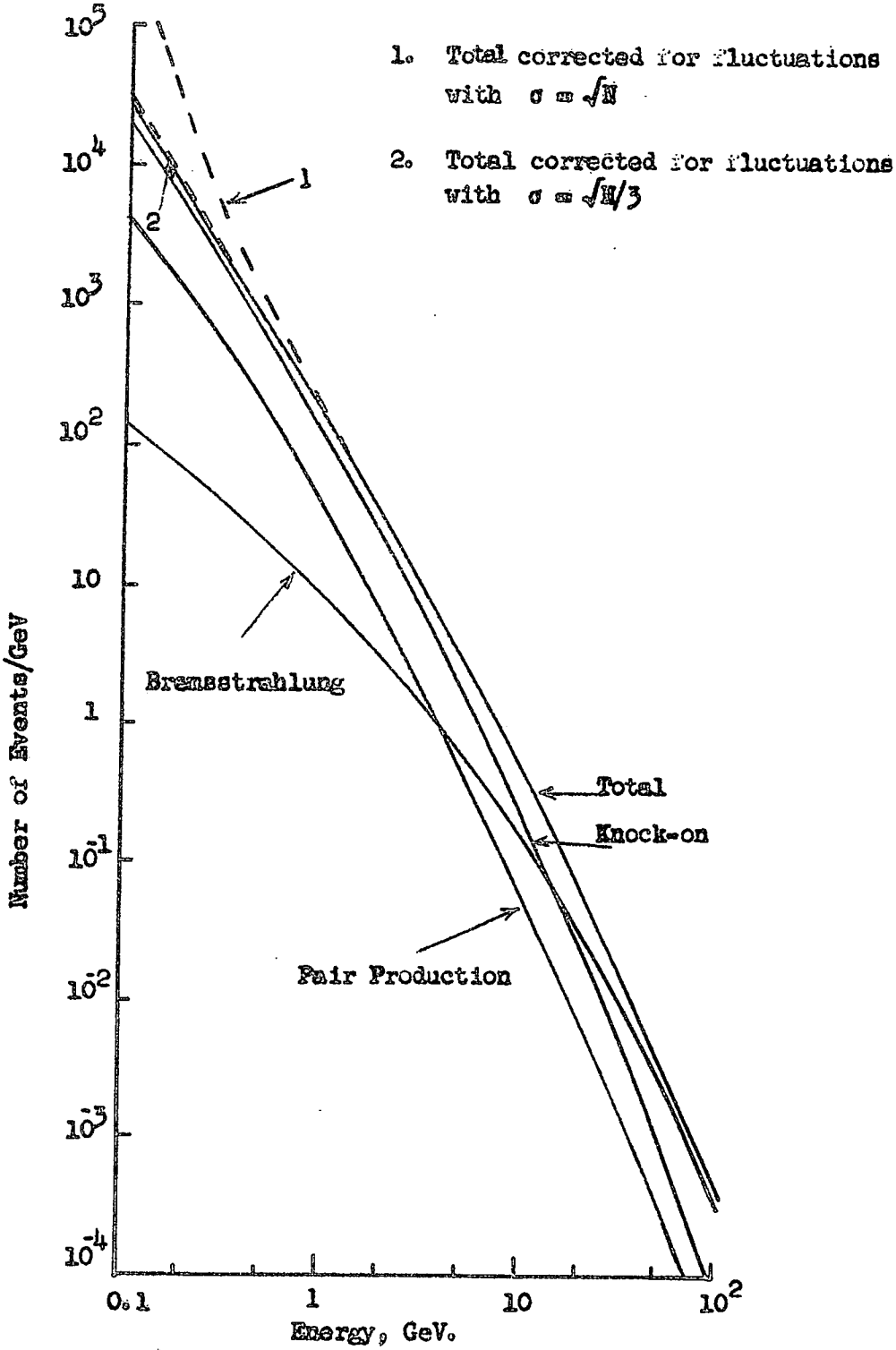

Predicted number of events for the unbiassed experiment.

9.2.7 The Effect of Fluctuations

During the calculation of the predicted number spectra two assumptions have been made concerning the growth of cascade showers. These are 1) that the development of the shower is that calculated by Buja, i.e. a shower of a certain energy, E, always reaches its maximum after a distance x radiation lengths, and 2) that a shower of energy E always contains the same number of particles at its point of maximum development. Neither of these assumptions is correct, however, since both the distance to the maximum of a shower and the number of particles at this maximum are subject to fluctuations. Of these fluctuations an attempt has been made to allow for the fluctuation in the distance to the maximum when determining the experimental differential energy spectrum.

The effect of fluctuations in the number of particles was calculated using the formula due to Lloyd and Wolfendale (1955) (see §6.7.2) with a standard deviation on the number of particles, N, at the shower maximum of $\sqrt{N}$ and $\sqrt{N/3}$, these values being the standard deviation for fluctuations which fit a Poisson distribution and the value estimated from the results quoted in table 8.2. Of these values $\sqrt{N/3}$ is probably correct and $\sqrt{N}$ represents the absolute upper limit of the fluctuations. The predicted curves corrected for these fluctuations are shown as the dashed lines in figure 9.3.

9.2.8 Discussion

In the calculation of the predicted curves the main assumption used was that the development of a cascade shower depends only upon

the number of radiation lengths of material present, and not upon the type of material. While this assumption is not correct, as can easily be seen from the figures of Butcher and Messel (1960) which indicate that heavy elements have a greater effect upon shower development than light elements, it does lead to a maximum value, in units of the apparatus, for the target thickness. At the other extreme if it is assumed that only the lead plays any part in the shower development then a minimum value for the target thickness in units of the apparatus, §9.2.3, is obtained. In the case of the knock-on process the difference between the two values is of the order of a few percent while for bremsstrahlung and pair production it is approximately 11%.

9.3 The Experimental Results

9.3.1 Conversion from Maximum Channel Number to Energy

In order to convert the value of the maximum channel number obtained experimentally to the energy of the shower equations 8.1 and 8.2 were used with the value of $\bar{c}$, equation 8.1, taken as the arithmetic mean of all of the mean pulse heights for single particles. This value was found to be

$$\bar{c} = 9.55.$$

9.3.2 Final Selection of Data

During the calculation of the target thickness, §9.2.3, it was found that, as would be expected from the method used, as the shower energy increased the number of large scintillation counters in which a maximum could occur was reduced. When the data from both the unbiassed and biassed runs was examined it was found that events had

occurred for which the maximum was in a large scintillation counter which was not allowed from the theoretical point of view. In order to make the analysis of the experimental results consistent with the theoretical calculations it was decided to reject events of this type as being due to fluctuations in the distance from interaction to shower maximum.

The effect of this correction, which was only carried out for events with energy greater than 1 GeV, can be seen from figure 9.4 where both corrected and uncorrected points are plotted for the case of the unbiassed run. From this figure it can be seen that this correction, while having a noticeable effect upon the results, is not so great as to indicate an error in the nature of the correction.

While this correction takes into account the fact that some showers develop more quickly than others it does not allow for showers which take longer than the average to develop and thus would give maxima in the sixth scintillation counter and be rejected. However it seems probable that the number of these showers is approximately equal to the number which would be expected to have maxima in the sixth large scintillation counter but which, because of fluctuations, would show maxima in the fifth large scintillation counter.

9.3.3 The Unbiassed Results

The final results from the unbiassed run are shown in figure 9.4 where they are compared with the predicted results. From these results it can be seen that the agreement between theory and experiment is very good over the whole of the transferred energy range above 0.2 GeV.

Figure 9.4

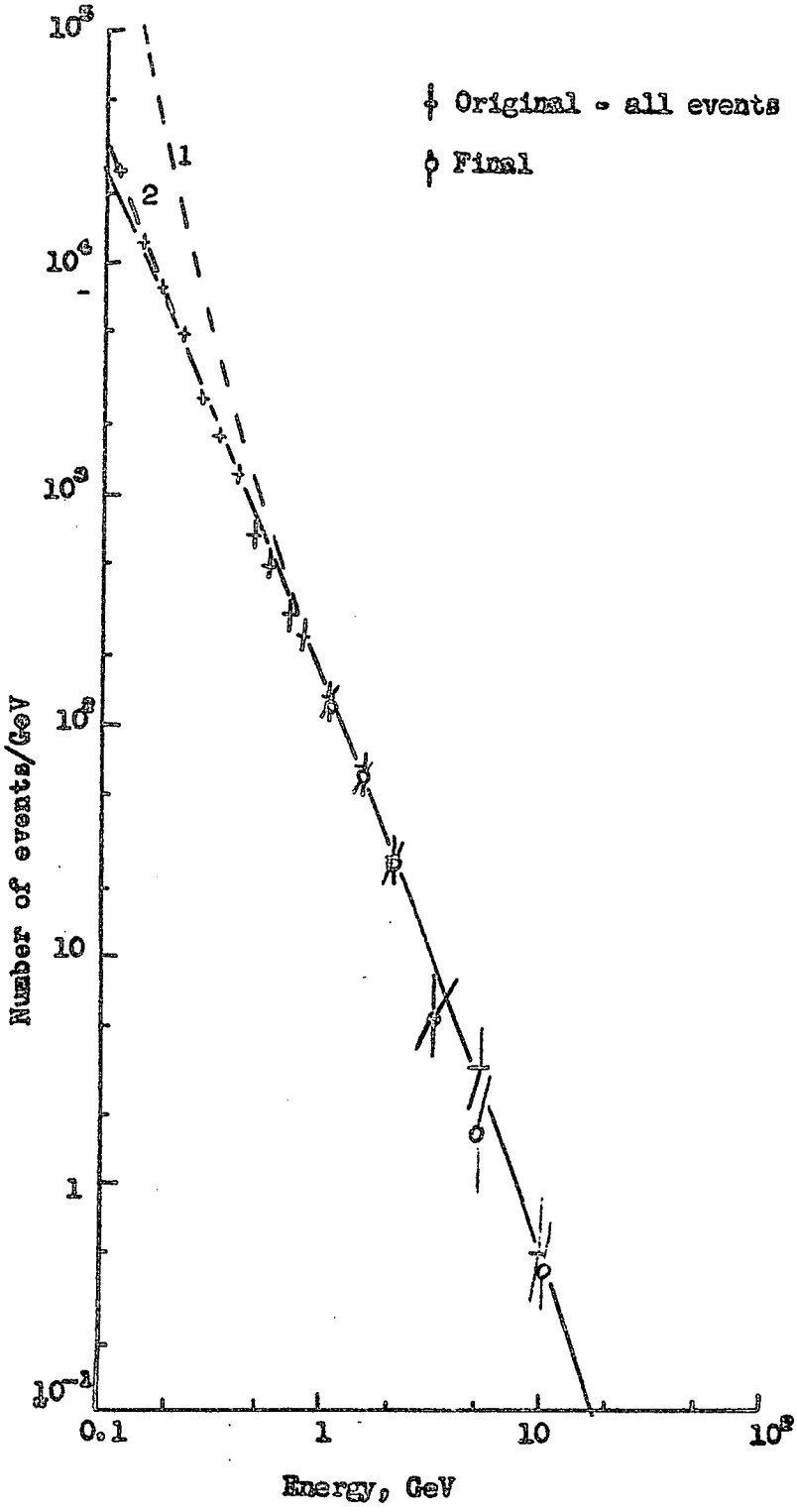

Comparison between the experimental and theoretical results for the unbiassed experiment.

Below this energy there is a slight excess of experimental results over theory but, as can be seen from the dashed lines, this excess can easily by explained as being due to fluctuations in the number of particles at shower maximum, §5.2.7.

9.3.4 The Biassed Results

The results from the biassed run are compared with the predicted results in figure 9.5. From this figure it can be seen that there is reasonable agreement between theory and experiment for transferred energies of greater than 2 GeV while below this energy there is a deficiency of experimental results. Since this region is that in which the biass on the fourth large scintillation counter has most effect it is probable that the deficiency is due to one of the following:

a) The mean pulse height for single particles varies according to the position in the scintillation counter through which the particle travels and the angle of incidence of the particle. Thus the number of particles required to give a pulse height greater than some value fixed by the biass level also depends upon the position and angle at which the shower traverses the counter. Because of this some showers traversing the fourth large scintillation counter will be detected with less efficiency than others. This effect decreases as the energy, and thus the distance traversed by the shower, increases.

b) In the case of low energy showers the total distance travelled by the shower is relatively small and thus any fluctuations in the growth and decay of the shower could have the effect of reducing the

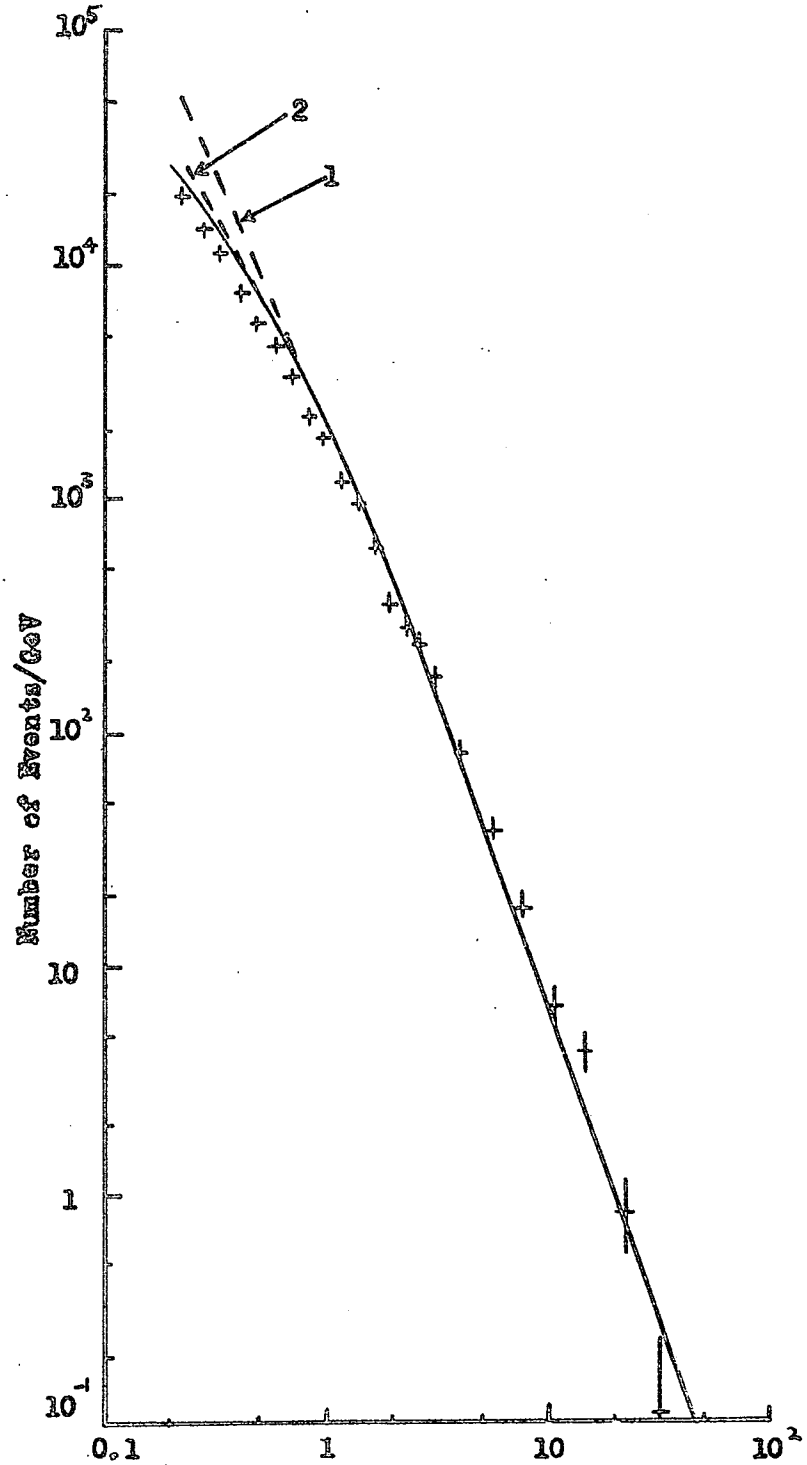

Figure 9.5 Differential energy spectrum of events from the biassed run.

number of particles present in the fourth large scintillation counter to below the bias level.

9.4 Conclusions from the London Experiment

In figure 9.6 the results obtained from both the unbiassed and biassed runs are shown plotted as the ratio between the observed and predicted number of events as a function of the transferred energy. Also shown are the predicted curves which are obtained when the cross-section for direct pair production is taken as one half that given by theory (cf Gaebler et al., 1961).

From the graphs in figure 9.6 it can be seen that, as has already been stated, §9.3.3 and §9.3.4, the agreement between theory and experiment is good in the case of the unbiassed run over the whole of the transferred energy range. For the biassed run, while results below 2 GeV are completely different from theory, for reasons which are stated in §9.3.4, there is no evidence above this energy for any marked discrepancy.

When the modified predicted curves are considered, dashed line, the agreement is not sufficiently good in the unbiassed case to be taken as evidence for any discrepancy in the theory of direct pair production such as is proposed by Gaebler et al. (1961).

The final conclusion that can be drawn from the results of the London experiment is that, for energy transfers up to 30 GeV the electromagnetic interactions of muons in a sandwich target of lead, carbon and aluminium are in agreement with theory.

Figure 9.6 Ratio of experimental to theoretically predicted number of events for the London experiment. ($\sigma = 0$)

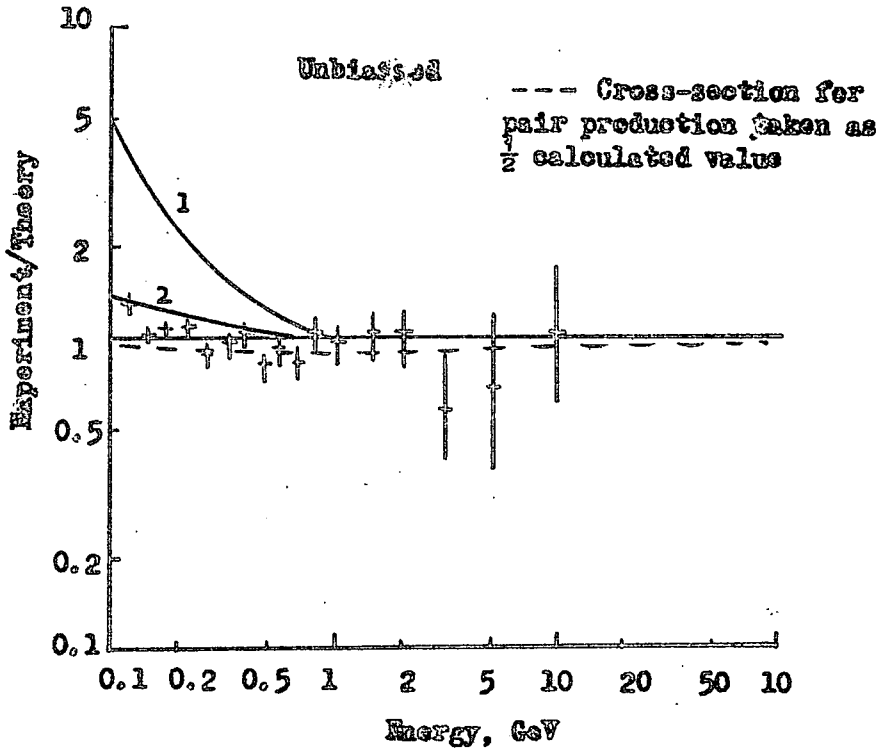

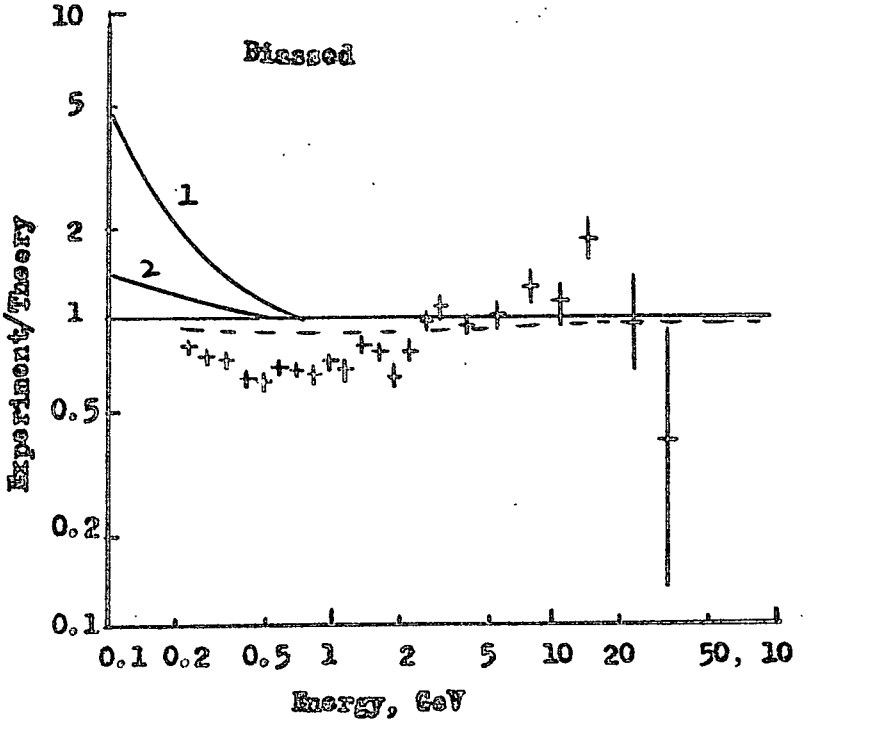

CHAPTER 10

CONCLUSIONS

The results from both of the experiments described in this thesis are in the range of transferred energies from 0.1 to 30 GeV (figures 6.2, 6.3, 9.3 and 9.4). Since over most of this energy region (up to 15 GeV in the case of the Durham experiment, and up to 20 GeV in the case of the London experiment) the dominant process is that of knock-on production these experimentsmay be considered primarily as being tests of the theory of this interaction.

Because of the greater statistical accuracy achieved in the London experiment, and the fact that there are less uncertainties in the analysis of this experiment, especially in the case of the unbiassed run, than in the analysis of the Durham experiment, the conclusions must be based mainly upon this experiment. At the same time the results of the Durham experiment, while being subject to large uncertainties, do provide some evidence in support of the conclusions from the London experiment.

The final conclusion obtained from the two experiments is that, in the region of energy transfer where the knock-on process is dominant, the results are fully consistent with the theory of Bhabha (1938). This conclusion, while in agreement with the results of Backenstoss et al. (1963b), is contradictory to that of Deery (1960) (see also Deery and Neddermeyer, 1961), who found an excess of events over the number predicted by theory which, furthermore, increased with increasing energy above 1 GeV. Since, as reported by these workers, it is

not possible, with any degree of certainty, to exclude the possibility that this excess is due to a statistical fluctuation, and also because the energy transfers do not extend into the region where bremsstrahlung is dominant, and where the evidence is that theory is correct, it is doubtful whether much reliance can be placed upon this result.

Apart from Deery, McDiarmid and Wilson (1962)also found indications of an excess of events in the region where knock-on production is dominant. However in this case the statistical accuracy was rather poor and uncertainty existed in the energy estimates. Thus, by decreasing the energy estimates for the secondary particles, obtained from cascade shower curves, by 10% (a reasonable estimate of the uncertainty) the authors showed that the disagreement between experiment and theory was considerably reduced.

In conclusion the evidence of the experiments carried out in Durham and London, when taken along with statistically very accurate work of Backenstoss et al. (1963h) at lower energies (up to 3.4 GeV energy transfer) indicates complete agreement between experiment and theory for the knock-on process for transferred energies covering the whole range from 0.1 GeV to 20 GeV. By combining this with the result from the CERN g-2 experiment, in which it was found that the anomalous magnetic moment of the muon was equal to the theoretical value to within 0.5% (Charpak et al., 1961), it can be stated that, at the present time, there is no evidence for the muon differing from a heavy electron.

ACKNOWLEDGMENTS

The author wishes to thank Professor G.D. Rochester for the provision of the facilities for this work and for his continued interest and support.

The author acknowledges with gratitude the help and guidance which he has, at all times, received from his supervisor, Dr. A.W. Wolfendale, and from Dr. M.G. Thompson.

Dr. J.C. Barton of the Northern Polytechnic, London, is thanked for the use of the data from his experiment and also for the help given through discussions of various aspects of the work.

The technical staff of the Physics Department, in particular Mr. W. Threadgill, Mr. E. Lincoln, Mr. P. Finley, Mr. W. Leslie and Miss C. Guyll, are thanked for their willing help.

The assistance of Mrs. G. Brooke and Miss P. Stewart in the preparation of this thesis is acknowledged with thanks.

Finally, the Department of Scientific and Industrial Research is thanked for the provision of a Research Studentship which enabled this research to be carried out.

REFERENCES

Allkofer, O.C., 1960, Z.f. Physik, 158, 274.

Avan, M., and Avan, L., 1957, Nuovo Cimento, 6, 1590.

Backenstoss, G., Hyams, B.D., Knop, G., and Stierlin, U., 1963a, Nuclear Inst. and Methods, 21, 155.

Backenstoss, G., Hyams, B.D., Knop, G., Marin, P.C., and Stierlin, U., 1963b, Phys. Rev., 129, 2759.

Barrett, P.H., Bollinger, L.M., Cocconi, G., Eisenberg, Y., and Greisen, K., 1952, Rev. Mod. Phys., 24, 133.

Barton, J.C., Barnaby, C.F., Jasani, B.M., and Thompson, C.W., 1962, J. Sci. Instr., 39, 360.

Barton, J.C., and Crispin, A., 1962, Nuclear Inst. and Methods, 16, 39.

Belenkii, S.Z., and Ivanenko, I.P., 1959, Soviet Physics Uspekhi, 2, 912.

Bertanza, L., and Martelli, G., 1954, Nuovo Cimento, 11, 217.

Bethe, H.A., and Heitler, W., 1934, Proc. Roy. Soc., 146, 84.

Bhabha, H.J., 1935A, Proc. Roy. Soc., 152A, 559.

Bhabha, H.J., 1935B, Proc. Camb. Phil. Soc., 31, 394.

Bhabha, H.J., 1938, Proc. Roy. Soc., A 164, 257.

Bhabha, H.J., and Chakrabarty, S.K., 1948, Phys. Rev., 74, 1352.

Block, M.M., King, D.T., and Wada, W.W., 1954, Phys. Rev., 96, 1627.

Brooke, G., Hayman, P.J., Taylor, F.E., and Wolfendale, A.W., 1962, J. Phys. Soc. Japan, 17, Suppl. AIII, 311.

Buja, Z., 1963, Acta Physica Polonica, 24, 381.

Butcher, J.C., and Messel, H., 1960, Nuclear Physics, 20, 15.

Charpak, G., Farley, F.J.M., Garwin, R.L., Muller, T., Sens, J.C., and Zichichi, A., 1961, Nuovo Cim., 22, 1043.

Chaudhuri, N., and Sinha, M.S., 1964, Nuovo Cimento, 32, 853.

Christy, R.F., and Kusaka, S., 1941, Phys. Rev., 59, 405.

Conversi, M., and Gozzini, A., 1955, Nuovo Cimento, 2, 189.

Conversi, M., Pancini, E., and Piccioni, O., 1947, Phys. Rev., 71, 209.

Coxell, H., 1961, Ph.D. Thesis, Durham.

Coxell, H., Meyer, M.A., Scull, P.S., and Wolfendale, A.W., 1961, Nuovo Cimento, Suppl. 21, 7.

Crawford, D.F., and Messel, H., 1962, Phys. Rev., 128, 2352.

Deery, R.F., 1960, Ph.D. Thesis, University of Washington.

Deery, R.F., and Neddermeyer, S.H., 1961, Phys. Rev., 121, 1803.

Fowler, G.N., and Wolfendale, A.W., 1958, Elementary Particles and Cosmic Ray Physics, Editors J.G. Wilson and S.A. Wouthuysen (North Holland Publishing Company, Amsterdam, 1958), Chapter 3.

Gaebler, J.F., Hazen, W.E., and Hendel, A.Z., 1961, Nuovo Cimento, 19, 265.

Hayman, P.J., Palmer, N.S., and Wolfendale, A.W., 1963, Proc. Roy. Soc., A 275, 391-410.

Hayman, P.J., and Wolfendale, A.W., 1962, Proc. Phys. Soc., 80, 710.

Hazen, W.E., 1955, Phys. Rev., 99, 911.

Kearney, P.D., 1962, Private Communication.

Lattes, C.M.G., Muirhead, H., Occhialini, G.P.S., and Powell, C.F., 1947, Nature, 159, 694.

Lloyd, J.L., and Wolfendale, A.W., 1955, Proc. Phys. Soc., A68, 1045.

Lloyd, J.L., and Wolfendale, A.W., 1959, Proc. Phys. Soc., 58, 178.

Massey, H.J., and Corben, J.C., 1939, Proc. Camb. Phil. Soc., 35, 463.

McDiarmid, I.B., and Wilson, M.D., 1962, Canad. J. Phys., 40, 698.

Messel, H., Smirnov, A.D., Varfolomev, A.A., Crawford, D.F., and Butcher, J.L., 1962, Nuclear Physics, 39, No. 1.

Murota, T., Ueda, A., and Tanaka, H., 1956, Progr. Theor. Phys., (Kyoto), 16, 482.

Neddermeyer, S.H., and Anderson, C.D., 1937, Phys. Rev., 48, 486.

Neddermeyer, S.H., and Anderson, C.D., 1939, Rev. Mod. Phys., 11, 191.

Nichiparuk, B., and Strugal'skii, Z.S., 1964, J.E.T.P., 18, 13.

Nishina, Y., Tomonaga, S., and Kobayasi, M., 1935, Sci. Pap. Inst. Phys. Chem. Research, Japan, 27, 137.

Ott, K., 1954, Z. Naturforsch, 9A, 488.

Pine, J., Davisson, R.J., and Greisen, K., 1959, Nuovo Cim., 14, 1181.

Racah, G., 1937, Nuovo Cim., 14, 93.

Roe, B.P., and Ozaki, S., 1959, Phys. Rev., 116, 1022.

Rossi, B., 1948, Rev. Mod. Phys., 20, 537.

Rossi, B., 1952, High Energy Particles (Prentice Hall Inc.).

Stoker, P.H., Bornman, C.H., and Van der Merwe, J.P., 1963, Nuclear Physics, 45, 505.

Stoker, P.H., and Haarhoff, P.C., 1960, Nuclear Physics, 14, 512.

Stoker, P.H., Hofmeyr, C., and Bornman, C.H., 1961, Proc. Phys. Soc., 78, 650.

Wilson, R.R., 1950, Phys. Rev., 79, 204.

Wilson, R.R., 1951, Phys. Rev., 84, 100.

Wilson, R.R., 1952, Phys. Rev., 86, 261.

Yukawa, H., 1935, Proc. Phys. Math. Soc. Japan, 17, 48.

APPENDIX

CASCADE SHOWERS

1. Introduction

In order to determine the energy of an electron or photon from the electromagnetic cascade shower which this produces in an absorber it is necessary to know the variation of the parameters of the shower with the energy of the incident particle.

This chapter contains a qualitative description of the way in which a cascade shower develops. This is then followed by descriptions of the results, obtained from a) cascade shower theory, b) Monte Carlo calculations, and c) experimental measurements, for the shower shape, the variation of total track length with energy, and the variation of the number of particles at a given depth in the shower with energy. In particular the special case of the number of particles at the shower maximum is considered.

Finally a comparison is made between the various results and an indication is given of the types of experiments for which the parameters are most suitable.

2. Cascade Shower Development

When an electron is incident upon an absorber with an energy greater than the critical energy then it is likely to lose energy through the emission of a photon, i.e. the bremsstrahlung process, and will carry on with reduced energy. This process continues until the energy of the electron falls below the critical energy when the dominant way by which the electron loses energy is by the ionization process. Each of

the photons produced in the passage of the original electron may materialise to form an electron-positron pair after travelling a short distance through the absorber and these particles will then behave in exactly the same way as the incident electron.

Thus it can be seen that the number of particles in a cascade shower will increase with increasing depth, while the average energy of these particles decreases. This continues until the average energy falls to the critical energy, beyond which point the number of particles decreases. The final result is that all the energy of the incident particle is lost through ionisation, energy being lost by ionisation the whole of the way through the shower.

From this simple description of the development of a cascade shower it can be seen that:

1) The number of particles at the shower maximum would be expected to be $N = E_o/\epsilon_o$ where E_o is the energy of the incident electron and ϵ_o is the critical energy of the absorber, and

2) The total track length in the shower would be E_o/ϵ_o radiation lengths since, in the end, all of the incident energy would be lost through ionisation and the critical energy is defined as the ionisation loss per radiation length.

3. Theoretical Results

3.1 Introduction

Because the theory describing all of the processes involved in the development of a cascade shower is extremely complex most calculations have been carried out to describe only the average behaviour of

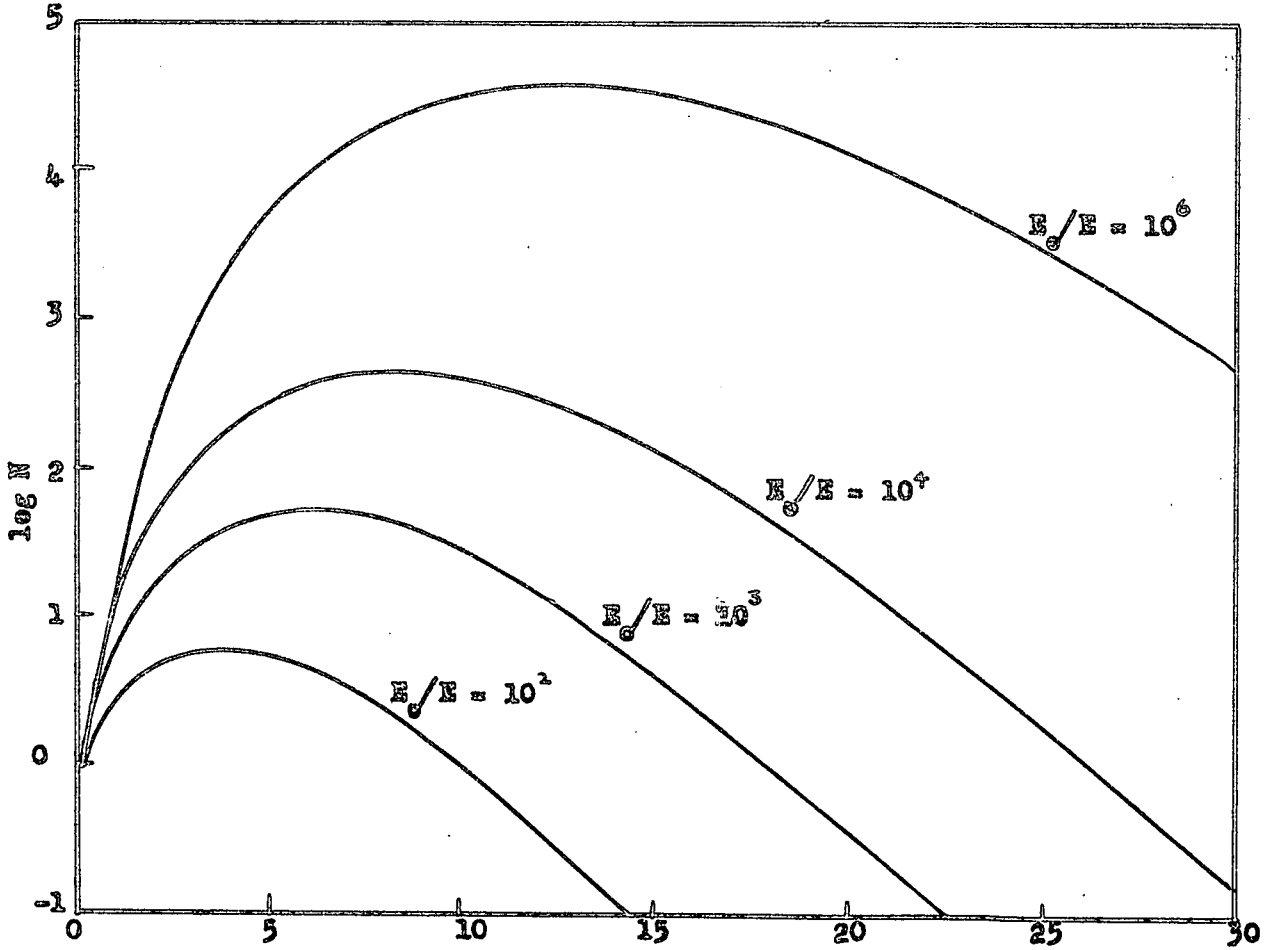

Figure A1 Average cascade shower curves for electron initiated showers
Approximation A

showers as they traverse matter. In this section the results considered are those due to Approximation A and Approximation B (as given by Rossi, 1952) and the results quoted by Buja (1963).

In what follows the approximations used in each of the calculations are outlined and the results obtained are indicated. Finally the results are compared with each other and any discrepancies are explained.

3.2 Approximation A (Rossi, 1952)

In the calculation of shower behaviour under Approximation A the only processes considered as contributing to the shower development are bremsstrahlung and pair production. The calculations are further simplified by using the asymptotic formulae for complete screening to describe these processes. Because of this the results only apply to shower electrons with energies greater than that given by $137\, m_e c^2\, Z^{-\frac{1}{3}}$, where Z is the atomic number of the absorber.

Examples of the average shower curves obtained by Approximation A, which apply for all absorbers so long as the distances are measured in terms of the radiation length, are given in figure A.1.

3.3 Approximation B (Rossi, 1952)

The Approximation B method of calculating the behaviour of cascade showers is an extension of the Approximation A method. In this method, instead of the energy loss through knock-on production and ionisation being neglected, this is taken into account by subtracting a constant energy per radiation length, equal to the critical energy, from the energies of the shower electrons.

The results obtained from this method of calculation, examples of which are shown in figure A.2, apply to all absorbers if the distances are measured in terms of the radiation length and the energy in terms of ϵ_o. It is important to note, however, that the calculations are most accurate for low Z absorbers, for which the asymptotic formulae used apply down to the critical energy, than for high Z absorbers for which the theory is expected to overestimate the shower development.

3.4 Buja (1963)

The results due to Buja, which are an extension of the results obtained by Ott (1954), were calculated using exact formulae for bremsstrahlung and pair production and taking into account the Compton effect. In order to take into account ionisation losses the electron energy, E, in the integral energy spectrum for the shower electrons is replaced by $E + \bar{\epsilon}$, where $\bar{\epsilon}$ is proportional to the critical energy ϵ_o. As a further modification of the theory $\bar{\epsilon}$ is replaced by a function $\bar{\epsilon}'$, proportional to the critical energy and the mean angle of scattering, to allow for the increase in track length due to Coulomb scattering.

The average shower curves obtained from these calculations are shown in figure A.3 for the case of electrons incident upon lead.

3.5 Comparison of the Theoretical Results

In order to compare the various sets of theoretical results the Approximation A and Approximation B results will be converted to apply to the case of a Pb absorber. Also the comparison will also be carried out with regard to the variation of total track length and number of particles at shower maximum with energy.

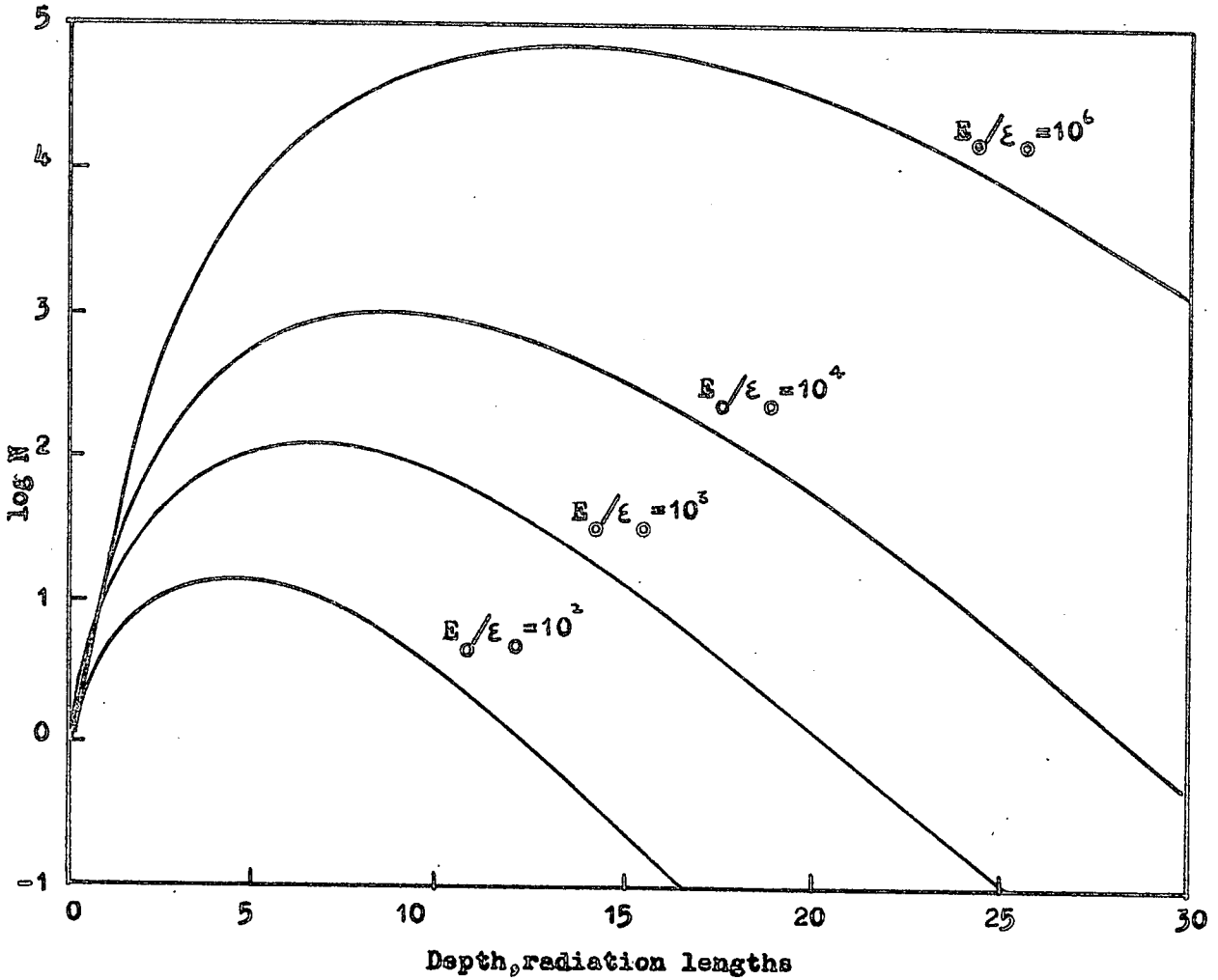

Figure A2 Average cascade shower curves for electron initiated showers Approximation B

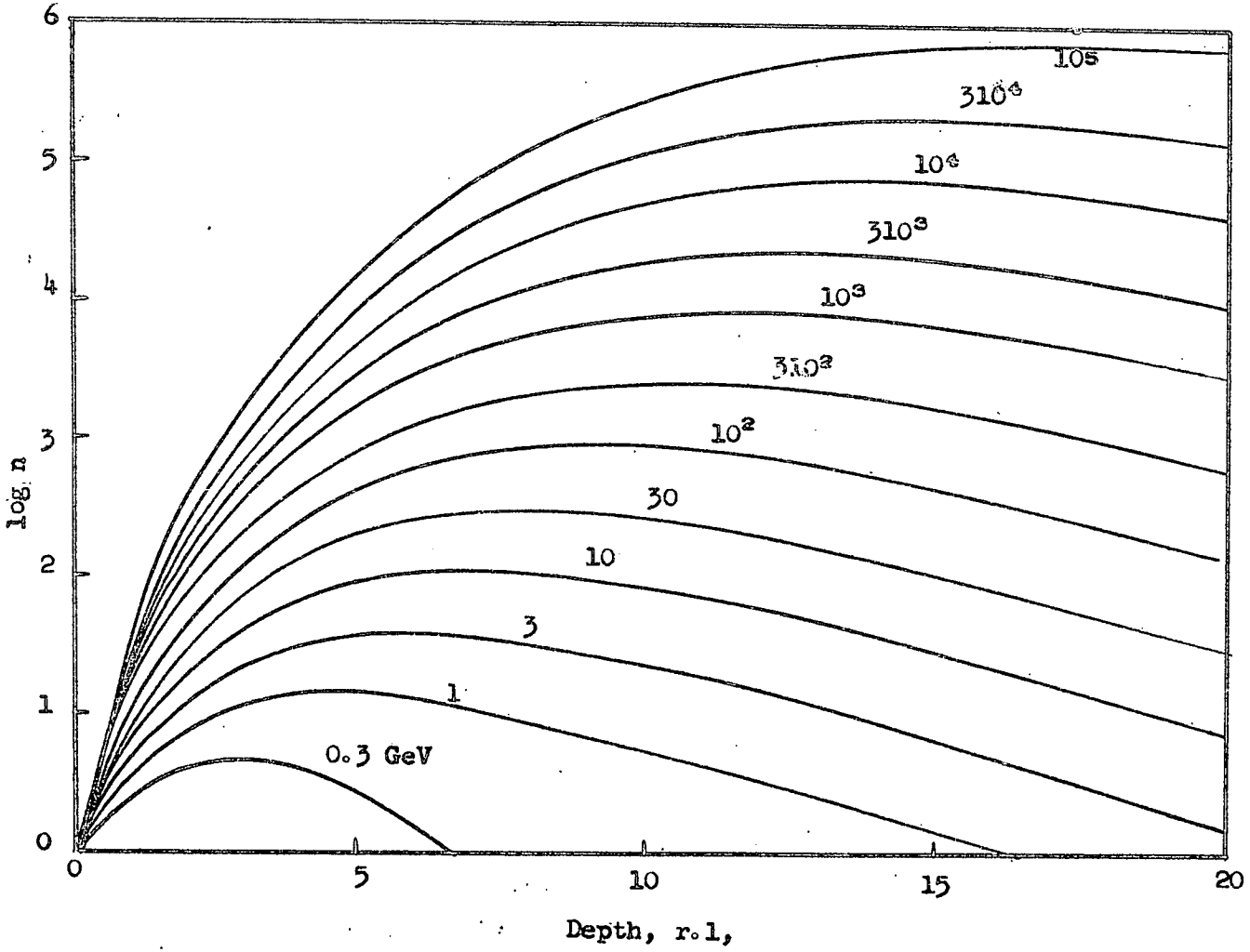

Figure A3 Cascade shower curves in Pb (Buja, 1963)

The results obtained from the various theories are given in table A.1 below.

TABLE A.1

Theory	E_{min}	Track length vs. E	N_{max} vs. E
App. A	10 MeV	$T = 0.04\ E$	$6.40\ E^{0.94}$
App. B	0	$T = 0.12\ E$	$18.22\ E^{0.93}$
Buja	0	$T = 0.11\ E$	$13.60\ E^{0.91}$

In this table the total track length, T, is in radiation lengths and the energy E is in MeV.

From table A.1 it can be seen that, as would be expected from conservation of energy, the values of K in the expression $T = KE$ obtained from Approximation B and the results due to Buja are very nearly equal, any slight difference being due to the integration under the shower curves.

A more interesting fact is that, in spite of the different factors included in the calculation of the shower curves, the exponent b in the expression

$$N_{max} = aE^{b}$$

is practically constant no matter which of the theories is considered. Thus, the differences in the value of a, which are due to the minimum shower electron energy considered and the approximations used, only affect the absolute values of the energies assigned to showers using this expression and not the relative energies.

4. Monte Carlo Calculations

4.1 Wilson (1952)

The first Monte Carlo calculations of cascade shower development were due to Wilson who used a 'wheel of chance' to investigate the behaviour of each of the component particles of a shower as they travelled through a lead block. In this way it was possible to calculate the behaviour of individual showers and, from a large number of these, to determine the average behaviour of a shower initiated by an electron or photon of a known energy.

The cross-sections used in these calculations were the values predicted by Bethe and Heitler (1934) adjusted to fit experimental results. To allow for ionisation a constant energy per radiation length, equal to the critical energy, was subtracted from the electrons.

In order to satisfy energy conservation the average shower curves were normalised so that the area under the curve times the critical energy, i.e. the total energy lost by ionisation, was equal to the energy of the incident particle.

The calculations were carried out in two parts. In the first no allowance was made for multiple scattering while in the second the electron was assumed to travel in the direction of the shower axis until it reached an energy, E_r, below which the motion was considered as being random.

Examples of the results obtained by Wilson are shown in figure A.4 for photons incident upon lead and no multiple scattering. In figures

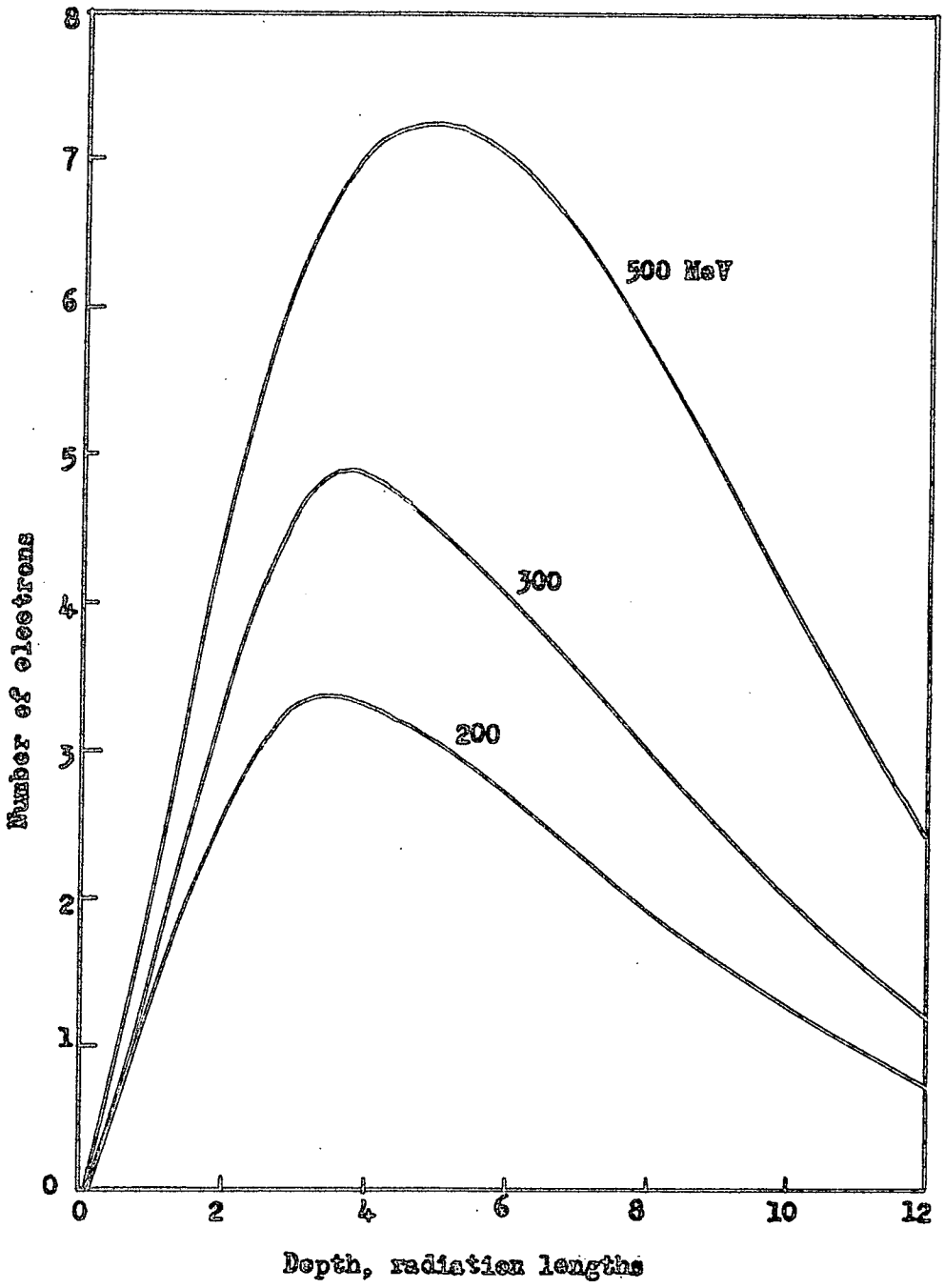

Figure A4 Cascade shower curves for photon initiated showers - Wilson (1952).

A.5 and A.6 the average shower curves for lead which were obtained when all shower electrons with energy less than 8 MeV, E_r for lead, were neglected.

4.2 Crawford and Messel, (1962)

Some of the most recent Monte Carlo calculations have been those of Messel and his colleagues (Butcher and Messel (1960), Crawford and Messel (1962) and Messel et al. (1962)). Of these the most useful results for the present work are those of Crawford and Messel which give the number of electrons and photons with energy greater than 10 MeV, the number with energy less than 10 MeV, the number back scattered, the total track length for electrons with greater than 10 MeV, and the degradation of energy, as a function of the depth in the shower.

These results, which were calculated on the SILLIAC computer, take into account a) bremsstrahlung, b) pair production, c) Compton effect, d) multiple scattering, and e) ionisation loss. For processes a), b) and c) the accurate cross-sections were used, and for d) the Molière theory of multiple scattering, as given by Bethe, was applied. Finally, in order to take into account ionisation loss an amount of energy E was subtracted from the electron energy after each flight through t radiation lengths, where

$$E = 0.346\ t \left\{19.15 + \log_e\ (E_0/2m_e c^2)\right\} \text{ MeV for lead.}$$

The results of the computations are shown in figures A.7 and A.8 which refer to showers initiated by electrons incident upon lead.

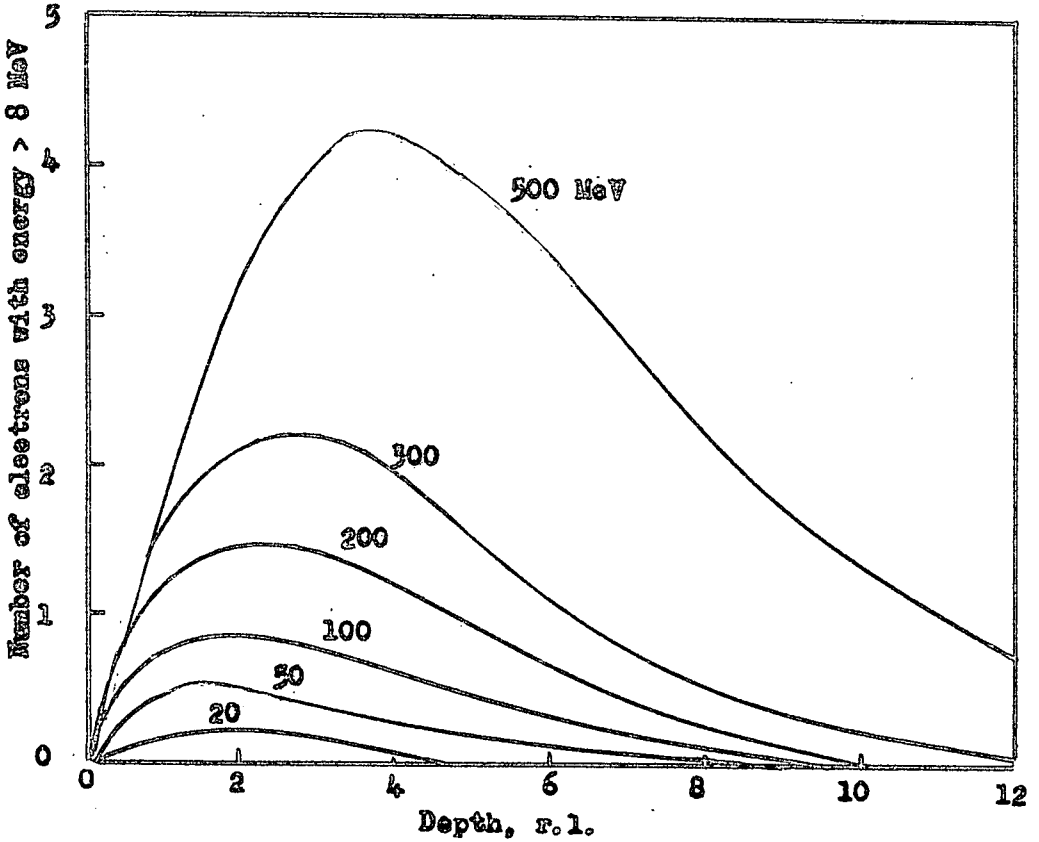

Figure A5 Cascade shower curves for photon induced showers - Wilson, 1952.

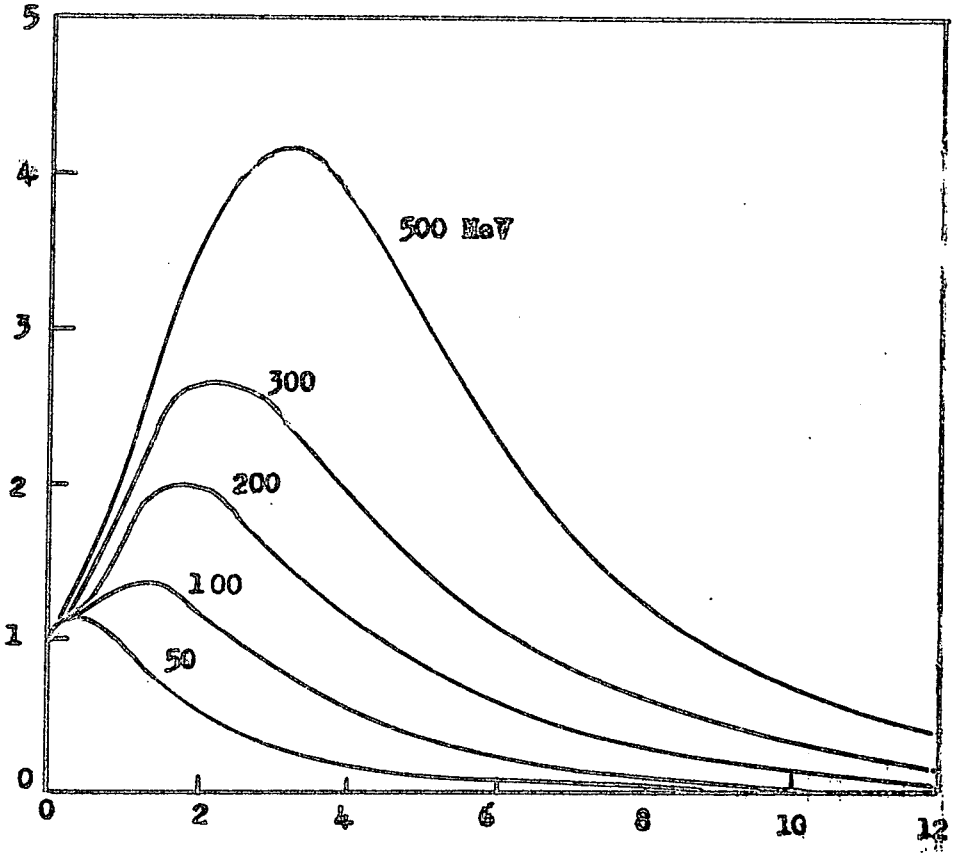

Figure A6 Number of electrons with energy greater than 8 MeV in electron initiated showers - Wilson (1952).

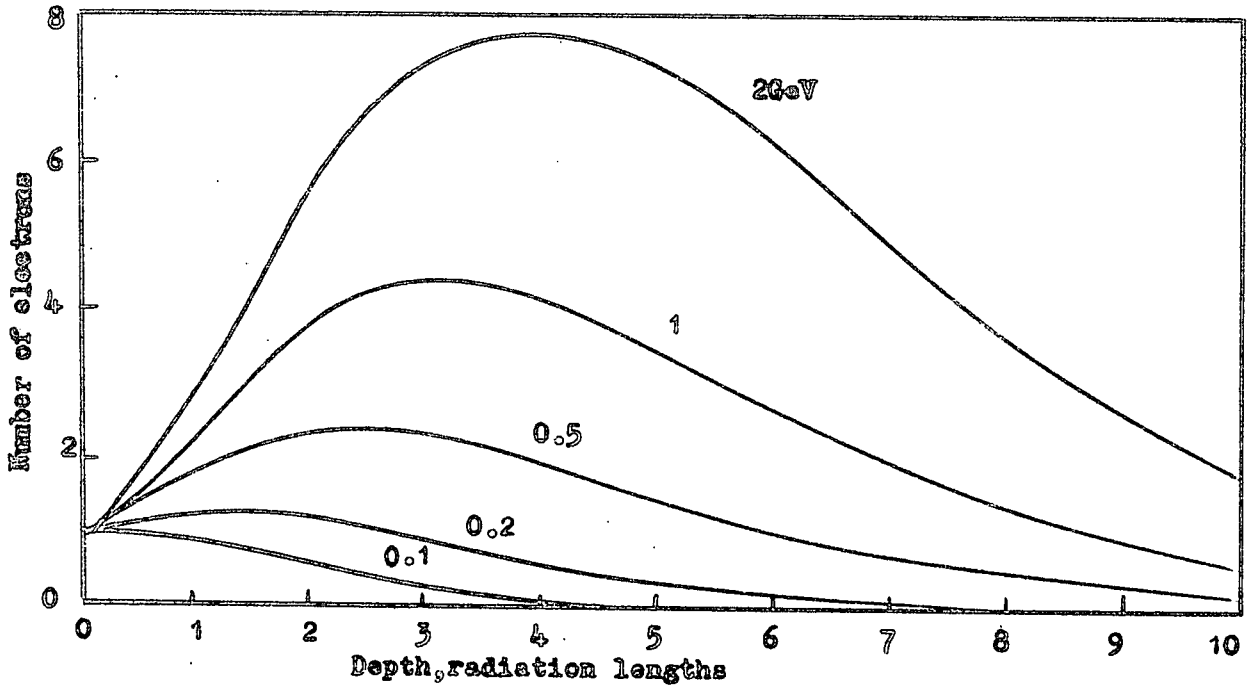

Figure A7 Number of electrons with energy greater than 10MeV in cascade showers in lead(Crawford and Messel, 1962).

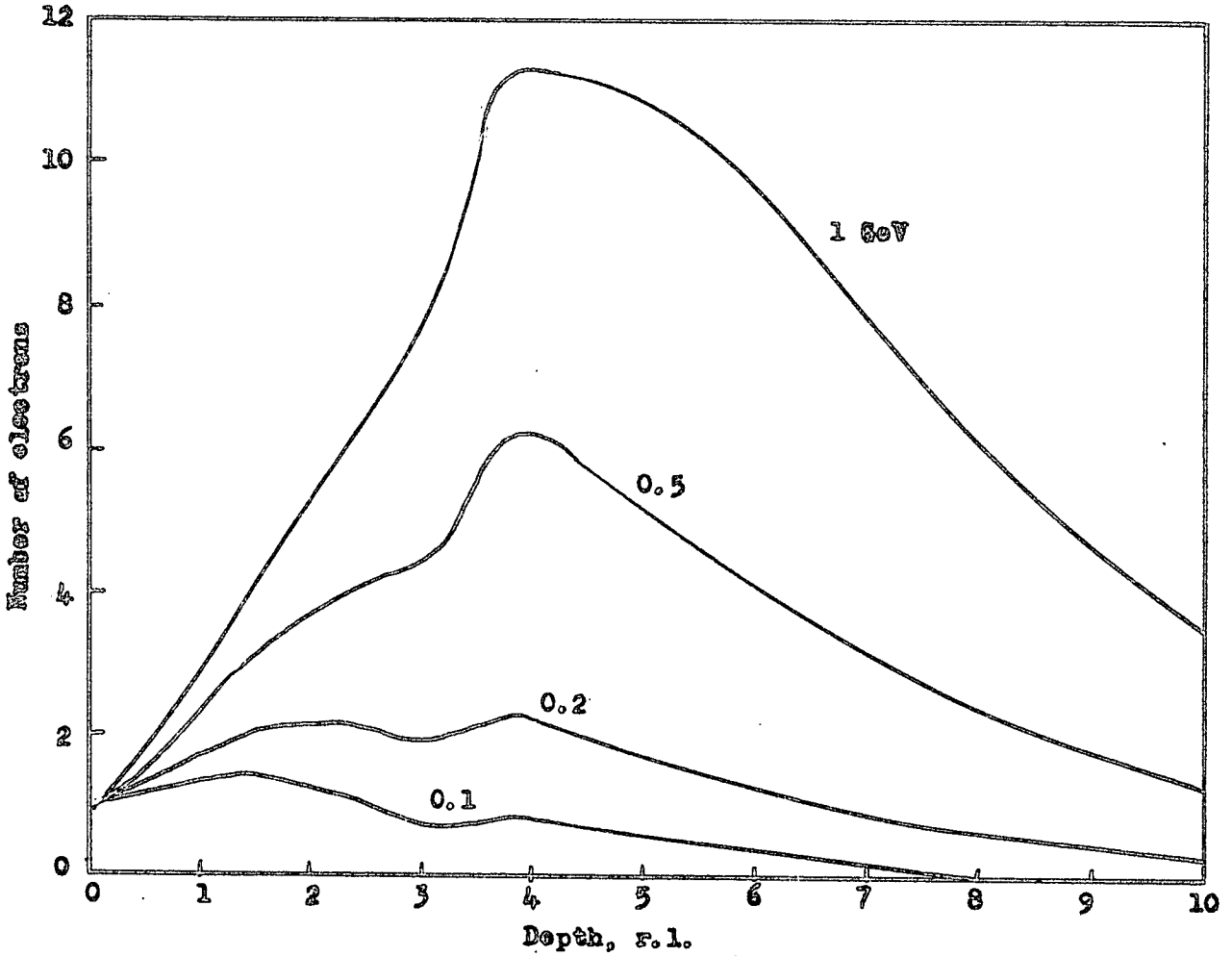

Figure A8 Total number of electrons, of all energies, in electron initiated cascade showers in Pb

4.3 Discussion and Comparison of the Monte Carlo Results

The most noticeable point when the shower curves of figure A.6, which give Wilson's results for the number of electrons with energy greater than 8 MeV, are compared with those of figure A.7, Crawford and Messel results for the number of electrons with energy greater than 10 MeV, is the large difference between the numbers of particles in showers of the same energy i.e. for a 0.5 GeV shower Wilson gives a maximum of 4.15 particles while Crawford and Messel give 2.51 particles. While some of this difference could be explained as being due to electrons with energies between 8 MeV and 10 MeV it seems likely that the most probable explanation of the discrepancy is that the energy degradation found by Crawford and Messel is greater than that found by Wilson due to the different methods of allowing for the ionisation loss and the effect of multiple scattering in the former work increasing the path lengths of electrons through the absorber.

If the variation of total track length with energy is determined for the two sets of results the values obtained are:

Wilson $T = 0.045\ E_o$ radiation lengths

Crawford and Messel $T = 0.032\ E_o$ radiation lengths.

Where E_o is the incident energy in MeV and T is the total track lengths.

Hence, the rate of energy loss is

22.2 MeV/radiation length from Wilson

and 31.2 MeV/radiation length from Crawford and Messel, and it is almost certain that the discrepancy between the results is due to the rate of energy degradation of the showers in the two cases.

5. Experimental Results

5.1 Hazen, (1955)

The results due to Hazen were obtained from an analysis of cloud chamber photographs of cascade showers produced in a multiplate cloud chamber by electrons whose energies were measured in a magnet cloud chamber.

The conclusion reached from this work is that for showers of energy between 100 and 1000 MeV the total track length in copper, defined as the sum of the number of track segments below each plate of the cloud chamber multiplied by the thickness of the plate, is related to the shower energy by

$$E = (24 \pm 3)\ T \text{ MeV}$$

i.e. $$T = (0.042 \pm 0.005)\ E \text{ radiation lengths.}$$

5.2 Backenstoss et al., (1963a)

The most recent investigation of cascade shower development is that of Backenstoss et al. who used a total absorption spectrometer in a beam of electrons from the C.E.R.N. proton synchrotron. From this experiment they obtained average shower curves for the case of both lead and iron absorbers. Examples of the shower curves obtained are shown in figure A.9 which refers to the case of an iron absorber. From these curves it is found that the variation of N_{max} and T with energy are given by

$$T = 0.039\ E^{0.96} \text{ radiation lengths with E in MeV}$$

and $$N_{max} = 5.95\ E^{0.75} \text{ with E in GeV.}$$

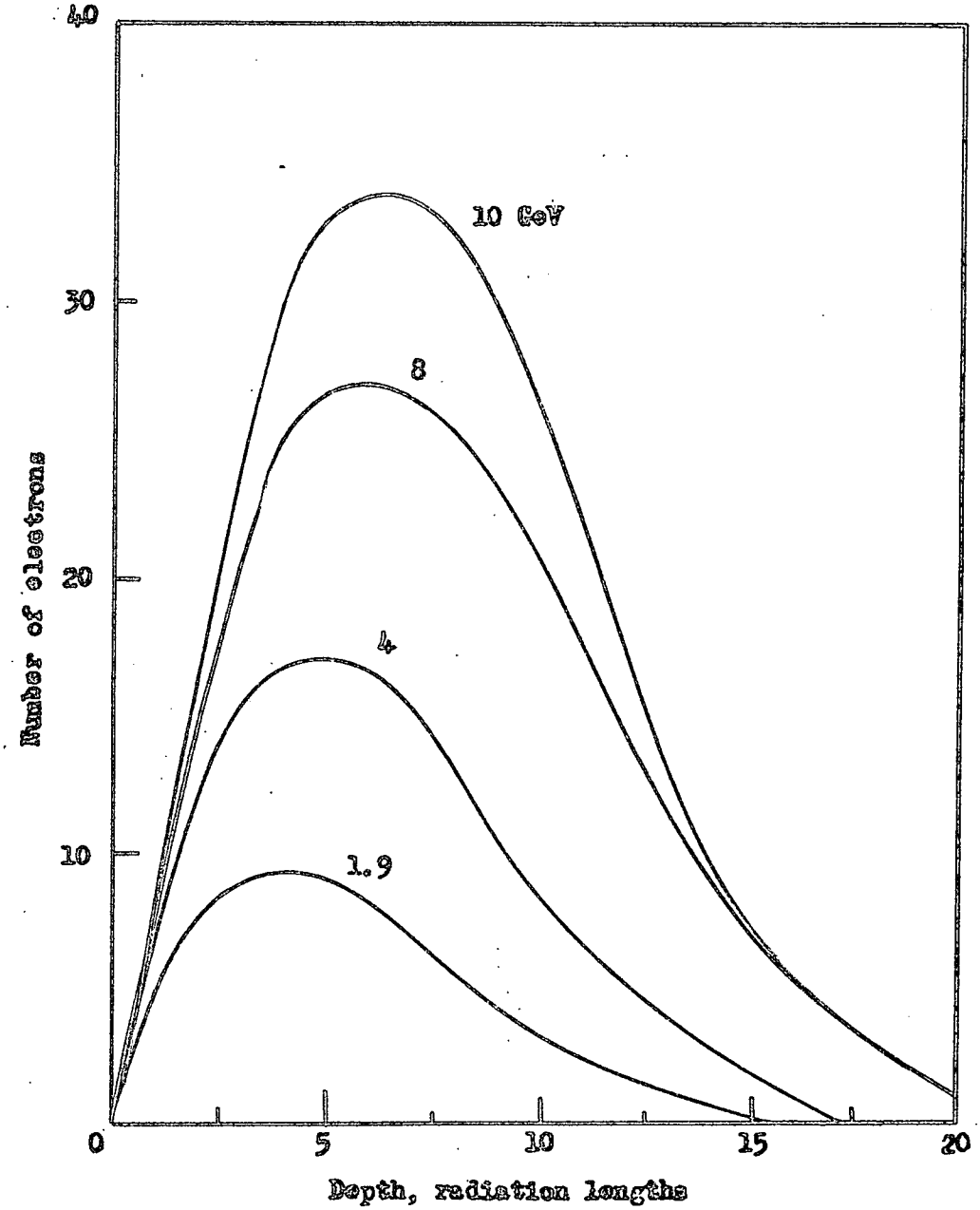

Figure A9 Experimental shower curves in Fe.
(Rackenstross et al., 1965).

6. Comparison of Results

6.1 Introduction

In order to compare the results of the various theories it is advantageous to consider the energy estimates which would be obtained for showers obtained experimentally. To do this consider three types of experiments, namely:

1) An experiment in which the absorber is in the form of numerous thin sheets separated by layers of detector e.g. a multiplate cloud chamber experiment or a total absorbtion spectrometer.

2) An experiment in which the absorber is in a number of thick sheets separated by detectors e.g. the London experiment described in this thesis.

3) An experiment in which the absorber is in the form of a solid block e.g. a cosmic ray burst experiment.

For each of these types of experiment the shower parameters which can be used to determine the energy are limited by the design of the experiment. These parameters and the variation of estimated energy with the shower theory used are described in the following paragraphs.

6.2 Thin plate experiment

In this type of experiment it is possible, since the shower is sampled at many points in its development, to use the following parameters to determine the shower energy, i.e.

1) The shower profile,

2) The number of particles at the shower maximum, and

3) The total electron track length in the shower.

Of these only the second and third will be considered. Of these the parameter which gives the best statistical accuracy is the total electron track length, although this may only be used when the shower is completely developed in the absorber. Thus there is an upper limit to the shower energy which can be determined using this parameter. On the other hand, the number of particles at the shower maximum, while giving less statistical accuracy, can be used to extend the range of energies which can be determined with a piece of apparatus.

Consider two cascade showers, in a multiplate cloud chamber containing thin lead plates, with total track lengths of 120 radiation lengths and 1200 radiation lengths respectively when all electrons are counted. From the values given for Approximation B and Buja's results in table A.1 it can be seen that the estimated energies for these showers would be as given in table A.2.

TABLE A.2

Total track length	120 r.l.	1200 r.l.
Approximation B	1 GeV	10 GeV
Buja	1.09 GeV	10.9 GeV

If, however, the electrons used in the determination of the total track length have energies greater than 10 MeV then the theoretical results which can be applied to determine the shower energies are those of Approximation A, Crawford and Messel, and Wilson. The estimated energies in these cases are shown in Table A.3.

TABLE A.3

Total track length	120 r.l.	1200 r.l.
Approximation A	3 GeV	30 GeV
Crawford and Messel	3.75 GeV	37.5 GeV
Wilson	2.67 GeV	26.7 GeV

From tables A.2 and A.3 it can be seen immediately that the variation of estimated energy with the theory considered is much less when all shower electrons are considered, of the order of 9% variation between the two theories considered, than when only electrons of energy greater than 10 MeV are considered. In this latter case a difference between the estimated results of 25% is quite probable.

One important point to notice here is that the difference between the theories leads to a constant factor between the energy estimates obtained and thus the uncertainties may be removed by normalisation of experimental data.

If the shower energy is to be estimated from the number of particles at the shower maximum then the calibration curves shown in figure A.10 would be used. From this figure the ratios of the energies estimated using the different theories are given in table A.4.

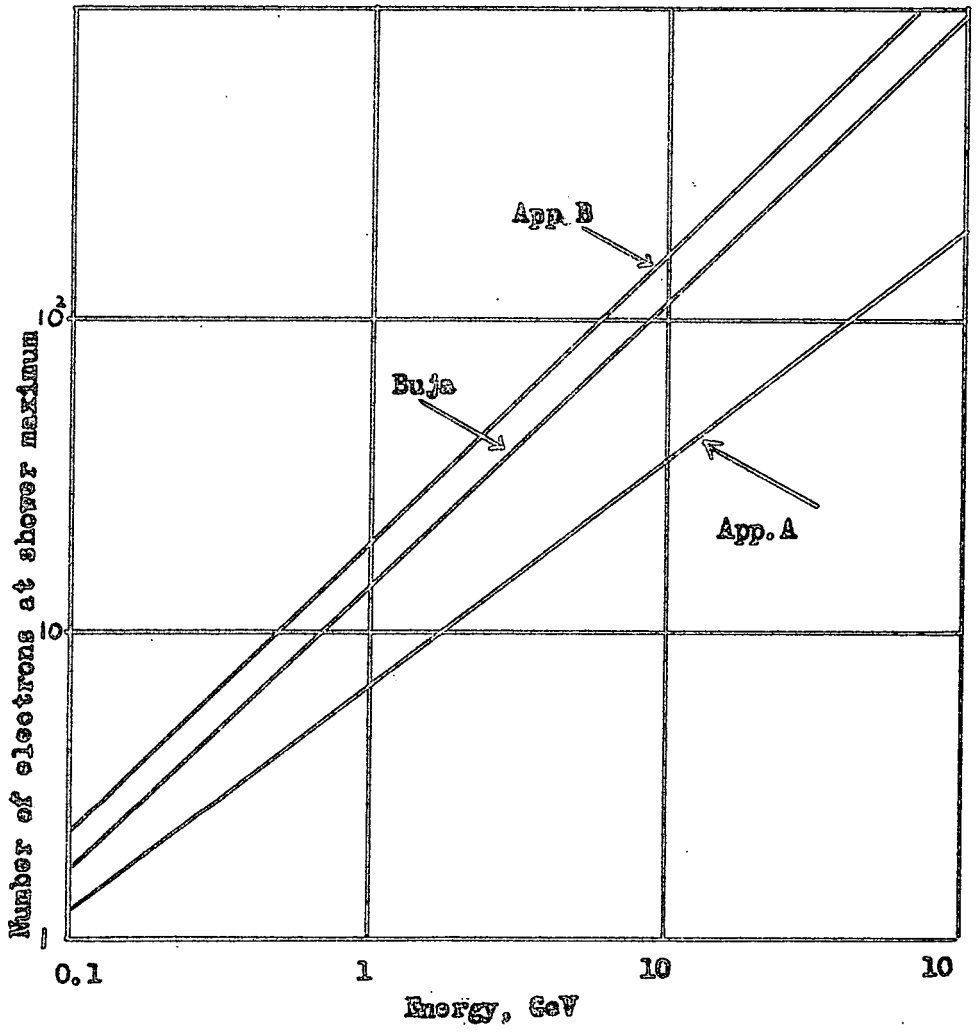

Figure A10 Cascade shower calibration curves

TABLE A.4

Number of electrons	10	10^2
Buja : App. B	1.38	1.41
(App. A : Buja)	(2.86)	(4.76)
(App. A : App. B)	(3.55)	(6.88)

From this table it can be seen that the discrepancy between the estimated energies increases with increasing number of particles at the shower maximum.

6.3 Thick plate experiment

In this type of experiment only the number of particles at the shower maximum can be used to estimate the energy and so the same reasoning applies as in the thin plate experiment.

6.4 Burst experiments

In this type of experiment the only measurable shower parameter is the number of particles leaving the block of absorber. To indicate the effect of the theory used in estimating the shower energy curves are plotted in figures A.11, A.12 and A.13 of the number of particles at a fixed depth in a cascade shower as a function of the shower energy for the different theories.

From these curves, which apply to Approximation B results and the results due to Buja, it can be seen that as the number of particles increases the ratio between the energy obtained from Approximation B and that from the results of Buja decreases. Also, as the depth in the shower increases the number of particles for which both theories give

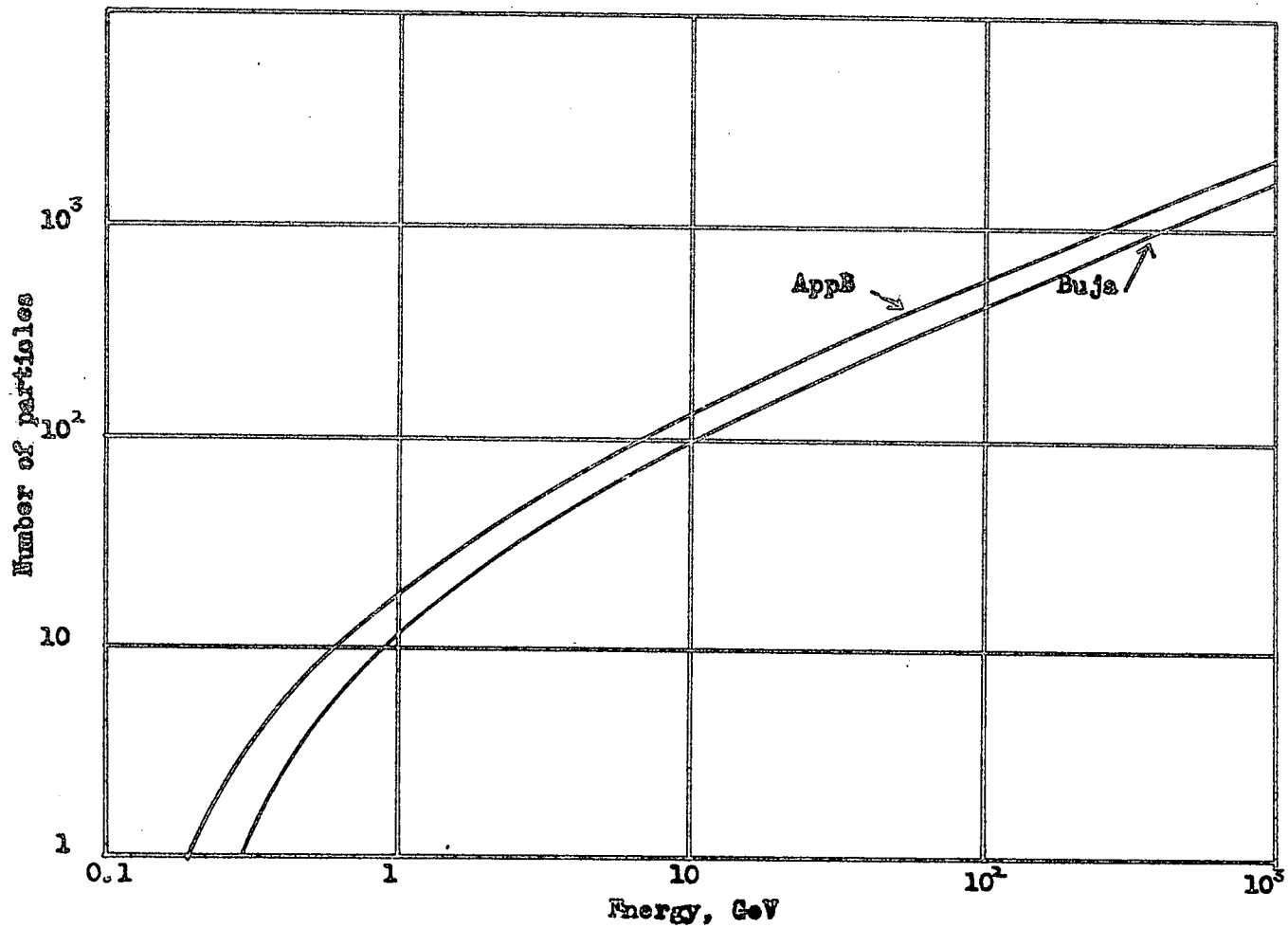

Figure A11 Number of particles at a depth of 5 r.l. Pb in an electron initiated shower.

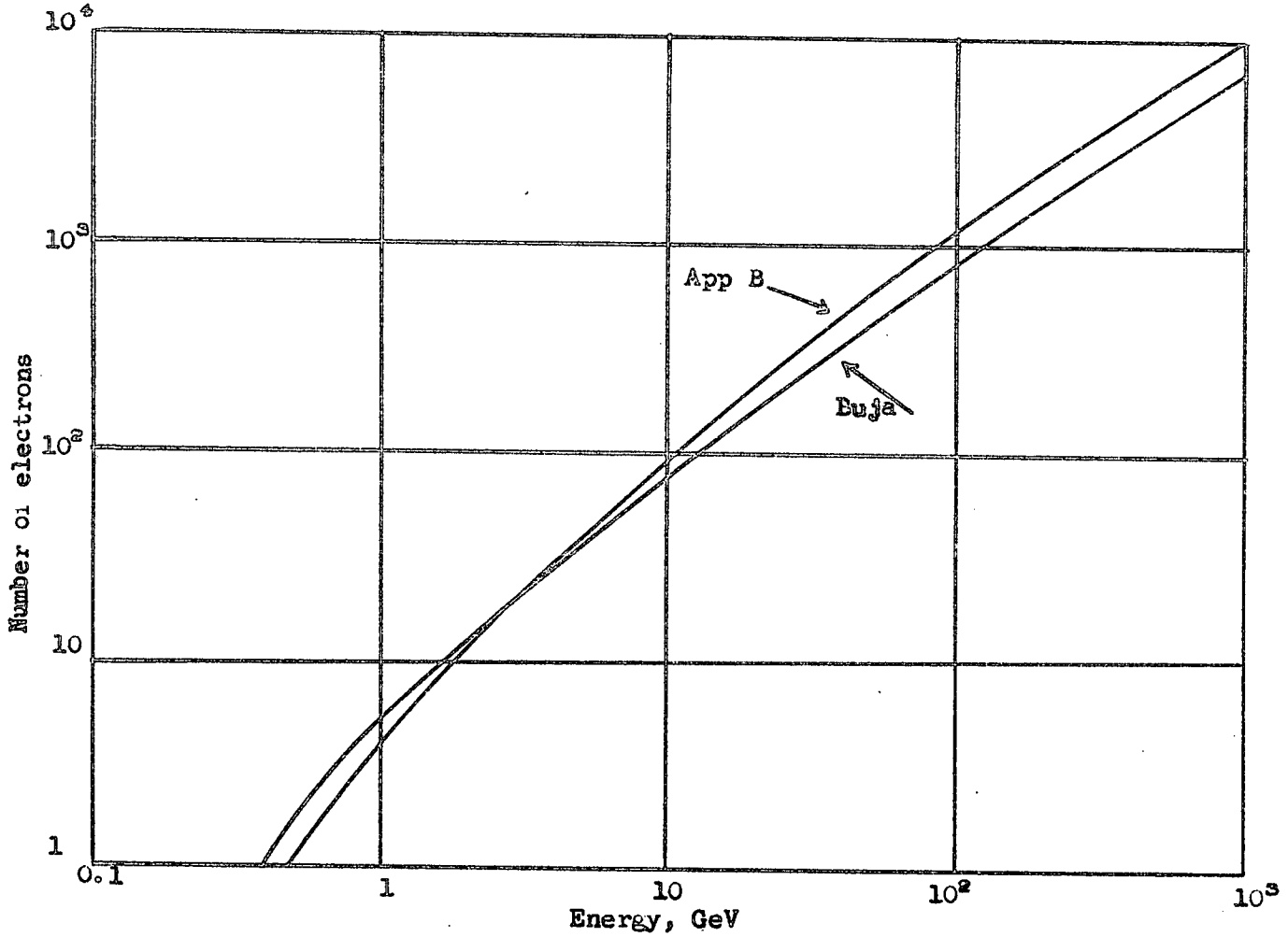

Figure A12 Number of electrons in electron initiated showers at a depth of 10 r.l. Pb

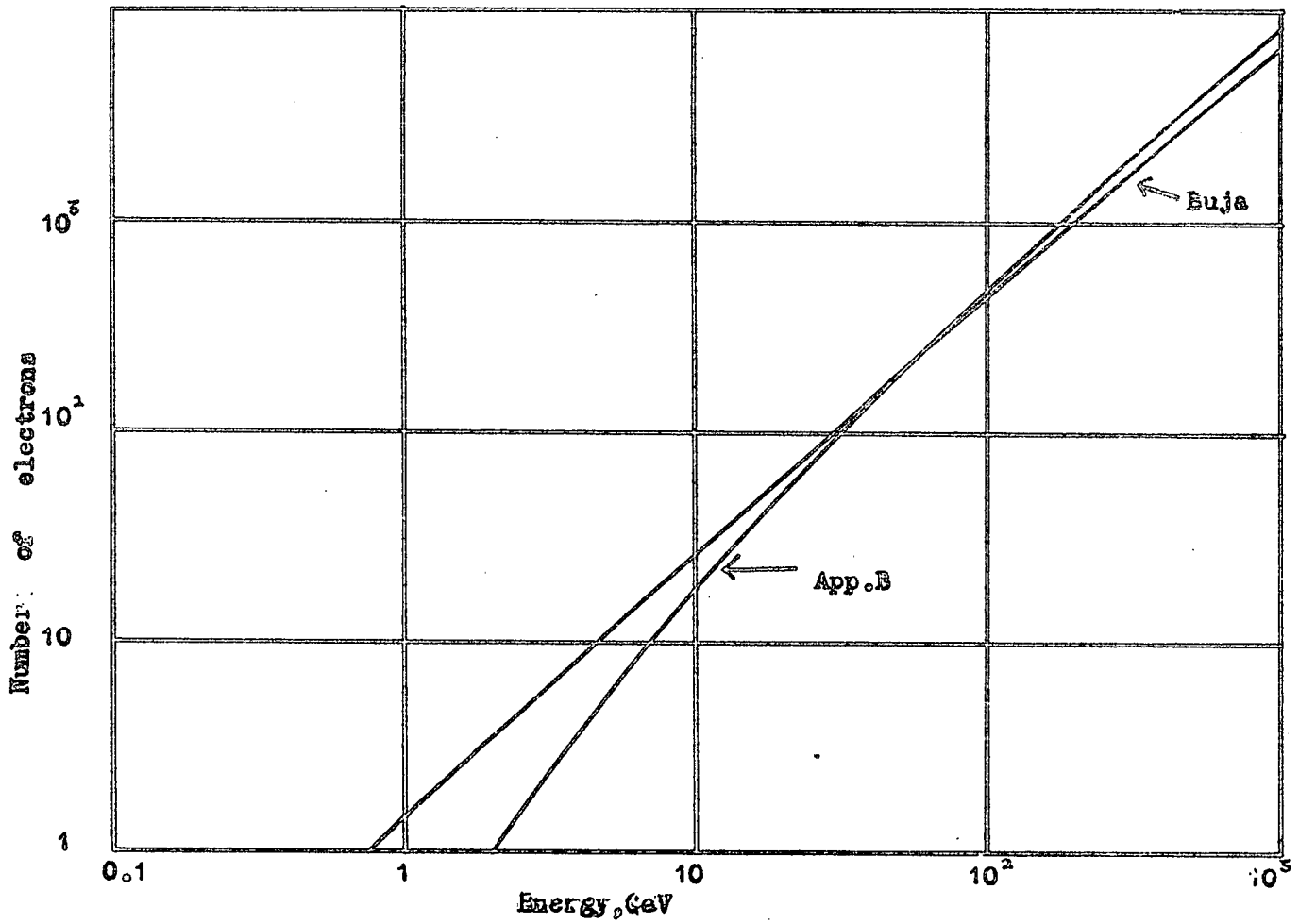

Figure A 13 Number of electrons in cascade showers at a depth of 15r.l. in Pb.

the same energy increases, below this number Approximation B gives the greatest energy, while above it Buja's results give the greatest energy.

7. Discussion

From the preceding paragraphs it can be seen that the method of energy estimation which is least likely to introduce uncertainties is that using the total electron track length in the shower. Thus, if electron, or photon, energies are to be determined from the cascade showers which these produce an experiment in which the absorber is in the form of a number of thin plates will give the most accurate values.

GUJARAT UNIVERSITY
COLLEGE
25 FEB 1955